# European Journal of Biomedical and Life Sciences

№ 1–2 2021

PREMIER
Publishing

Vienna
2021

# European Journal of Biomedical and Life Sciences

Scientific journal

**№ 1–2 2021**

ISSN 2310-5674



**Proofreading** Kristin Theissen
**Cover design** Andreas Vogel
**Additional design** Stephan Friedman
**Editorial office** Premier Publishing s.r.o.
Praha 8 – Karlín, Lyčkovo nám. 508/7, PSČ 18600
**E-mail:** pub@ppublishing.org
**Homepage:** ppublishing.org

**European Journal of Biomedical and Life Sciences** is an international, German/English/Russian language, peer-reviewed journal. It is published bimonthly with circulation of 1000 copies.

The decisive criterion for accepting a manuscript for publication is scientific quality. All research articles published in this journal have undergone a rigorous peer review. Based on initial screening by the editors, each paper is anonymized and reviewed by at least two anonymous referees. Recommending the articles for publishing, the reviewers confirm that in their opinion the submitted article contains important or new scientific results.

Premier Publishing s.r.o. is not responsible for the stylistic content of the article. The responsibility for the stylistic content lies on an author of an article.

**Instructions for authors**

Full instructions for manuscript preparation and submission can be found through the Premier Publishing s.r.o. home page at: http://www. ppublishing.org.

**Material disclaimer**

The opinions expressed in the conference proceedings do not necessarily reflect those of the Premier Publishing s.r.o., the editor, the editorial board, or the organization to which the authors are affiliated.

Premier Publishing s.r.o. is not responsible for the stylistic content of the article. The responsibility for the stylistic content lies on an author of an article.

**Included to the open access repositories:**

ULRICHSWEB GLOBAL SERIALS DIRECTORY · НАУЧНАЯ ЭЛЕКТРОННАЯ БИБЛИОТЕКА eLIBRARY.RU · CYBERLENINKA · Google scholar

GIF GLOBAL IMPACT FACTOR The journal has the GIF impact factor .562 for 2018.



Typeset in Berling by Ziegler Buchdruckerei, Linz, Austria.
Printed by Premier Publishing s.r.o., Vienna, Austria on acid-free paper.

# Section 1. Clinical Medicine

**https://doi.org/10.29013/ELBLS-21-1.2-3-7**

*Soltanova I. F.,*
*Mehdiyeva N. I.,*
*Oncology Department of Azerbaijan Medical University*
*E-mail:*

## CLINICAL AND PROGNOSTIC ANALYSIS OF THE EXPRESSION OF PD-L1 AND COX-2

**Abstract.** In modern oncology, the determination of PD-L1and COX-2 in the tumor tissue is one of the promising areas of research that allow you to correctly and adequately make a plan for further treatment of the patient and assess the prognosis of the disease. Determination of the expression level of the PDL-1 molecule and COX-2 is considered as a potential biomarker for predicting the effectiveness and duration of treatment of malignant neoplasms.

**Keywords:** cervical cancer, programmed death-ligand 1(PDL-1), cyclooxygenase-2 (COX-2).

The presence of metastatic lymph nodes in cervical cancer is one of the unfavorable prognostic factors that significantly affect the survival rates of patients. Thus, according to Y. Chen et al. metastases in the pelvic lymph nodes are associated with a decrease in the 5-year survival rate of patients from 85% to 53% [1]. Tumor lesion of regional nodes in cervical cancer is considered an indicator of the risk of distant metastasis, and therefore, this patient category needs adjuvant therapy, which specificity and volume vary depending on many factors [2]. On the other hand, the recent extensive study of biological markers of cervical tumors (PD-L1, COX-2) is also aimed at optimizing systemic therapy regimens [3]. Therefore, the study of the correlation between metastasis to the lymph nodes and the presence of PD-L1 [4] and COX-2 receptors in the tumor will allow a more targeted approach to the identification of patients in need of adjuvant treatment.

**The purpose of the study:** The study of the dependence between the expression of PD-L1 and COX-2 in tumor cells at cervical cancer (CC) and the frequency of metastasizing in regional lymph nodes.

**Materials and Methods.** The research included 70 women with a histologically confirmed diagnosis of primary CC at I–IIA and IIIC1 stages. The patients underwent surgical treatment at the Oncology Clinic of AMU for the period from 2015 to 2019. Along with the standard morphological examination, the standard immunohistochemical (IHC) treatment regimen was used (VENTANA Bench Mark Ultra) with the help of rabbit monoclonal antibodies to COX-2 (SP21) and PD-L1 (VD21R) of the Medaysis company. The expression level of PD-L1 was assessed by the number of cells tropic to antibodies – when staining less than 1.0% of the general population, the result was considered negative, and when staining more than 1.0% – positive. Based on the level of COX-2 expression in the squamous epithelium, four groups with cytoplasmic staining were identified: 0 (negative reaction), 1+ (weak expression

level), 2+ (medium), and 3+ (pronounced). Statistical processing of the obtained results was performed using discriminant – $\chi^{2-}$ Pearson and nonparametric analysis of variance – Kruskal-Wallis H test based on the SPSS-26 program. The difference was considered significant with a confidence level of at least 95% ($p < 0.05$).

**Results.** The age of the patients varied between 32–71 years, the average age was 50.2 ± 1.0 years. All patients underwent standard volumes of examinations, intended for CC: clinical examination, laboratory and instrumental methods (ultrasound, MRT, etc.). In the context of the work performed, MRT is valuable as a source of information on the status of regional lymph nodes at the preoperative stage. According to MRT data, enlarged lymph nodes (up to 14 mm in size) were found in four patients, including 2 cases of presacral and 2 cases of mesorectal lymph nodes. All patients underwent extirpation of the uterus with appendages in various versions, depending on the degree of prevalence of the tumor process. The stage distribution was as follows: IA – 7 (10.0 ± ± 3.6%), IB – 49 (70.0 ± 5.5%), IIA – 4 (5.7 ± 2.8%) and IIIC1–10 (14.3 ± 4.2%) patients. The results of IHC staining with antibodies to COX-2 receptors are presented in Table 1. In general, the incidence of COX-2-expressing tumors with the severity of 1+, 2+, and 3+ was 17 (24.3 ± 5.1%), 28 (40.0 ± 5.9%), and 25 (35.7 ± 5.7%) cases, respectively. As seen in the above data, the 1+, 2+, and 3+ expression levels of COX-2 at stage IA were in 5 (71.4 ± 17.1%), 0, and 2 (28.6 ± 17.1%) cases, respectively. At stage IB, these indicators were 10 (20.4 ± 5.8%), 21 (42.9 ± ± 7.1%), and 18 (36.7 ± 6.9%), respectively. At stage IIA, the number of patients with the 1+, 2+ and 3+ expression levels of COX-2 was 1 (25.0 ± 21.7%), 0 and 1(75.0 ± 21.7%), at stage IIIC1–1(10.0 ± ± 9.5%), 7(70.0 ± 14.5%) and 2(20.0 ± 12.6%), respectively ($P\chi^2 = 0.010$, $P_H = 0.224$). The results obtained indicate that there is no significant correlation (not confirmed by Kruskal-Wallis) between the severity of the COX-2 status and the stage.

Table 1.– Dependence of the expression level of COX-2 receptors in cervical cancer on the stage of the disease

| COX-2 expression level | IA | | IB | | IIA | | IIIC1 | | Total |
|---|---|---|---|---|---|---|---|---|---|
| | n/(%) | | | | | | | | |
| 1+ | 5 | 71.4±17.1 | 10 | 20.4±5.8 | 1 | 25.0±21.7 | 1 | 10.0±9.5 | $P\chi^2$=0.01 $P_H$=0.224 |
| 2+ | 0 | 0 | 21 | 42.9±7.1 | 0 | 0 | 7 | 70.0±14.5 | |
| 3+ | 2 | 28.6±17.1 | 18 | 36.7±6.9 | 3 | 75.0±21.7 | 2 | 20.0±12.6 | |

In (Figure 1), the dependence between the COX-2 expression levels and lymph node metastasis is presented. In the group of patients without lymph node metastases (N0), the incidence of the 1+, 2+ and 3+ expression levels of COX-2 in cervical cancer was 16 (26.7 ± 5.7%), 21 (35.0 ± 6.2%), and 23 (38.3 ± ± 6.3%) cases, respectively.

In the group of patients with lymph node metastases (N1), the distribution was as follows: 1(10.0 ± ± 9.5%), 7(70.0 ± 14.5%) and 2(20.0 ± 12.6%), respectively. $P = 0.110$, $P_H = 0.865$. As the results show, there is no significant correlation for this category. Therefore, the presence and severity of COX-2 expression do not affect the frequency of regional metastasis. Table 2 shows the results of IHC studies of PD-L1 receptors in cervical cancer, depending on the stages of the disease.

According to the data presented, at stage IA, PD-L1-positive tumors were not observed, at stage IB, the incidences of PD-L1 + and PD-L1- forms of cervical cancer were 11(22.4 ± 6.0%) and 38(77.6 ± ± 6.0%) cases, respectively. At stage IIA, all tumors were PD-L1-negative. At stage IIIC1, the expression of PD-L1 was absent in 2(20.0 ± 12.6%) cases, the remaining 8(80.0 ± 12.6%) were PD-L1-positive ($P < 0.001$, $P_H < 0.001$).

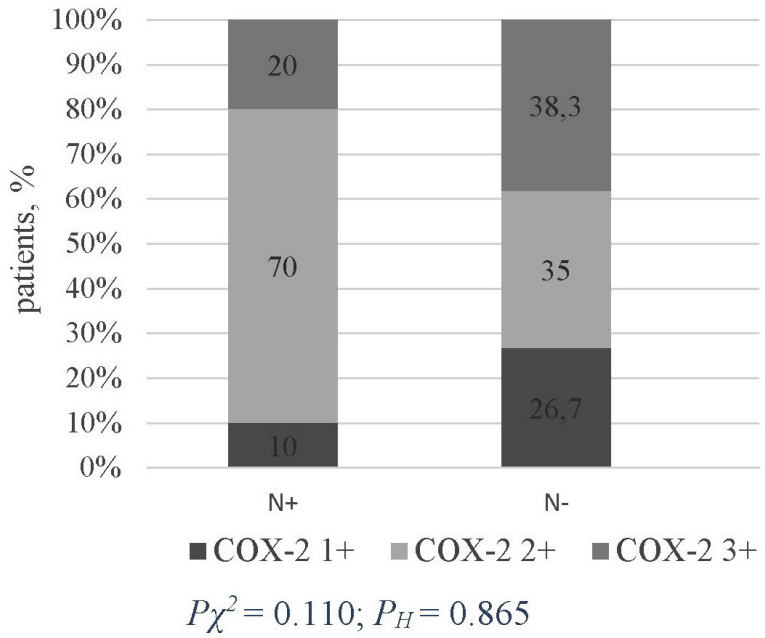


Figure 1. Ratio of COX-2-expressing tumors in patients with metastases in lymph nodes

Table 2.– Dependence of the expression level of PD-L1 receptors on the stage of the cervical cancer disease

| PD-L1 expression | IA | | IB | | IIA | | IIIC1 | | Total |
|---|---|---|---|---|---|---|---|---|---|
| | n /% | | | | | | | | $P\chi^2$<0.001 $P_H$ <0.001 |
| PD-L1-negative | 7 | 100 | 38 | 77.6±6.0 | 4 | 100 | 2 | 20.0±12.6 | |
| PD-L1-positive | 0 | 0 | 11 | 22.4±6.0 | 0 | 0 | 8 | 80.0±12.6 | |

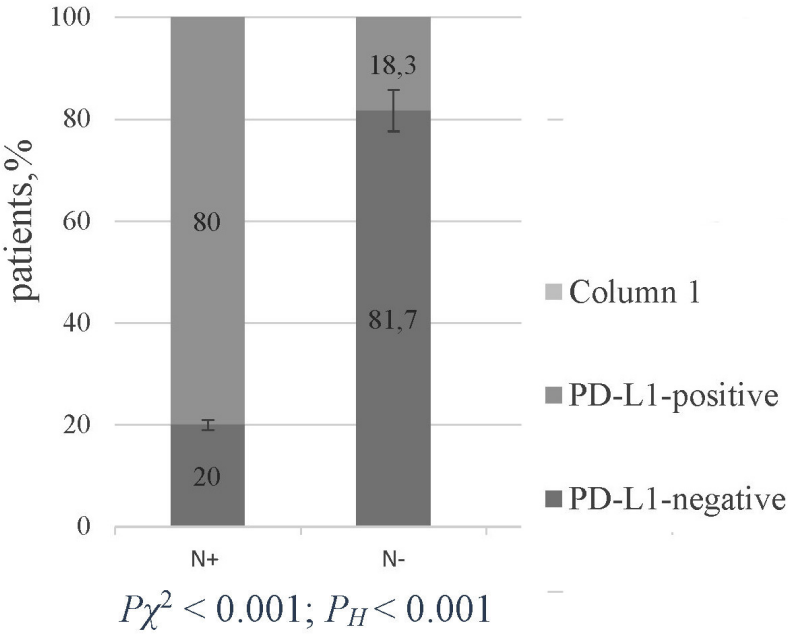


Figure 2. Ratio of PD-L1-negative and PD-L1-positive variants of tumors in patients with metastases in lymph nodes

Thus, PD-L1 expression is significantly associated with stage IIIC1 of the disease, characterized by the presence of metastases in the pelvic lymph nodes.

Figure 2 shows a diagram of the distribution of PD-L1 + and PD-L1- tumors among patients with lymph node metastases. According to the diagram, in the group of patients without metastases in the pelvic lymph nodes (N0), the ratio of PD-L1 + and PD-L1- variants was 18.3% and 81.7% (11 and 49 cases), respectively.

In the group of patients with metastases in the lymph nodes (N1), the given ratio is equal to 80.0% to 20.0% (8 and 2 cases), respectively ($P < 0.001$; $P_H < 0.001$). The data obtained confirm the availability of statistically reliable dependence between the cellular expression of PD-L1 receptors and metastasis in lymph nodes, which is very important in the assessment of the risk of tumor progression. When comparing the frequency of distant metastasis, a significant dependence of this indicator on the N status was revealed. Thus, in the N0 group, the number of patients with distant metastases (M1) was 12(20.0 ± ± 5.2%), patients without metastases (M0) – 48 (80.0 ± 5.2%), while in the group N1, the respective values were 6 (60.0 ± 15.5%) and 4 (40.0 ± 15.5%); $P = 0.007$; $\chi^2 = 7.179$; $P_H = 0.008$. The structure of the frequency of recurrence when comparing both groups is as follows: N0 – recurrence developed in 10(16.7 ± 4.8%), and absent in 50(83.3 ± 4.8%) cases; N1 recurrence developed in 4(40.0 ± 15.5%) and 6(60.0 ± 15.5%) cases, respectively, $P = 0.088$; $\chi^2 = 2.917$; $P_H = 0.090$. Statistical analysis confirms the presence of a correlation between lymph node metastasis and distant dissemination of the disease.

**Conclusion.** The conducted analysis of the results in immunohistochemical staining of preparations of patients with primary operable cervical cancer revealed the presence of certain patterns between the frequency of regional metastasis and status of PD-L1 and COX-2. Thus, it was established that the severity of COX-2-expression does not affect the frequency of metastases in lymph nodes ($P = 0.110$, $P_H = 0.865$), and also does not correlate with the clinical stage of CC ($P\chi^2=0$, $P_H=0.224$). The reliable dependence of PD-L1 status on regional metastasis was revealed. Thus, in 80.0% of the cases, N1 tumors were PD-L1-positive, while N0 tumors were PD-L1-positive only in 18.3% of the neoplasms ($P < 0.001$; $P_H < 0.001$). Correlation between PD-L1 expression and IIIC1 level of the disease was also established ($P < 0.001$, $P_H < 0.001$). It was found that the presence of N1 correlates with the development of distant metastases – 60.0% versus 20.0% at N0($P = = 0.007$; $P_H = 0.008$). The study of the frequency of local recurrences of cervical cancer showed the absence of a significant relationship between this indicator and the N status ($P = 0.088$; $\chi^2 = 2.917$).

Thus, in cervical cancer patients with lymph node metastases, the diagnosis of PD-L1 expression has a great clinical and prognostic importance, in other words, PD-L1-positivity can be regarded as an indicator of the risk of disease progression.

**Summary**

The lesion of the lymph nodes in cervical cancer is one of the main risk factors for the dissemination of the disease. Metastases in the pelvic lymph nodes are associated with a decrease in the 5-year survival rate of patients from 85% to 53%. From this position, due to the expansion of the opportunities of adjuvant therapy in this category of patients, the study of the receptor profile (PD-L1, COX-2) of tumor cells is of particular relevance. Interpretation of the results of immunohistochemical staining of cervical cancer with antibodies to PD-L1 and COX-2 in a cohort of patients with lymph node metastases (N1) revealed the presence of certain regularities between the expression of PD-L1 and COX-2 and clinical prognostic parameters. No correlation was found between the severity of COX-2 expression and metastases in the lymph nodes. Reliable dependence between PD-L1-positivity and tumor lesions of lymph nodes was revealed. In 80.0% of cases, N1 tumors were PD-L1-positive, while only 18.3% of N0 neoplasms were PD-L1-positive ($P < 0.001$; $P_H < 0.001$). The presence of N1 was found to correlate

with the development of distant metastases-60.0% vs 20.0% in N0 (P = 0.007; $P_H$ = 0.008). The study of the frequency of local CC recurrences showed the absence of reliable dependence between the indicator and the N status (P = 0.088; $\chi^2$ = 2.917).

Thus, the expression of PD-L1 in cervical cancer cells correlates with the frequency of regional metastasis, which should be taken into account in assessing the risk of progression and planning systemic therapy.

**References:**

1. Chen Y., Fang C., Zhang K. et al. Distribution patterns of lymph node metastasis in early stage invasive cervical cancer Medicine (Baltimore). Oct 16. 2020.– 99(42).– 22285 p.
2. Chen Ch.,Ou Y.,Lin H.,Wang Ch. Analysis of prognostic factors and clinical outcomes in uterine cervical carcinoma with isolated para-aortic lymph node recurrence. Am. J. Transl. Res. 2019.– 11(12).– P. 7492–7502.
3. Liu Z., Hu K., Liu A., Shen J. Patterns of lymph node metastasis in locally advanced cervical cancer Medicine (Baltimore). Sep, 2016.– 95(39).– 4814 p.
4. Heeren M., Punt S., Bleeker M. et al. Prognostic effect of different PD-L1 expression patterns in squamous cell carcinoma and adenocarcinoma of the cervix Mod Pathol. Jul, 2016.– 29(7).– P. 753–763.

**https://doi.org/10.29013/ELBLS-21-1.2-8-13**

*Kubrakov Konstantin Mikhailovich,*
*Candidate of medical sciences (PhD), Associate professor,*
*the Department of Neurology and Neurosurgery*
*EI "Vitebsk State Order of Peoples' Friendship Medical University",*
*Vitebsk, Belarus*
*E-mail: k-kubrakov@yandex.ru*

*Kornilov Artem Viktorovich,*
*Candidate of medical sciences (PhD), assistant,*
*of the Department of Hospital Surgery*
*EI "Vitebsk State Order of Peoples' Friendship Medical University"*
*Vitebsk, Belarus*
*E-mail: joda_jedi@mail.ru*

*Alekseev Denis Sergeevich,*
*Clinical intern, EI "Vitebsk State Order of Peoples'*
*Friendship Medical University", Vitebsk, Belarus*

# APPLICABILITY OF VAC-SYSTEM IN TREATMENT OF PATIENTS WITH RETRODURAL SPINAL EPIDURAL ABSESSES

**Abstract:** The study included 23 patients with the retrodural spinal epidural abscesses (SEA) who underwent surgical debridement. 13 patients underwent classical laminectomy, removal of a purulent focus with flow-washing drainage of the wound. In 10 patients, SEA was removed using the developed technology with performing the interlaminar openings for access to the posterior epidural space, debridement, and vacuum-assisted closure (VAC). The use of the developed method made it possible to reduce reliably the number of relapses of the purulent process (pFisheri = 0.0016), to shorten the duration of hospitalization (pMann-Whitney = 0.004) and to obtain a good functional treatment outcome according to the Frankel scale (pWilcoxon = 0.027).

**Keywords:** spinal epidural abscess, vacuum-assisted closure, interlaminectomy, mortality.

**Introduction.** SEA is an inflammatory process in the epidural space of the spinal column, located between the dura mater and the periosteum [1]. Spinal epiduritis is relatively rare and accounts for 0.22% of all pathology of the spine and spinal cord [2].

The SEA clinical characteristics has no specific symptoms at the disease onset, which leads to the diagnosis delay as well as the development of severe neurological (paresis and paralysis) and systemic purulent complications such as the systemic inflammatory response syndrome and sepsis [3].

At present, the systematic approach to the surgical treatment of SEA has been provided by the authors headed by E. Pola (2018). – New Classification Pyigenic Spondylodiscitis (NCPS). However, in this algorithm, the treatment of an epidural abscess is viewed only within the framework of spondylodiscitis – type C1-C4. Also, this classification does not take into account the retrodural location of SEA, the

presence of extravertebral purulent foci, the severity of systemic inflammatory reactions to set indications or contraindications for surgical treatment [4, 5].

Therefore, until now, the most common method of SEA treating is a conventional laminectomy followed by debridement and drainage of the epidural tissue. Unfortunately, the instability of the posterior supporting complex, especially after multilevel laminectomy with an extended purulent epiduritis leads to the development of severe post-laminectomy syndromes with pronounced lumbodynia and spinal deformity, which often require surgical correction [6].

Thus, the development of new methods of surgical treatment of SEA will help to supplement modern algorithms for the treatment of patients with purulent epiduritis and improve the results of surgical interventions in patients with this pathology.

Thereby, the development of new methods of SEA surgical treatment will help to supplement modern algorithms for management of patients with purulent epiduritis and to improve the surgery results in patients with this pathology.

**Aim of the research.** To assess the effectiveness of VAC systems in the surgical treatment of retrodural spinal epidural abscesses.

**Materials and methods.** The study included 23 patients with retrodural SEA (G06.1 – code according to ICD-10), who were being treated at Vitebsk Regional Clinical Hospital and Mogilev Emergency Hospital from 2008 to 2020 inclusive. There were 15 men (65.2%) and 8 women (34.8%) among them, the median age of patients was 52 (48–60) years. Patient participation was voluntary. The research protocol was approved by the decision of the Ethics Committee of the educational institution "Vitebsk State Order of Peoples' Friendship Medical University".

The neurological examination included history taking of complaints from patients with the assessment of the severity of pain on a visual analogue scale (VAS) from 0 to 10 points, a study of higher cerebral activity, disorders of the motor and sensory spheres, and dysfunction of the pelvic organs.

Neurological status was assessed at hospitalization, throughout the treatment period and on discharge in accordance with the international standards for the neurological classification of spinal cord injury with the completion of the ISNCSCI (International Standards for Neurological Classification of Spinal Cord Injury) revision form of 2015. However, taking intoconsideration the number of patients with the extended SEA localization and below the L2 vertebral body, the use of the AIS-2015 scale was not always correct. Therefore, we used the Frankel scale.

On admission, laboratory and instrumental research methods were carried out in the patients (CT and MRI of the spine, ultrasound examination of the abdominal organs). According to MRI data, in 78.3% of patients, SEA was localized in the lumbar spine (Table 1).

Table 1. – Levels of SEA location in the spine

| Regions of the spinal column | n(%) |
|---|---|
| Isolated SEA of the lumbar spine | 18(78,3%) |
| Multilevel SEA involving the thoracic and lumbar regions | 3(13,0%) |
| Extended SEA involving more than 6 segments in different parts of the spinal column | 2(8,7%) |
| **Total** | **23**(100%) |

Patients with retrodural SEA (n = 23) were divided into 2 groups depending on the type of surgical treatment.

Group I included 13 patients (56.5%). Surgical treatment of a purulent focus in which was performed through decompressive laminectomy followed by flow-washing drainage of the wound.

Group II included 10 (43.5%) patients. Operations in this group were performed according to the technology developed by the authors with the resection formation of interlaminar openings throughout SEA, debridement of purulent foci. At the end of the operation VAC-system was applied for wound drainage (patent BY22947 «Method for the treatment of nonspecific epiduritis with paravertebral abscess»). The scheme of the operative access and installation of VAC is shown in (Figure 1) [7].

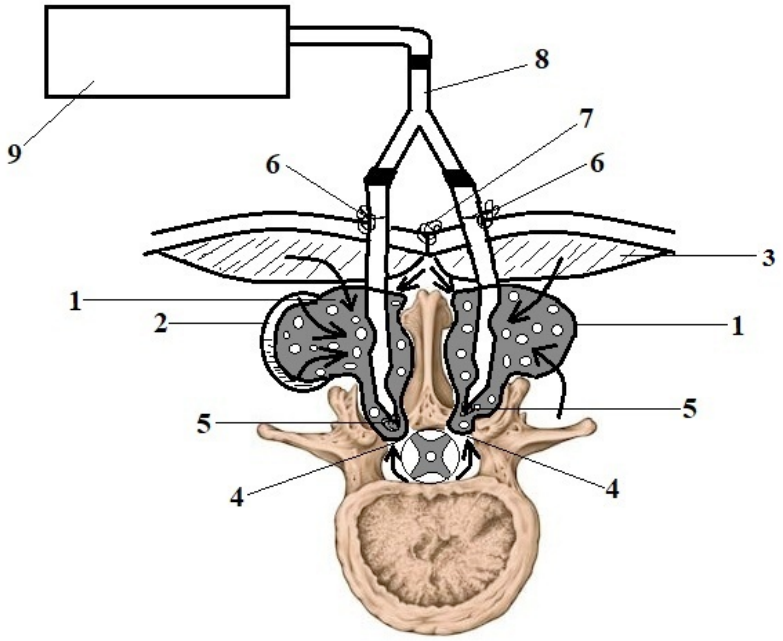


Figure 1.– Scheme of the SEA removal operation with the VAC system:
1 – polyurethane porous material, 2 – paravertebral abscess, 3 – paraspinal muscles, 4 – interlaminar access area, 5 – fixing suture, 6 – counteropening, 7 – seam on the skin, 8 – drainage tube, 9 – aspirator

Comparative analysis on the effectiveness of surgical methods for the treatment of retrodural SEA was carried out according to the assessment of the severity of pain syndrome based on the VAS scale, regression of neurological disorders, the number of recurrences of the purulent process and reoperations, according to the mortality rate and duration of inpatient treatment in the groups.

Statistical processing was performed using the STATISTICA 10.0 program. The normality of features distribution was determined by the Kolmagorov-Smirnov and Shapiro-Wilk criteria. For qualitative variables, the frequency of cases (n) and the proportion (in %) were determined; for quantitative ones, the median, upper and lower quartiles of Me (LQ–UQ). Comparison of the frequency of the trait in independent samples was carried out according to the $\chi^2$ test, according to the exact two-sided Fisheri, Mann-Whitney test. The obtained results were considered reliable at $p < 0.05$.

**Results.** The assessment of the pain syndrome severity according to the VAS scale was carried out only in the patients of group II. There was only a statement of the presence of pain in the corresponding part of the spinal column in group I. When assessing the severity of pain using the VAS scale, all 9(90%) patients of group II scored more than 8 points, one person had a maximum VAS score of 10 points. The median of the pain severity among the patients of group II was 8.5 (8–9) points on the VAS scale.

In patients with retrodural SEA, focal neurological deficit was revealed in 10 cases (43.5%). Spastic tetraparesis was diagnosed in 1 patient, lower spastic paraplegia – in 3, lower flaccid paraparesis – in 6 people, dysfunction of the pelvic organs – in

4. Sensitivity disorders of hypesthesia type were observed in 4 patients (18.18%).

In the early postoperative period, in all 23 patients a clinical positive result was achieved. In 10 patients of group II, the intensity of pain syndrome 2–3 after surgery significantly decreased from 8.5 (8–9) to 5 (4–5) points according to the VAS scale. On discharge, in 6 patients of group II, the pain syndrome completely regressed to 0 points according to the VAS; in 3 patients, mild pain (VAS1–2 points) persisted in the area of the postoperative wound. There were no complaints of any pain among the patients (VAS – 0 points) at the follow-up examination one month after the operation (n = 9).

Restoring of neurological deficit in two groups included an increase in the strength and range of active movements in the lower and upper extremities up to 3–4 points, a decrease in paresthesia and a decrease in sensory disorders, and restoration of control over the pelvic disorders. No patient had postoperative kyphotic deformity of the spine.

The dynamics of changes in neurological disorders and pain syndrome according to VAS in patients of group II both on admission and on discharge from the hospital are presented in (Table 2).

Table 2.– Dynamics of functional changes in patients of group II with retrodural SEA on admission and on discharge from the hospital

| Indicators | Admission | Discharge | Frankel category upgrade | p |
|---|---|---|---|---|
| VAS, Me (LQ-UQ) | 8,5(8–9) | 1(0–2) | – | $P_{Wilcoxon}$ = 0,007 |
| Frankel A, n(%) | 0 | 0 | – | |
| Frankel B, n(%) | 1(11,1%) | 0 | 1 | |
| Frankel C, n(%) | 2(22,2%) | 1(11,1%) | 2 | |
| Frankel D, n(%) | 3(33,3%) | 2(22,2%) | 3 | |
| Frankel E, n(%) | 3(33,3%) | 6(66,6%) | – | $P_{Wilcoxon}$ = 0,027 |

*Note – Frankel A – 1, Frankel B – 2, Frankel C – 3, Frankel D – 4, Frankel E – 5*

According to (Table 2), it can be seen that patients of group II had a statistically significant decrease in the pain syndrome severity from 8.5(8–9) on admission to 1 (0–2) on discharge from their hospital according to the VAS scale (pWilcoxon = = 0.007), and there was also a progressive transition of neurological disorders (66.6%) to higher functional classes (pWilcoxon = 0.027) according to the Frankel scale. In group II, 1 patient died, the mortality rate was 10%. At the same time, readmissions and reoperations were not required in this group of patients. The median of inpatient treatment in group II was 26(22–31) days.

Out of 13 people in group I, 5 patients (39%) required 9 readmissions due to the progression of the purulent process. At the same time, one patient was re-hospitalized 3 times with 3 reoperations. Also, 2 people were treated at the hospital again, and one of them required surgery. Despite this, after 3 months, these 2 patients underwent the second course of antibiotic therapy in the hospital due to the development of complications. Also, 2 patients came back with pains in the spine and fever; they were examined and treated with antibacterial drugs. Therefore, in this group, 4 reoperations were performed because of the developed intermuscular abscesses in the area of surgical intervention. In the group, 2 people died, the mortality rate was 15.4%. During readmissions, 5 patients stayed 285 days in the hospital. The terms of in-patient treatment in group I made up 51(38–81) days. The treatment results in groups are presented in (Table 3).

Table 3.– Comparative data on the effectiveness of surgical treatment in patients with retrodural SEA in the groups

| Indicators | I(n=13) | II(n=10) | p |
|---|---|---|---|
| Survived | 11 | 9 | $P_{Fisheri} = 1,0$ |
| Died | 2 | 1 | $P_{Fisheri} = 1,0$ |
| Lethality,% | 15,4% | 10% | $P_{Fisheri} = 0,601$ |
| Number of readmissions | 9 | 0 | $P_{Fisheri} = 0,0016$ |
| Number of reoperations | 4 | 0 | $P_{Fisheri} = 0,104$ |
| Length of in-patient treatment, Me (LQ-UQ), bed-days | 51(38–81) | 26(22–31) | $P_{Mann-Whitney} = 0,004$ |

**Discussion.** A new technology for the surgical treatment of retrodural SEA has been developed and applied, including access to the posterior epidural space by marginal resection of adjacent vertebral arches and widening of interlaminar spaces along the purulent focus from one or both sides using the VAC system [7]. Patients received reliably significant positive results of changes in clinical status, including a decrease in the severity of pain syndrome according to the VAS scale from 8.5(8–9) points on admission to 1(0–2) points on discharge (pWilcoxon = 0.007), as well as neurological deficit regression with a progressive transition of 66.6% of patients to higher functional classes according to the Frankel scale (pWilcoxon = 0.027).

Also, despite the absence of significant differences in the decrease in mortality in patients with retrodural SEA from 15.4% in group I to 10% in group II (pFisheri = 0.601), a statistically significant decrease in the number of readmissions from 39% to 0% was obtained (pFisheri = 0.0016) and required reoperations for recurrent purulent-inflammatory process (pFisheri = 0.104), as well as a decrease in the duration of inpatient treatment from 51(38–81) to 26 (22–31) bed-days (pMann-Whitney = 0.004), which indicates the high efficiency of the developed approach to prompt removal of SEA using VAC systems.

**Conclusions.** The use in clinical practice of the advanced technology of surgical removal of retrodural SEA with the use of the VAC-system allows optimizing the treatment of patients with the improvement of functional outcomes and lowering financial expenses due to shortening the terms of the inpatient treatment stage.

## References:


1. Leopold Arko 4th, Eric Quach, Vincent Nguyen, Daniel Chang, Vishad Sukul, Bong-Soo Kim. Medical and surgical management of spinal epidural abscess: a systematic review. Neurosurg Focus [Electronic resource].– Vol. 37. 2014. Mode of access: URL: https://doi.org/10.3171/2014.6.FOCUS14127.– Date of access: 27.04.2021
2. Amit R. Patel, Timothy B. Alton, Richard J. Bransford, Michael J. Lee, Carlo B. Bellabarba, Jens R. Chapman. Spinal epidural abscesses: risk factors, medical versus surgical management, a retrospective review of 128 cases. Spine J.– Vol. 14. 2014.– P. 326–330.
3. Steven F. De Froda J. Mason De Passe, Adam E. M Eltorai, Alan H. Daniels, Mark A. Palumbo. Evaluation and management of spinal epidural abscess. J Hosp Med. [Electronic resource].– Vol. 11. 2016. Mode of access: URL: https://www.journalofhospitalmedicine.com/jhospmed/article/127631/evaluation-spinal-epidural-abscess.– Date of access: 27.04.2021.

4. Enrico Pola, Taccari F., Autore G., Giovannenze F., Pambianco V., Cauda R., Maccauro G., Fantoni M. Multidisciplinary management of pyogenic spondylodiscitis: epidemiological and clinical features, prognostic factors and long-term outcomes in 207 patients. Eur. Spine J.– Vol. 27. 2018.– P. 299–236.
5. Enrico Pola, Autore G., Formica V. M., Pambianco V., Colangelo D., Cauda R., Fantoni M. New classification for the treatment of pyogenic spondylodiscitis: validation study on a population of 250 patients with a follow-up of 2 years. Eur. Spine J.– Vol. 26. 2017. suppl. 4.– P. 479–488.
6. Farhan Siddiq, Ashish Chowfin, Robert Tight, Abe E. Sahmoun, Raymond A. Smego Jr. Medical vs surgical management of spinal epidural abscess. Arch Intern Med.– Vol. 164(22). 2004.– P. 2409–2412.
7. Kubrakov K. M., Petukhov V. I., Kornilov A. V. Vacuum therapy application in surgical treatment of spinal epidural abscesses. Novosti Khirurgii.– Vol. 27(1). 2019.– P. 59–65.

**https://doi.org/10.29013/ELBLS-21-1.2-14-19**

*Panchuk O. V.,*
*MD, MMed, Phd student,*
*Bogomolets National medical university, Kiev, Ukraine*
*Susak Y. M.,*
*doctor of medicine, professor, head of department of surgery,*
*Bogomolets National medical university, Kiev, Ukraine*
*Markulan L. Y.,*
*Phd, MD, associate professor department of surgery*
*Bogomolets National medical university, Kiev, Ukraine*
*E-mail: orestpv@gmail.com*

# ASSESSMENT OF QUALITY OF LIFE IN PATIENTS WITH COSMETIC ANTERIOR ABDOMINAL WALL DEFECTS, VENTRAL HERNIATION AND I–II DEGREE OF OBESITY

**Abstract.** In the study, we determined the reference values of the quality of life using the international questionnaire MOS-SF-36 and we additionally conducted a questionnaire using the questionnaire we developed. In the study after 1 year, the patients of the main group, who underwent both abdominoplasty and liposuction, noted a significant improvement in body contours, had better quality of life and were more satisfied with the aesthetic result of the operation.

**Keywords:** abdominoplasty, lipoabdominioplasty, quality of life.

*Панчук О. В.*
*Аспирант кафедры хирургии, Национальный медицинский университет им. А. А. Богомольца, Киев, Украина*
*Сусак Я. М.*
*доктор медицинских наук, профессор, заведующий кафедрой хирургии*
*Национальный медицинский университет им. А. А. Богомольца, Киев, Украина*
*Маркулан Л. Ю.*
*кандидат медицинских наук, доцент кафедры хирургии*
*Национальный медицинский университет им. А. А. Богомольца, Киев, Украина*
*E-mail: orestpv@gmail.com*

# ОЦЕНКА КАЧЕСТВА ЖИЗНИ У ПАЦИЕНТОВ С КОСМЕТИЧЕСКИМИ ДЕФЕКТАМИ ПЕРЕДНЕЙ БРЮШНОЙ СТЕНКИ, ВЕНТРАЛЬНЫМИ ГРЫЖАМИ И ОЖИРЕНИЕМ I–II СТЕПЕНИ

**Аннотация.** В исследовании мы определили референтные значения качества жизни с помощью международного опросника MOS-SF-36 и мы дополнительно проводили анкетирование по

разработанной нами анкете. При исследовании через 1 год, пациенты основной группы, которым было выполнено одновременно абдоминопластику и липосакцию, отмечали значительное улучшение контуров тела, имели лучшие показатели качества жизни и были более довольны эстетическим результатом операции.

**Ключевые слова:** абдоминопластика, липоабдоминиопластика, лазерная доплеровская флоуметрия, ультразвуковая допплеровская флоуметрия.

**Анализ последних публикаций и исследований**

Липосакция довольно распространенная операция в мире, по данным Международного общества эстетической пластической хирургии (ISAPS), она занимает второе место по количеству, уступая аугментационной маммопластике [4].

Современная тенденция сочетать абдоминопластику и липосакцию направлена для улучшения результатов и получения лучших эстетических результатов [11; 12]; проведены исследования, которые показывают безопасность сочетание этих операций [1].

Saldanha разработал и описал методику липоабдоминопластики. Он предложил проводить диссекции проксимального лоскута поверхностно, для сохранения фасции Скарпа. Согласно автору, это сохраняет сеть лимфатических сосудов передней брюшной стенки, которые расположены глубже фасции Скарпа в гипогастральных участке. Этот хирургический прием также помогает лучшему плоскостном сопоставлению проксимального лоскута, который обычно тоньше дистального [7; 8].

Costa-Ferreira et al., опубликовали в 2013 результаты рандомизированного клинического исследования о безопасности и эффективности сохранения фасции Скарпа. Это исследование показало уменьшение выделения количества секрета, который выделялся по дренажам на 65% и их можно было удалять на 3 дня раньше чем у пациентов без сохранения фасции Скарпа [2; 3].

Lockwood описал основные дефектные зоны после абдоминопластики, среди них: «напряженную» зону в центральной части живота, избыток кожи и дряблость в боковой и паховой областях, надлобковая депрессия рубца, проксимальное смещение волос на лоне, плохая выразительность талии, и гипертрофические и асимметричные рубцы [5].

Во время проведения липоабдоминопластики с ультразвуковой и PAL липосакцией, снижается потеря крови и потребность в послеоперационной гемотрансфузии, но в этих исследованиях не исследованы объемную липосакцию с резекцией массивных лоскутов [10].

Натуральный вид пупка является важным в эстетике тела, неестественной вид объясняется искаженной форме и цвету. Пупочный рубец – это главная стигма липоабдоминопластики. Меняется его внешний вид вследствие старения, беременности, развития грыж и гиперхромия [9].

Операция влияет на вид пупка и передней брюшной стенки и имеет значительное влияние на психоэмоциональное самочувствие пациентов и удовлетворенность эстетическим результатом [6, 11].

Цель работы: исследовать влияние результата операций абдоминопластики отдельно или в сочетании с липосакцией на качество жизни и на психоэмоциональное состояние у пациентов с косметическими дефектами передней брюшной стенки, вентральными грыжами и с ожирением I–II ст.

**Материалы и методы**

Исследование было проведено в 132 больных, из них женщины – 116(87,9%), мужчины – 16(12,1%). Средний возраст пациентов составил 43,2 ± ± 10,3 года. Пациенты были разделены на 2 группы: основная группа – 64(48,5%) пациентов, которым выполняли абдоминопластики в сочетании с липосакцией группа сравнения – 68(51,5%) пациентов,

которым выполняли абдоминопластики без липосакции. Кроме основной и контрольной группы, мы также определили референтные значения качества жизни в 42 пациентов, которые были прооперированы в нашей клинике (группа О), и были репрезентативными с пациентами из основной и группы сравнения по возрасту, полу, ИМТ (индексу массы тела) и типом деформации передней брюшной стенки и не выполняли себе абдоминопластику и липосакцию. Все пациенты, включенные в исследование, были с ожирением I, II степени (средний ИМТ 32,8 ± 2,67 кг/м$^2$). Средний возраст пациентов в группе сравнения составил 43,3 ± 10,4 года, а в основной группе – 43,1 ± 10,1 года (p = 0,301). По степени косметических деформаций передней брюшной стенки все пациенты относились к III или IV типа по классификации дефектов передней брюшной стенки по Matarasso. Все пациенты в трех исследуемых группах статистически не отличались по возрасту, индексу массы тела, типом деформации передней брюшной стенки (все p < 0,05).

**Результаты исследования**

В нашем исследовании приняли все пациенты основной и контрольной групп и группы В, которым исследовали качество жизни с помощью международного опросника MOS-SF-36.

Таблица 1.– Средние показатели качества жизни в исследуемых группах до операции и через 1 год после операции

| Показатель | Группа | Средние значения | | p |
|---|---|---|---|---|
| | | До | 1 год | |
| PF | Основная | 82,78±7,28 | 89,44±4,76 | 0,001 |
| | Сравнения | 83,31±6,96 | 83,89±6,27 | 0,452 |
| | Группа О | 83,1±7,01 | 83,68±5,72 | 0,399 |
| Rp | Основная | 76,11±5,51 | 84,45±7,24 | <0,001 |
| | Сравнения | 76,17±5,38 | 77,79±6,67 | 0,036 |
| | Группа О | 76,43±6,31 | 77,1±+6,17 | 0,049 |
| BP | Основная | 78,73±5,41 | 82,54±5,66 | <0,001 |
| | Сравнения | 79,78±4,48 | 80,21±4,57 | 0,068 |
| | Группа О | 79,76±4,7 | 79,81±4,61 | 0,432 |
| GH | Основная | 74,22±5,91 | 76,37±7,13 | 0,056 |
| | Сравнения | 73,85±9,46 | 74,57±9,83 | 0,068 |
| | Группа О | 73,59±10,81 | 74,2±9,58 | 0,059 |
| VT | Основная | 69,37±9,57 | 80,39±9,81 | <0,001 |
| | Сравнения | 68,16±11,41 | 72,07±11,28 | <0,001 |
| | Группа О | 68,31±12,01 | 69,5±1,87 | 0,351 |
| SF | Основная | 76,31±8,03 | 84,97±8,27 | <0,001 |
| | Сравнения | 76,79±9,94 | 77,33±6,58 | 0,422 |
| | Группа О | 77,02±8,71 | 77,32±6,54 | 0,385 |
| RE | Основная | 64,75±13,60 | 72,98±9,11 | 0,001 |
| | Сравнения | 64,79±12,17 | 68,37±8,41 | 0,028 |
| | Группа О | 64,52±13,97 | 67,42±8,81 | 0,041 |
| MH | Основная | 65,87±10,92 | 75,6±12,07 | <0,001 |
| | Сравнения | 65,91±11,25 | 66,31±10,91 | 0,594 |
| | Группа О | 66,04±10,01 | 67,11±10,42 | 0,384 |

При исследовании данных было выявлено отсутствие статистически значемой разницы между тремя группами пациентов по показателям качества жизни до проведения оперативного вмешательства, таблица 1, где условными знаками обозначены: PF – физическое функционирование; Rp – ролевое функционирование, что обусловлено физическим состоянием; BP – интенсивность боли; GH – общее состояние здоровья; VT – жизненная активность, SF – социальное функционирование; RE – ролевое функционирование, обусловленное эмоциональным состоянием; MH – психическое здоровье.

Во всех группах пациенты оценивали состояние своего здоровья как хорошее или удовлетворительное и все они хотели его улучшить. Характерным до оперции было то, что они отмечали снижение возможности концентрироваться и соответственно выполнять работу не так аккуратно как могли раньше, другим проявлением было наличие определенной нервозности, чувства тревоги и раздражительности.

Через 1 год после оперативных вмешательств в основной и группе сравнения, увеличивались средние значения всех показателей качества жизни. В группе О увеличились средние показатели Rp и RE ($p < 0,05$). В основной группе отмечено улучшение всех показателей качества жизни ($p < 0,05$). В группе сравнения увеличились показатели Rp, VT, RE ($p < 0,05$). Средние показатели качества жизни через 1 год после операции представлены в сводной (таблице 1). Увеличение всех показателей здоровья в основной группе характеризует улучшение физического и психического компонента здоровья.

Для дополнительной оценки эстетического результата операций, нами было внедрено в практику проведение собственного анкетирования пациентов, перенесших данные оперативные вмешательства. В ее структуре 3 пункта, первый пункт – это возраст пациента, во втором пункте был определен вид оперативного вмешательства и в соответствии с которой группы исследования принадлежал пациент, и в третьем пункте непосредственно определяли общее удовлетворение результатом операции. Данное анкетирование было анонимным и проводился всем пациентам основной группы и группы сравнения.

Эстетические результаты операции оценивали по 4 балльной шкале, основным критерием выделяли наличие осложнений в раннем и отдаленном периоде после операции. Градация «плохой результат» предусматривала наличие осложнений, требующих дальнейшей хирургической операции для спасения жизни пациента. Если была необходимость в незначительных вмешательствах в раннем послеоперационном периоде для коррекции серьезных послеоперационных осложнений, не угрожали жизни пациента, например гематома, лигатурные свищи, явные выраженные деформации, воспалительные процессы в области рубца, серомы, то считали удовлетворительным результатом. Когда возникала потребность только в эстетическом улучшении результата для пациента, таких как дополнительная липосакция или коррекция «ушек», качества и положения рубца, то относили к хорошему результату. Отличным результатом считали отсутствие потребности в оперативных вмешательствах и результат полностью удовлетворял пациента.

Оценку результата проводили через 1 и 12 месяцев после оперативного вмешательства. В выборке в основной группе из 64 пациентов через 1 месяц после операции результат был следующим: отличный в 58 случаях (90,6%), хороший в 4(6,3%) и удовлетворительное в 2(3,1%) случаях, в данной группе не было ни одного плохого результата. У пациентов с удовлетворительным результатом основной группы развилась у одного пациента гематома, которая требовала эвакуации и у одного пациента серома, которую лечили путем проведения пункции. В группе сравнения среди 68 пациентов отличный результат был в 50 случаях (73,6%), хоро-

ший в 12 (17,6%) и удовлетворительное в 6 (8,8%) случаях, и также не было ни одного плохого результата. При исследовании полученного эстетического результата между двумя группами пациентов в срок 1 месяц после операции, было обнаружено статистически достоверно лучший эстетический результат у пациентов основной группы при значениях $\chi^2 = 6,48$ и $p = 0,039$.

Через 12 месяцев проводили повторное анкетирование и оценка эстетического результата. Полученные данные несколько отличались от первоначальных, получивших через 1 мес после операции. В основной группе у 2 больных с отличным результатом послеоперационный рубец незначительно растянулся к ширине 6 и 7 мм в центральной части, что вызвало недовольство у пациента, и они были переведены в группу с хорошим результатом. Отличный результат был у 56 пациентов (87,5%). У всех пациентов с удовлетворительным результатом было проведено лечение серомы и устранения гематомы в раннем периоде, и они соответственно были перенесены в группу с хорошим результатом, где количество пациентов составляла 8 (12,5%).

В группе сравнения у 17 пациентов с отличным результатом через 12 мес проксимальный кожный лоскут за счет растяжения и птоза, образовывал складку над горизонтальным рубцом, которая создавала косметически неприемлемый результат, у 10 больных, 6 из них имели нависание над рубцом, горизонтальный рубец растянулся к ширине > 1 см, что вызвало недовольство эстетическим результатом, и всего 21 пациент был переведен в группу с хорошим результатом. В группе с отличным результатом осталось 29 пациентов (42,6%). Все пациенты из группы с удовлетворительным результатом были пролечены и в срок через 1 год после операции были переведены в группу с хорошим результатом, где их количество было 39 (57,4%). При исследовании эстетического результата через 1 год после операции выявлено статистически значимую разницу между основной, где результат был лучше, и группой сравнения при значениях $\chi 2 = 27,01$та $p < 0,001$. Исследовав динамику изменения доли пациентов в основной группе через 1 месяц и по сравнению с данными за 1 год, не было выявлено статистически значимых изменений при $\chi^2 = 3,37$ и $p = 0,186$. Зато, в группе сравнения выявлено уменьшение количества пациентов в динамике в течение года с отличным результатом, и преобладание пациентов хорошим эстетическим результатом операции, эти показатели статистически отличались через 1 месяц и один год при значениях $\chi^2 = 25,88$, $p < 0,001$.

Согласно полученным данным, пациентов, которые отлично оценили эстетический результат операции, было больше в основной группе. В группе сравнения через 1 год было выявлено ухудшение эстетического результата операции по сравнению с основной группой пациентов ($p < 0,001$), что связано с формированием кожно-жирового валика над горизонтальным рубцом и других косметических деформаций.

**Вывод**

Липоабдоминопластика – это безопасная комплексная методика выполнения абдоминопластики, которая дает возможность достичь хороших эстетических результатов и атлетических природных контуров тела. В основной группе статистически достоверно улучшилось физическое и психический компонент здоровья (при всех значениях $p < 0,05$), а в группе сравнения, статистически достоверные изменения произошли только для показателя Rp, VT, RE ($p < 0,05$).

Исследовав результаты анкетирования по разработанной нами анкете, определили изменения доли пациентов в основной группе через 1 месяц и по сравнению с данными за 1 год и не было выявлено статистически значимых изменений ($p = 0,186$). В группе сравнения выявлено уменьшение количества пациентов, в динамике в течение года, с отличным результатом и преобладание пациентов с хорошим эстетическим

результатом операции, эти показатели статистически отличались через 1 месяц и один год при значении $p < 0,001$. В конечном итоге пациенты основной группы имеют лучшие контуры тела, когда липосакция одновременно выполняется с абдоминопластика, имеют лучшие показатели качества жизни и удовлетворенности эстетическим результатом.

**Список литературы:**


1. Chow I., Hanwright P. J., Gutowski K. A., et al. Is there a limit? A risk assessment model of liposuction volume on complications in lipoabdominoplasty. Plast Reconstr Surg. 2015.– 136.– P. 92–93.
2. Costa-Ferreira A., Rebelo M., Silva A., et al. Scarpa fascia preservation during abdominoplasty: randomized clinical study of efficacy and safety. Plast Reconstr Surg. 2013.– 131(3).– P. 644–651. DOI: http://dx.doi.org/10.1097/PRS.0b013e31827c704b.
3. Costa-Ferreira A., Rebelo M., Vasconez L. O., et al. Scarpa fascia preservation during abdominoplasty: a prospective study. Plast Reconstr Surg 2010.– 125.– P. 1232–1239.
4. International Society of Aesthetic Plastic Surgery. The International Survey on Aesthetic/Cosmetic Procedures Performed in 2017. URL: http://www.isaps.org/news/isaps-global-statistics. Accessed 2018.
5. Lockwood T. E. Maximizing aesthetics in lateral-tension abdominoplasty and body lifts. Clin Plast Surg. 2004.– 31.– P. 523–537.
6. Regnault P. The history of abdominal dermolipectomy. Aesthetic Plast Surg. 1978.– 2.– P. 113–123.
7. Saldanha O. R., Federico R., Daher P. F., et al. Lipoabdominoplasty. Plast Reconstr Surg. 2009.– 124(3).– P. 934–942. PMID: 19730314. DOI: http://dx.doi.org/10.1097/PRS.0b013e3181b037e3.
8. Saldanha O. R., Pinto E. B.S., Matos Jr. W. N., et al. Lipoabdominoplastia – Técnica Saldanha. Rev Bras Cir Plást. 2003.– 18(1).– P. 37–46.
9. Shestak K. C., Walgenbach K. J., Azari K. Marriage: Abdominoplasty and short scar technique. Aesth Surg J. 2002.– 22.– P. 294–301.
10. Wall S. H. Jr, Lee M. R. Separation, aspiration, and fat equalization: SAFE liposuction concepts for comprehensive body contouring. Plast Reconstr Surg. 2016.– 138.– P. 1192–1201.
11. Панчук та О. В. ін. Ліпоабдомінопластика – комплексний метод корекції дефектів передньої черевної стінки// Art of Medicine. 2019.– № 1(9).– С. 105–110. [Panchuk OV, et al. Lipoabdominoplasty – complex method of correction of the anterior abdominal wall defects. Art of Medicine. 2019.– № 1(9).– P. 105–110. (In Ukr).]. DOI: https://doi.org/10.21802/artm.2019.1.9.105.
12. Панчук О. В., Мішалов В. Г., Лещишин І. М., та ін. Місце допплерівської флоуметрії у визначенні та оцінці характеристик кровотоку в судинах передньої черевної стінки при проведенні ліпоабдомінопластики. Серце і судини. 2018.– № 4.– С. 40–44. [O. V. Panchuk, V. H. Mishalov, I. M. Leshchyshyn, et al. Doppler flowmetry in the determination and evaluation of blood flow characteristics in the anterior abdominal wall vessels during lipoabdominoplasty. Blood and vessels. 2018.– № 4.– P. 40–44. (In Ukr).] DOI: https://doi.org/10.3978/HV2018–4–40.

**https://doi.org/10.29013/ELBLS-21-1.2-20-23**

*Lezhenko Hennadii Olexandrovych*
*Zaporizhzhia State Medical University*
*MD, PhD, DSc, Head of the Hospital Pediatrics Department*
*E-mail: genalezh@gmail.com*
*Pogribna Anastasiia Olexandrivna,*
*Zaporizhzhia State Medical University*
*PhD-Student, Hospital Pediatrics Department*
*Zaporozhye, Ukraine*
*E-mail: a.pogrebnaia@gmail.com*

# INFLUENCE OF VITAMIN D STATUS ON THE SEVERITY OF ANEMIA OF INFLAMMATION IN YOUNG CHILDREN WITH ACUTE INFLAMMATORY BACTERIAL RESPIRATORY DISEASES

**Abstract.** We have studied the effect of vitamin D status on the severity of anemia of inflammation in young children with acute inflammatory bacterial respiratory diseases. Some indicators of iron metabolism were analyzed depending on the level of vitamin D in the blood serum in the understanding the development of anemia of inflammation.

**Keywords:** anemia of inflammation, vitamin D, erythropoietin, ferritin, young children.

Due to the expansion of researches on the extraskeletal functions of vitamin D, its potential role in iron homeostasis and erythropoiesis has been described. An increase in pro-inflammatory cytokines suppresses erythropoiesis in the bone marrow and shortens the life span of erythrocytes due to increased activation of macrophages and erythrophagocytosis in anemia of inflammation (AI). A decrease in proinflammatory cytokines and, as a consequence, hepcidin caused by the influence of vitamin D can increase the bioavailability of iron for erythropoiesis and hemoglobin synthesis by restoring iron recirculation, preventing iron sequestration in macrophages, eliminating disorders of iron absorption, thereby preventing the development of AI. On the other side, inflammatory cytokines can disrupt erythropoiesis by suppressing the production of erythropoietin (EPO), as well as the differentiation and proliferation of erythroid progenitor cells [1, 1011–1023]. However, vitamin D supports erythropoiesis by increasing the proliferation of erythroid precursors and a synergistic effect with EPO [2, 403–409; 3, 121–127; 4, 432–438; 5, 1672–1679]. Previous studies suggest that an additional pleiotropic benefit of vitamin D supplementation may be to reduce the severity of anemia and increase sensitivity to EPO [6, 447–452].

**Aim.** To determine the relationship between the level of vitamin D in the blood serum and the severity of AI in young children with acute inflammatory bacterial diseases of the respiratory system.

**Materials and methods.** A total of 40 children aged between 1 month and 3 years (with an average age of 1,6 ± 0.4 years) were examined. The main group consisted of 20 children with acute bacterial diseases of the respiratory tract. In the main group, bronchitis was diagnosed in 14(70%) children, pneumonia – in 6(30%) children. Given the hematological picture, the main group was divided into two subgroups. The first subgroup included

10 children with AI, which was determined 4–5 days after the disease onset. The second subgroup consisted of 10 children without anemia. The comparison group was represented by 10 children with iron deficiency anemia (IDA) without inflammatory manifestations. The control group included 10 conditionally healthy children. The studied groups were representative in age and sex of the children. All study patients on a planned basis received a vitamin D3 supplement according to clinical guidelines.

The content of vitamin D in the blood serum of children of the observation group was determined. It was established that the level of 25(OH)$D_3$ ≤ 30 ng/ml was observed in the first subgroup in 4(40%) children, in the second subgroup – in 5(50%) children, in the comparison group – in 3(30%) children. In the control group, there was no evidence of vitamin D deficiency. The level of 25(OH)$D_3$ 30–45 ng/ml was found in the first subgroup in 5(50%) children, in the second subgroup in 4(40%) children, in the comparison group – in 6(60%) children, in the control group – in 6(60%) children. The level of 25(OH)$D_3$ ≥ 45 ng/ml was detected in the first, second subgroup, as well as in the comparison group in 1(10%) child, in the control group – in 4(40%) children.

Blood serum 25(OH)$D_3$, erythropoietin, and ferritin levels were measured by enzyme-linked immunosorbent assay (ELISA) using commercial kits: 25OH Vitamin D Total ELISA (DIAsourceImmunoAssays S.A., Belgium), EPO (Erythropoietin) ELISA (Biomerica, Germany), Ferritin ELISA (ORGENTEC DiagnostikaGmbH, Germany).

Statistical analysis of the data was performed using the statistical packages «EXCEL» and "Statistica 13.0" (StatSoft Inc. No. JPZ8041382130ARCN10-J). Normality of the data was checked using the Shapiro-Wilk test. We used the method of correlation analysis with the Spearman correlation coefficient calculation**.** Measurement data of a non-normal distribution and non-linear dependence were expressed as a median and quartile (Me (Q25; Q75)). To assess the differences in indicators, the nonparametric Mann-Whitney U-test was calculated as a nonparametric analogue of the Student criterion. Differences were considered at a significance level of $p < 0,05$.

All procedures performed in studies involving human participants were in accordance with the Ethical Standards of the Institutional and National Research Committee and with the 1964 Declaration of Helsinki and its later amendments or comparable ethical standards. An informed consent was obtained from all individual participants included in the study. The full data set of children, their parents, and physician that support the findings of this study were not publicly available due to the restrictions of the ethics approval originally obtained.

**Results.** In this study, we determined the change in markers of iron metabolism in the observation groups depending on the level of vitamin D in the blood serum. We have previously described the hematological picture in study patients [7, 473–478].

At a level of 25(OH)$D_3$≤30 ng/ml in the first subgroup moderate and mild anemia was observed with a hemoglobin content of 95(87; 106) g/L. With an increase in the content of 25(OH)$D_3$ in the blood serum of children with AI there was a tendency to an increase in the hemoglobin level, and the anemia was characterized by a mild severity: at a 25(OH)$D_3$ level of 30–45 ng/ml hemoglobin was 106(100; 109) g/L. Only in 1 patient from the first subgroup the 25(OH)$D_3$ content exceeded 45 ng/ml, while the hemoglobin index was 107 g/L, which is 1,3 times ($p<0,05$) higher than the indicators of the first quartile of the hemoglobin level detected at 25(OH)$D_3$ level ≤30 ng/ml. A similar clinical picture was observed in the comparison group: with vitamin D deficiency, the hemoglobin level was 96,5 (95; 106) g/l, with 25(OH)$D_3$ 30–45 ng/ml – 107 (96,5; 109) g/L, and only in one case 25(OH)$D_3$≥45 ng/ml, while the hemoglobin content was limited to 106 g/L. In the second subgroup, a tendency towards an increase in the hemoglobin level was also revealed, proportional to the increase in the 25(OH)$D_3$ content. At a level of 25(OH)$D_3$ ≥45 ng/ml, the hemoglobin content

reached 136 g/L, while with a level of vitamin D provision in the range of 30–45 ng/ml, the hemoglobin index was 119 (110; 129,5) g/L, at $25(OH)D_3 \leq$ ≤ 30 ng/ml – 113 (110; 129) g/L. In the control group there was no deficiency in the provision of vitamin D.

The data on the EPO level in the blood serum of the studied patients are quite indicative. Thus, in the first subgroup, the EPO level at $25(OH)D_3 \geq 45$ ng/ml was 1,8 times higher than its content at $25(OH)D_3 \leq 30$ ng/ml and 1,5 times higher at $25(OH)D_3$ 30–45 ng/ml (6,8 ng/ml versus 3,85 (3,5; 5,75) ng/ml and 4,5 (4,2; 4,5) ng/ml, respectively, $p<0.05$). 1,5 times the EPO content at $25(OH)D_3 \geq 45$ ng/ml its level at $25(OH)D_3 \leq 30$–45 ng/ml in the second subgroup (6,53 ng/ml, 4,35 (3,3; 4,5) ng/ml and 4,5 (4,35; 5,75) ng/ml, respectively, $p<0.05$) and the comparison group (27,0 ng/ml, 23,5(20,5; 29,5)ng/ml and 18,0 (14,0; 20,5) ng/ml, $p<0.05$).

In the first subgroup the ferritin content at $25(OH)D_3 \leq 30$ ng/ml was 1,3 times higher than its content in the groups of children with a sufficient level of vitamin D provision (63,0(48,0; 78,0) ng/ml, 47,75 (38,0; 55,0) ng/ml, 48 ng/ml, respectively, $p <0,05$). The tendency to its increase at $25(OH)D_3 \leq 30$ ng/ml was also observed in the second group (52,0 (45,0; 68,0) ng/ml, 47,7 (34,0; 50,2) ng/ml and 45 ng/ml, $p>0,05$). In the comparison group the ferritin level at $25(OH)D_3 \leq 30$ ng/ml was 2 times higher than its values at the content of vitamin $25(OH)D_3 \geq 45$ ng/ml (48,0 (43,5; 50,0) ng/ml, 23 ng/ml, $p<0.05$), and at $25(OH)D_3 \leq$ ≤ 30–45 ng/ml, there was a tendency to its decrease (39,8 (33,0; 47,5) ng/ml, $p<0.05$).

We revealed a weakening of correlations with an insufficient level of vitamin D. Thus, at $25(OH)D_3 \leq 30$ ng/ml, a weak inverse correlation was noted between it and ferritin ($r= –0,12$, $p<0,05$), and a moderate straight correlation – with hemoglobin ($r =0,31$, $p <0,05$) and EPO ($r =0,3$, $p <0,05$). At the same time, at $25(OH)D_3 >30$ ng/ml, a moderate inverse correlation was observed between it and ferritin ($r= –0,36$, $p<0,05$), and a moderate straight correlation – with hemoglobin ($r=0,6$, $p<0,05$) and EPO ($r=0,5$, $p<0,05$).

**Discussion.** In the course of this study, we examined the potential relationship between vitamin D status and the corresponding dynamics of some indicators of iron metabolism. We noted a statistically significant decrease in hemoglobin concentration proportional to an increase in vitamin D deficiency. This suggests that vitamin D deficiency may be a potential risk factor for the development of AI. In support of our hypothesis there is evidence from studies that described an investigative relationship between $25(OH)D_3$ and $1,25(OH)_2D_3$ deficiency and the prevalence of anemia [8, 715–720; 9, 564–572]. Determination of a positive correlation relationship between the concentrations of hemoglobin and erythropoietin with vitamin D in the blood serum probably indicates a protective role of vitamin D against erythropoietic disorders. Icardi A. et al. (2013) described the inverse relationship between $25(OH)D_3$ status and EPO [8, 715–720], which can be explained by the involvement of the reticuloendothelial system in the implementation of the immune defense reaction, due to which the synthesis of hepcidin increases with a decrease in the availability of iron, which will naturally lead to resistance to EPO and the development of anemia [5, 1672–1679]. The dynamics of ferritin value depending on the vitamin D status suggests that the need for iron sequestration as a protective reaction is inversely proportional to the protective function carried out by vitamin D, which may indicate ineffective erythropoiesis in patients with insufficient $25(OH)D_3$ provision. Another possible mechanism is that vitamin D directly stimulates erythroid precursors. Thus, it was studied that an increase in the concentration of $25(OH)D_3$ reduces the expression of ferritin mRNA, and immunohistochemical analysis of the ferritin protein confirmed that the effect of $25(OH)D_3$ also leads to a decrease in the expression of the protein itself [9, 564–572; 10, 1650–1658]. Based on the data presented in this study, we hypothesize that vitamin D metabolites are likely to maintain the expression of ferroportin in

the membrane, and its loss is associated with intracellular iron deposition through ferritin, which, in turn, leads to AI of the iron-redistribution genesis. This is of direct importance for the control of systemic homeostasis. In this situation, the functioning of vitamin D, aimed at protecting adequate erythropoiesis, is consistent with its intracellular antibacterial activity. The mechanisms described above support our hypothesis that low vitamin D status may be a contributing factor to AI. At the same time, the active form of vitamin D can affect erythropoiesis by stimulating the proliferation and maturation of erythroid progenitor cells, and this may explain the positive effect of vitamin D in reducing the severity of AI.

Thus, according to the results of the study, it can be argued that the severity of the course of anemia of inflammation is determined by the level of vitamin D deficiency, which is apparently due to its effect on erythropoiesis due to sensitivity to EPO and possible indirect effects on ferritin synthesis.

## References


1. Guenter Weiss, Lawrence T. Goodnough. N Engl J Med: Anemia of chronic disease,– Vol. 352.– Issue 10, 2005. Doi: 10.1056/NEJMra041809.
2. Dora Ben Alon, Cidio Chaimovitz, Alexander Dvilansky, Gilles Lugassy, Amos Douvdevani, Shraga Shany, Ilana Nathan. Exp Hematol: Novel role of 1,25(OH)(2) D(3) in induction of erythroid progenitor cell proliferation,– Vol. 30.– Issue 5. Doi: 10.1016/s0301–472x(02)00789–0.
3. Filippo Aucella, Rosario Potito Scalzulli, Giuseppe Gatta, Mimmo Vigilante, Angelo Michele Carella, Carmine Stallone. Nephron Clin Pract: Calcitriol increases burst-forming unit-erythroid proliferation in chronic renal failure. A synergistic effect with r-HuEpo,– Vol. 95.– Issue 4. 2003. Doi: 10.1159/000074837.
4. Ellen M. Smith Vin Tangpricha. Curr Opin Endocrinol Diabetes Obes: Vitamin D and anemia: insights into an emerging association,– Vol. 22.– Issue 6. 2015. Doi: 10.1097/MED.0000000000000199.
5. Andrea Icardi, Ernesto Paoletti, Luca De Nicola, Sandro Mazzaferro, Roberto Russo, Mario Cozzolino. Nephrol Dial Transplant: Renal anaemia and EPO hyporesponsiveness associated with vitamin D deficiency: the potential role of inflammation,– Vol. 28.– Issue 7. 2013. Doi: 10.1093/ndt/gft021.
6. John J. Sim Peter T. Lac, In Lu A. Liu Samuel O. Meguerditchian, Victoria A. Kumar, Dean A. Kujubu, Scott A. Rasgon. Ann Hematol: Vitamin D deficiency and anemia: a cross-sectional study,– Vol. 89.– Issue 5. 2010. Doi: 10.1007/s00277–009–0850–3.
7. Hennadii Lezhenko, Anastasiia Pogribna. Zaporozhye medical journal: The role of hepcidin in the pathogenetic mechanisms of anemia of inflammation development in young children with acute inflammatory bacterial diseases of the respiratory system,– Vol. 22.– Issue 4. 2020. Doi: 10.14739/2310–1210.2020.4.208356.
8. Neha M. Patel Orlando M. Gutiérrez, Dennis L. Andress, Daniel W. Coyne, Adeera Levin, Myles Wolf. Kidney Int: Vitamin D deficiency and anemia in early chronic kidney disease,– Vol. 77.– Issue 8. 2010. Doi: 10.1038/ki.2009.551.
9. Justine Bacchetta, Joshua J. Zaritsky, Jessica L. Sea, Rene F. Chun, Thomas S. Lisse, Kathryn Zavala, Anjali Nayak, Katherine Wesseling-Perry, Mark Westerman, Bruce W. Hollis, Isidro B. Salusky and Martin Hewison. JASN: Suppression of Iron-Regulatory Hepcidin by Vitamin D,– Vol. 25.– Issue 3. 2014. URL: https://doi.org/10.1681/ASN.2013040355.
10. Sana Syed, Ellen S. Michalski, Vin Tangpricha, Supavit Chesdachai, Archana Kumar, Jarod Prince, Thomas R. Ziegler, Parminder S. Suchdev, Subra Kugathasan. Inflammatory Bowel Diseases: Vitamin D Status Is Associated with Hepcidin and Hemoglobin Concentrations in Children with Inflammatory Bowel Disease,– Vol. 23.– Issue 9. 2017. Doi.org/10.1097/MIB.0000000000001178.

**https://doi.org/10.29013/ELBLS-21-1.2-24-33**

*Tang Diane,*
*YK Pao School, Shanghai, China*
*E-mail: 2928599264@qq.com; xxjnicole@hotmail.com*

# HEART DISEASE PREDICTION WITH LOGISTIC REGRESSION AND RANDOM FOREST MODEL

**Abstract:** Heart disease is the leading cause of death for men, women, and people of most racial and ethnic groups in the United States. (Centers for Disease Control and Prevention, 2018) [3]. The early prognosis of CVDs can inspire better lifestyle choices among high-risk patients and in turn reduce the risk of CVD. This research aims to pinpoint the most relevant/risk factors of heart disease and to build a predictive model for the overall risk of heart disease using logistic regression and compare its performance to the random forest model with hyperparameter tuning. Due to the imbalance of the data and the nature of this study, the Average Precision score, the Recall score, and the area under Receiver Operating Characteristic curve are all important metrics. The Synthetic Minority Oversampling Technique (Smote) method with the logistic regression model performed the best among the various techniques implemented in this study.

**Keywords:** heart disease, logistic regression, random forest, hyperparameter tuning.

## 1. Introduction

Cardiovascular diseases (CVDs) are a group of disorders of the heart and blood vessels. Coronary heart disease (CHD) is the most common type of CVD. World Health Organization has estimated 17.9 million people died from CVDs in 2016, representing 31% of all global deaths. Of these deaths, 85% are due to heart attack and stroke (World Health Organization [15]).

Heart disease is the leading cause of death for men, women, and people of most racial and ethnic groups in the United States (Centers for Disease Control and Prevention, 2018) [3].

Coronary heart disease (CHD) is the most common type of heart disease, killing 365,914 people in 2017 (Benjamin E.J. [2]). About 655,000 Americans die from heart disease each year – that's 1 in every 4 deaths (Virani S. S. [13]).

The early prognosis of CVDs can inspire better lifestyle choices among high-risk patients and in turn reduce the risk of CVD.

## 2. Exploratory Data Analysis and Data Preprocessing

The dataset used in this study is from an ongoing cardiovascular study on residents of the town of Framingham, Massachusetts (Framingham heart study, n.d.) [4]. The dataset includes 4,238 records and 16 columns. Each of the 15 feature variables is a potential risk factor. There are both demographic, behavioral and medical risk factors.

The histogram plot of the 16 variables is shown in (figure 1). All columns are already numerical and one hot encoding is not needed. From figure 1, BPM eds, current Smoker, diabetes, male, prevalent Hyp, prevalent Stroke, and Ten Year CHD are binary, 0 represents negative cases and 1 represents positive cases.

The classification variable (Ten Year CHD) is the patients' 10-year risk of coronary heart disease (CHD). A count plot of the classification variable made using Seaborn is shown in figure 2. (Seaborn Countplot, n.d.) [11; 12]. Count plot shows the counts of observations in each categorical bin using

bars. From (figure 2) we can see the classification variable is imbalanced which could cause a classification model to over-favor predictions of the class or classes with the overwhelming majority of the data, crippling the model's ability to classify others with the small minority.

Table 1.– Feature variables in the dataset

| | Feature variables | Description | Data type |
|---|---|---|---|
| Demographic | Sex | Male or female | Nominal |
| | Age | Age of the patient | Continuous |
| | Education | Education level of the patient | Continuous |
| Behavioral | Current smoker | Whether or not the patient is a current smoker | Nominal |
| | Cigs per day | The number of cigarettes that the person smoked on average in one day | Continuous |
| Medical (history) | BP Meds | Whether or not the patient was on blood pressure medication | Nominal |
| | Prevalent stroke | Whether or not the patient had previously had a stroke | Nominal |
| | Prevalent Hyp | Whether or not the patient was hypertensive | Nominal |
| | Diabetes | Whether or not the patient had diabetes | Nominal |
| Medical (current) | Tot Chol | Total cholesterol level | Continuous |
| | Sys BP | Systolic blood pressure | Continuous |
| | Dia BP | Diastolic blood pressure | Continuous |
| | BMI | Body Mass Index | Continuous |
| | Heart Rate | Heart rate | Continuous |
| | Glucose | Glucose Level | Continuous |

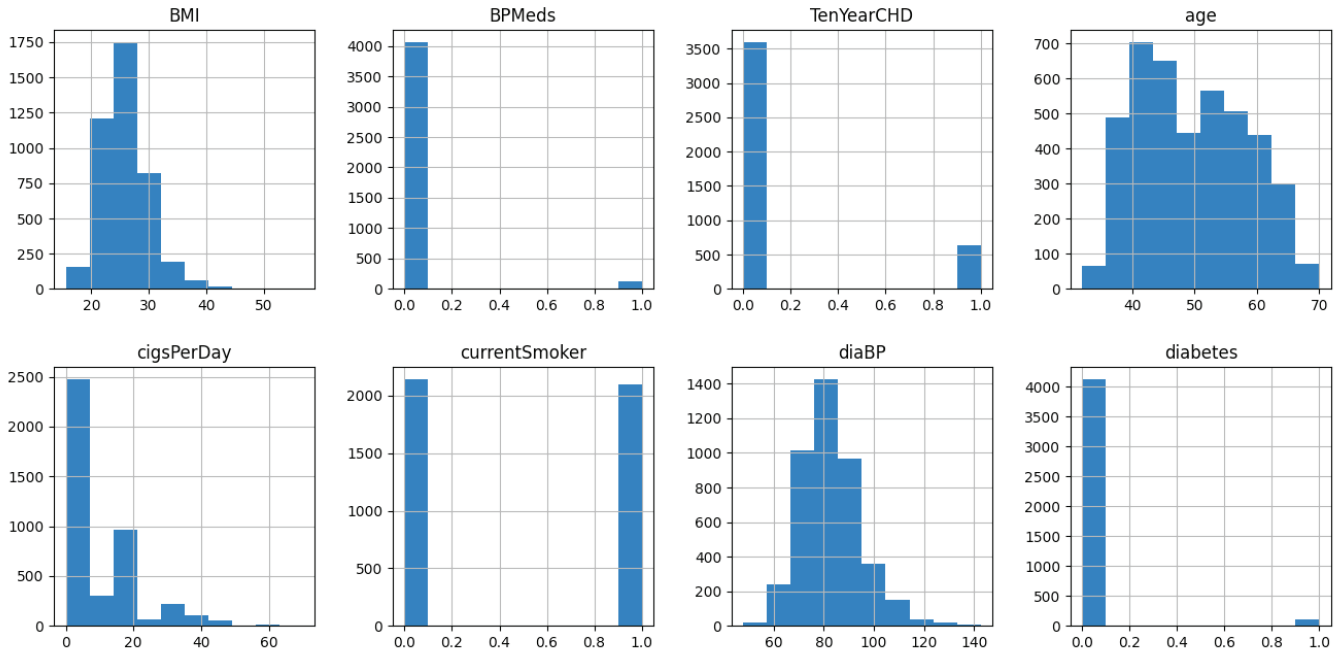

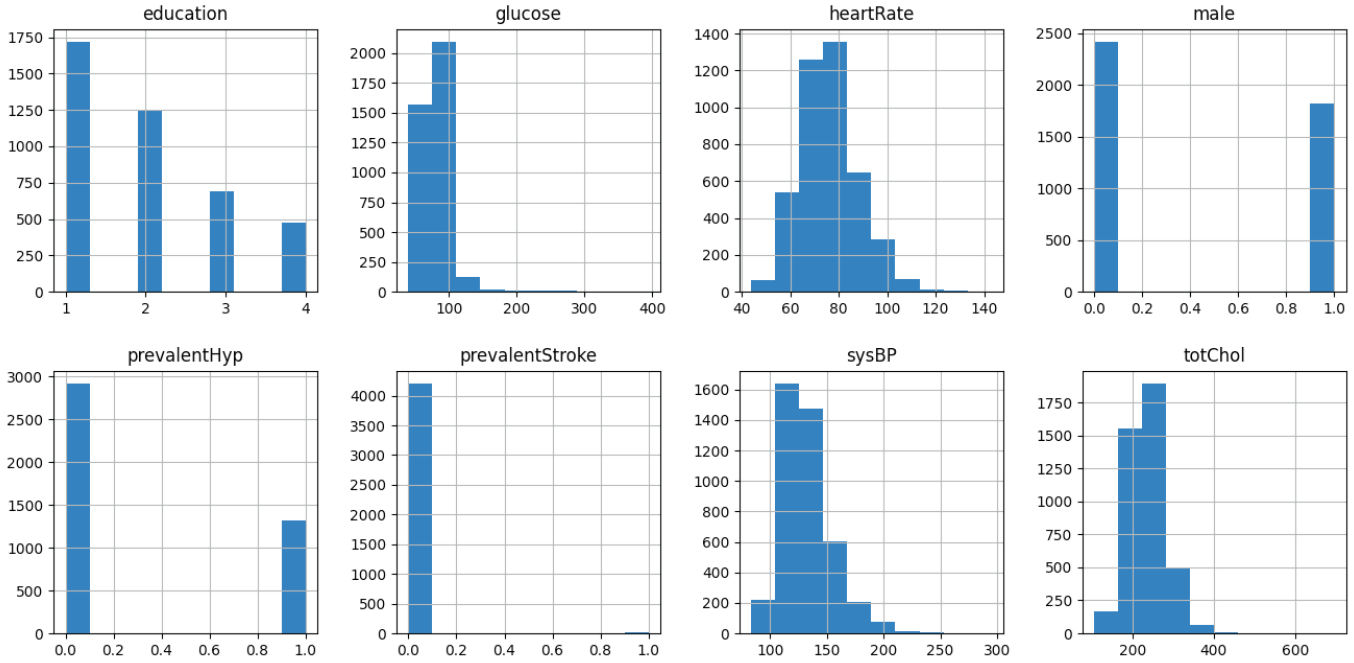


Figure 1. Histogram plot of feature variables

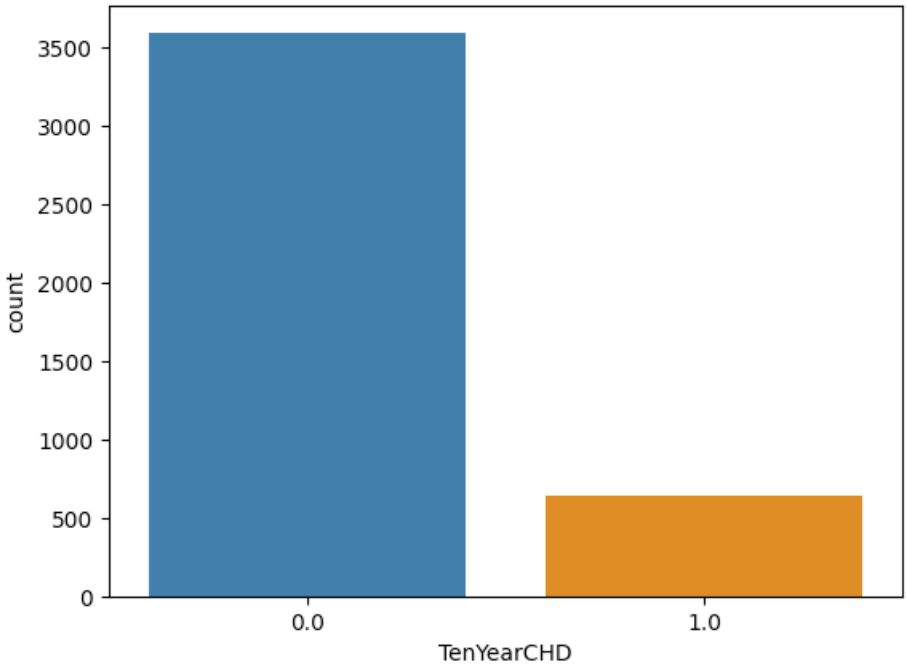


Figure 2. Count plot of classification variable (0 means the patient won't have CHD in ten years, 1 means the patient will have CHD in ten years)

Figure 3 presents the distribution plots of the 15 feature variables, color coded by the outcome variable (Ten Year CHD). Blue curves in each subplot represent the variable's distribution with the outcome variable being negative and red curves represent the variable's distribution with the outcome variable being positive. The distribution plot made by the Seaborn library combines the matplotlib histogram function with the Seaborn kernel density estimate (KDE) plot and rugplot (marginal distributions) functions.

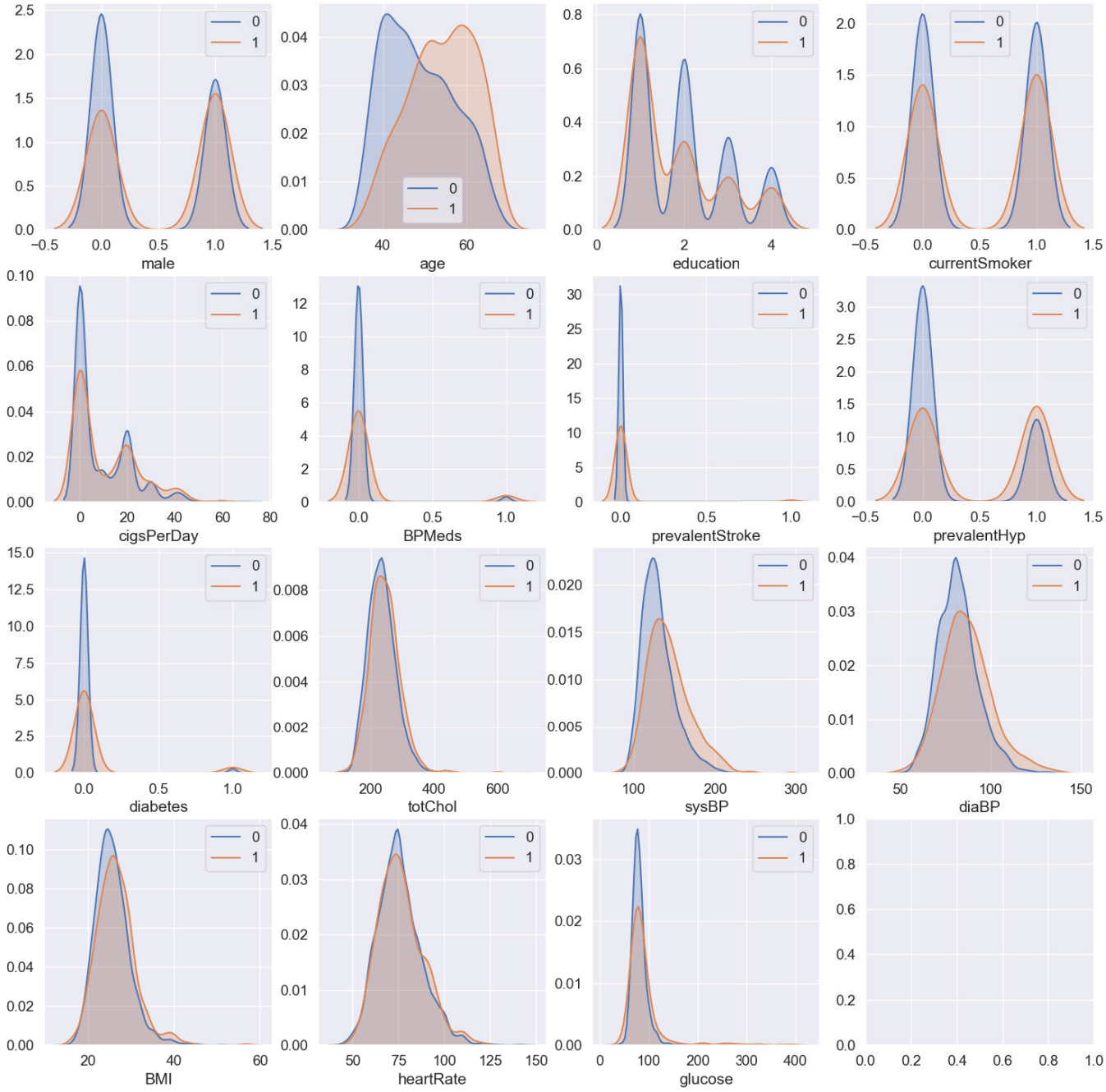


Figure 3. Distribution plot of 15 feature variables, colored by the classification variable ("Ten Year CHD"), blue curves

(Seaborn distplot, n.d.) The x-axis shows bins (ranges) of the variable and the y-axis is the probability density function for the kernel density estimation. The total area of each density plot is 1. From (figure 3), males, older people, less educated, smokers, all have higher probabilities of having CHD.

Missing values in the dataset have been imputed using K Nearest Neighbors (KNN) imputer function from Scikit-learn. Scikit-learn is a Python module integrating a wide range of state-of-the-art machine learning algorithms for medium-scale supervised and unsupervised problems (Pedregosa [10]). This imputer replaces the missing values with the mean value

from k nearest neighbors found in the dataset. By default, it uses a Euclidean distance metric to impute the missing values (KNN imputation, n.d.) [7].

MinMax Scaler from Scikit-learn was used to center the variables and bring them to the same scale to ensure the proper performance of the machine models. After standardization, the data was separated into two groups using Train_test_split function from Scikit-learn: the training sample with 80% of the data and the testing sample with 20%. The train set would be used to train the model, and the test set would be used to test the accuracy and performance of the model.

**3. Models and Results**

***3.1 Logistic Regression Model***

The first model trained by the train set was the logistic regression model implemented from Scikit-learn. Since the classification variable is categorical and binary, binomial logistic regression is a natural first step. It is based on sigmoid function where output is a probability. The key argument "class_weight" was set to be balanced to compensate for the imbalanced dataset. The classification report, confusion matrix, cross validated roc_auc score and average precision score were calculated, and the precision recall curve was shown in figure 4. The cross validated roc_auc score and aps score for the logistic regression are: 0.725 and 0.3448.

Table 2 shows the classification report of the logistic regression model. The classification report shows the main performance metrics of the machine learning model in predicting each class, including the precision, recall, f1-score, their macro and weighted averages, their counts, and the overall accuracy. (Kohli [8]). Table 3 shows the confusion matrix of the logistic regression model. A confusion matrix presents the count of the true positives, false positives, true negatives, and false negatives of each class.

Table 2. – Logistic regression base model classification report

| Class | Precision | Recall | F1-score | Support |
|---|---|---|---|---|
| 0.0 | 0.93 | 0.67 | 0.78 | 733 |
| 1.0 | 0.25 | 0.70 | 0.37 | 115 |
| | | | | |
| Accuracy | | | 0.68 | 848 |
| **Macro avg** | 0.59 | 0.68 | 0.57 | 848 |
| **Weighted avg** | 0.84 | 0.68 | 0.73 | 848 |

Table 3. – Logistic regression base model confusion matrix

| | |
|---|---|
| True Positive (**TP**) 493 | False Positive (**FP**) 240 |
| False Negative (**FN**) 35 | True Negative (**TN**) 80 |

⇒ TP: positive samples predicted as positive.

⇒ Accuracy – Percentage of true/correct predictions: $\frac{TP + TN}{TP + FP + TN + FN}$

⇒ Precision – Percentage of correctly predicted positive predictions: $\frac{TP}{TP + FP}$

⇒ Recall (Sensitivity / True Positive Rate) – Percentage of the positive cases that were predicted true: $\frac{TP}{TP + FN}$

⇒ F1-score – Harmonic mean of precision and recall: $\frac{2}{\frac{1}{precision} + \frac{1}{recall}} = \frac{2 * precision * recall}{precision + recall}$

⇒ Specificity (1 – False Positive Rate) – Percentage of the negative cases that were predicted true: $\frac{TN}{TN + FP}$

⇒ 'macro avg' – Unweighted average of each metric.

⇒ 'weighted avg' – Weighted average of each metric. This accounted for class imbalance.

Accuracy is a great measure but only when you have symmetric datasets (false negatives & false positives counts are close), also, false negatives & false positives have similar costs. F1 is best if you have

an uneven class distribution and if the cost of false positives and false negatives are different. Precision is how sure you are of your true positives whilst recall is how sure you are that you are not missing any positives (Ghoneim [5]).

In the case of predicting heart disease risks, false positives are far better than false negatives, so Recall is an important metric in this study. For a model of which the purpose is to predict illness, leaving a higher risk person labeled healthy is far less desirable than getting some healthy people labeled positive for the illness.

Cross-validation is a model validation method that tests whether the model is overfitted to the specific training and testing samples, which could result in bad performance with any other dataset that the model has not seen yet (Shaikh [3]).

Figure 4 shows the precision-recall curve which focuses mainly on the performance of the positive class which is crucial when dealing with imbalanced classes. In the PR space, the goal is to be in the upper-right-hand corner – the top right corner (1, 1) means that we classified all positives as positive (Recall=1) and that everything we are classifying as positive is true positive (Precision=1) – the latter translates to zero False Positives (Azevedo, n.d.) [1]. Average Precision Score is basically the "area under curve" of Precison-Recall curve.

Using both roc_auc and average_precision_ score to evaluate the model. roc_auc is the area under curve for ROC curve. The ROC curve is plotted with TPR (True Positive Rate / Recall / Sensitivity) against the FPR (False Positive Rate / 1-Specificity) where TPR is on y-axis and FPR is on the x-axis. Roc_auc ranges from 0 to 1, 1 means the model has excellent performance where the positive and negative cases are perfectly distinguishable.

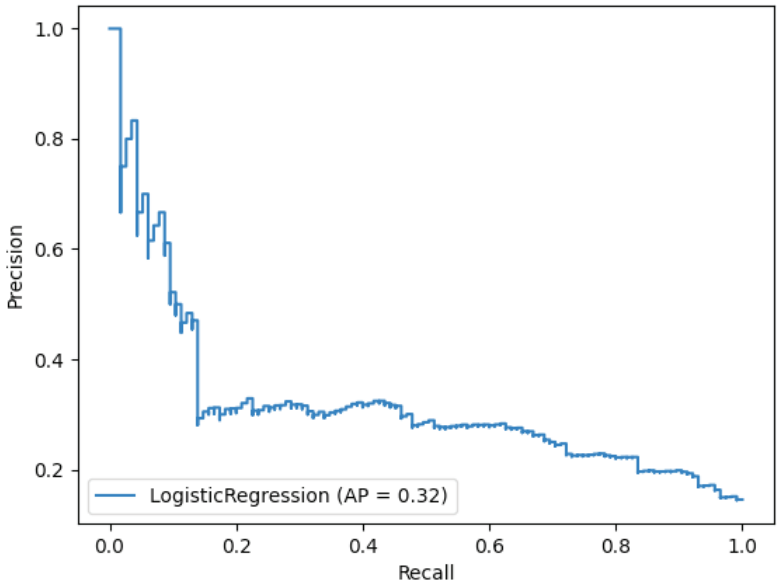


Figure 4. Precision Recall curve

### *3.2 Logistic Regression Hyperparameter Turning*

Grid search is an approach to parameter tuning that will methodically build and evaluate a model for each combination of algorithm parameters specified in a grid. Grid Search CV from Scikit-learn will try all combinations of those parameters, evaluate the results using cross-validation, and the scoring metric provided. In the end, it will output the best parameters for the dataset. It will work both for regression and classification machine learning algorithms.

Grid search tunes hyperparameter C in logistic regression model and the best C is 0.4. The resulting model's classification report and confusion matrix are shown in table 2 and 3. The cross validated roc_auc score and aps score are 0.7256 and 0.352136.

Table 4. – Logistic regression after Grid Search CV classification report

| Class | Precision | Recall | F1-score | Support |
|---|---|---|---|---|
| 0.0 | 0.94 | 0.67 | 0.78 | 733 |
| 1.0 | 0.25 | 0.71 | 0.37 | 115 |
| | | | | |
| Accuracy | | | 0.67 | 848 |
| Macro avg | 0.59 | 0.69 | 0.58 | 848 |
| Weighted avg | 0.84 | 0.67 | 0.72 | 848 |

Table 5. – Logistic regression after GridSearchCV confusion matrix

| | |
|---|---|
| TP 489 | FP 244 |
| FN33 | TN82 |

### *3.3 Logistic Regression Imbalance Sampling*

Synthetic Minority Oversampling Technique (Smote) is an approach to the construction of classifiers from imbalanced datasets (Chawla N. V., [9]). Smote works by utilizing a k-nearest neighbor algorithm to create synthetic data. Smote first start by choosing random data from the minority class, then the k-nearest neighbors from the data are set (Wijaya, n.d.) [14]. Synthetic data would then be made between the random data and the randomly selected k-nearest neighbor. In this case, SMOTE is imported from the imbalanced-learn API. (imbalanced-learn API, n.d.) It'll create synthetic positive cases to match the number of negative cases in the dataset. The resulting model's classification report is shown in (table 4). Cross validated roc_auc score and aps score are 0.7284 and 0.7073. The aps score improved significantly.

Table 6. – Logistic regression (SMOTE) classification report

| Class | Precision | Recall | F1-score | Support |
|---|---|---|---|---|
| 0.0 | 0.93 | 0.67 | 0.78 | 733 |
| 1.0 | 0.25 | 0.70 | 0.37 | 115 |
| | | | | |
| Accuracy | | | 0.67 | 848 |
| Macro avg | 0.59 | 0.69 | 0.57 | 848 |
| Weighted avg | 0.84 | 0.67 | 0.72 | 848 |

Another strategy was to resample the minority cases (y=1) to match majority cases (y=0) with Scikit-learn's resample function. The resulting classification report is shown in table 5. Cross validated roc_auc score and aps score did not improve.

Table 7. – Logistic regression (resample) classification report

| Class | Precision | Recall | F1-score | Support |
|---|---|---|---|---|
| 0.0 | 0.94 | 0.67 | 0.78 | 733 |
| 1.0 | 0.25 | 0.70 | 0.37 | 115 |
| | | | | |
| Accuracy | | | 0.68 | 848 |
| Macro avg | 0.59 | 0.69 | 0.58 | 848 |
| Weighted avg | 0.84 | 0.68 | 0.73 | 848 |

### *3.4 Random Forest Model*

Random forest is an ensemble learning method which consists of a large number of individual decision trees that operate as an ensemble. Each individual tree in the random forest outputs a class prediction and the class with the most votes becomes the model's prediction shown in figure 5 (Yiu, [16]). The idea behind ensemble learning is that a large number of relatively uncorrelated models operating as a committee will outperform any of the individual constituent models.

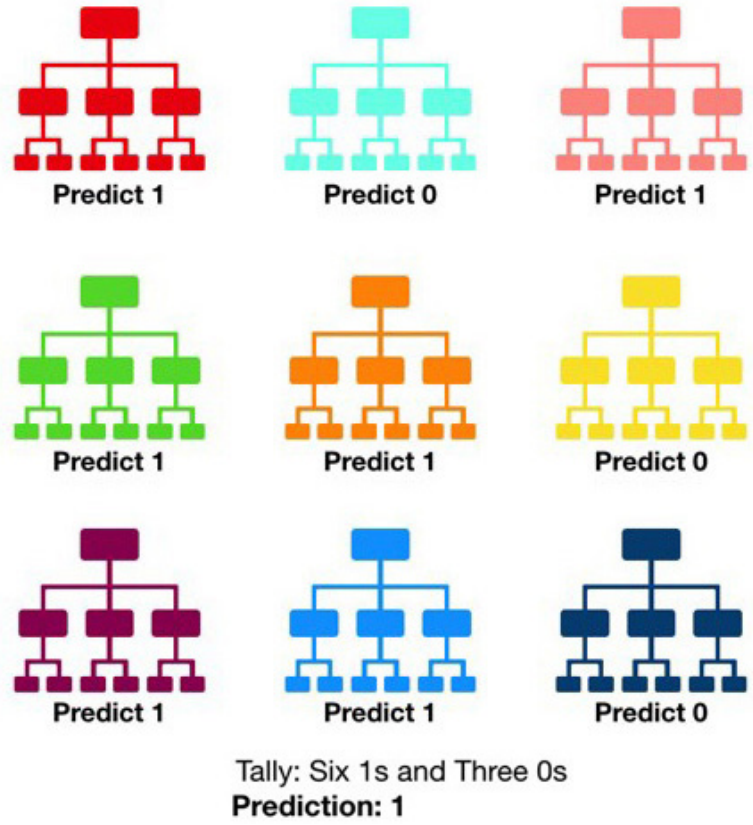


Figure 5. Visualization of a random forest model making a prediction (Yiu, [16])

The resulting classification report is shown in (table 6). Cross validated roc_auc and aps scores are 0.689 and 0.297 which are not higher than logistic regression.

Table 6.– Random forest base model classification report

| Class | Precision | Recall | F1-score | Support |
|---|---|---|---|---|
| 0.0 | 0.87 | 0.99 | 0.93 | 733 |
| 1.0 | 0.60 | 0.08 | 0.14 | 115 |
| | | | | |
| Accuracy | | | 0.87 | 848 |
| Macro avg | 0.74 | 0.54 | 0.53 | 848 |
| Weighted avg | 0.84 | 0.87 | 0.82 | 848 |

### *3.5 Random Forest Model Hyperparameter Tuning*

Using Grid Search CV again to tune the hyperparameters in random forest model. The criterion for hyperparameter tuning is to achieve the highest roc_auc. The best roc_auc score was 0.7178 and the corresponding best parameters are {'class_weight': 'balanced', 'criterion': 'entropy',

'max_depth': 20, 'max_features': 'auto', 'max_leaf_nodes': 650, 'min_samples_split': 0.07, 'n_estimators': 100}. The classification report with the best parameters is shown in (table 7). The recall improved drastically from the random forest base model.

Table 7.– Random forest hyperparameter tuned classification report

| Class | Precision | Recall | F1-score | Support |
|---|---|---|---|---|
| 0.0 | 0.92 | 0.65 | 0.76 | 733 |
| 1.0 | 0.22 | 0.64 | 0.33 | 115 |
| | | | | |
| Accuracy | | | 0.65 | 848 |
| Macro avg | 0.57 | 0.65 | 0.55 | 848 |
| Weighted avg | 0.83 | 0.65 | 0.70 | 848 |

The roc_auc measures the overall performance of a model, but in this case, to find as many true positive heart disease cases as possible, models with higher recall (for class 1) score are more desirable. Taking recall into consideration, grid search was used again to choose the most suitable model. Among the models with reasonably high roc_auc score (>=0.71), models with highest recall scores were picked. The results of the grid search were stored in an attribute ("cv_results") including every parameter comb, and its corresponding scores. There are 244 models with roc_auc score higher than 0.71, the best cross validated recall score among them is 0.634. Cross validated roc_auc and aps scores are 0.713 and 0.325. The corresponding classification report is shown in (table 8).

Table 8.– Random forest best recall classification report

| Class | Precision | Recall | F1-score | Support |
|---|---|---|---|---|
| 0.0 | 0.93 | 0.67 | 0.78 | 733 |
| 1.0 | 0.24 | 0.67 | 0.35 | 115 |
| | | | | |
| Accuracy | | | 0.67 | 848 |
| Macro avg | 0.58 | 0.67 | 0.57 | 848 |
| Weighted avg | 0.84 | 0.67 | 0.72 | 848 |

**4. Conclusion**

It is difficult to manually determine the odds of getting heart disease based on risk factors. However, machine learning techniques are useful to predict the output from existing data.

From the data, males, older people, less educated, smokers, all have higher probabilities of having CHD. The random forest model did not perform better than logistic regression model except for the accuracy score. Since the data is severely imbalanced, area under Receiver Operating Characteristic curve and Average Precision Score were both used to evaluate the models' performances. Recall (Sensitivity) is another important metric for this project. Since the model is predicting Heart disease, a false negative (ignoring the probability of disease when there actually is one) is more dangerous than a false positive in this case. In other words, more sensitive than specific is desirable for this project. The Synthetic Minority Oversampling Technique (SMOTE) method in combination with the logistic regression model achieved the highest Average Precision score, area under Receiver Operating Characteristic curve, and Recall score.

## References:


1. Azevedo C. (n.d.). On ROC and Precision-Recall curves. Retrieved from towards data science: URL: https://towardsdatascience.com/on-roc-and-precision-recall-curves-c23e9b63820c
2. Benjamin E. and Muntner P. and ather Heart disease and stroke statistics-2019 update: a report from the American Heart Association. Circulation. 2019.
3. Centers for Disease Control and Prevention. Underlying Cause of Death, 1999–2018. CDC WONDER Online Database. 2018.
4. Framingham heart study. (n.d.). Retrieved from URL: https://www.kaggle.com/amanajmera1/framingham-heart-study-dataset/data
5. Ghoneim S. Accuracy, Recall, Precision, F-Score & Specificity, which to optimize on? 2019. Retrieved from towards data science: URL: https://towardsdatascience.com/accuracy-recall-precision-f-score-specificity-which-to-optimize-on-867d3f11124
6. Imbalanced-learn API. (n.d.). Retrieved from imbalanced-learn.org: URL: https://imbalanced-learn.org/stable/api.html
7. KNN imputation. (n.d.). Retrieved from Medium: URL: medium.com/@kyawsawhtoon/a-guide-to-knn-imputation-95e2dc496e
8. Kohli S. Understanding a Classification Report For Your Machine Learning Model. 2019, November 18. Retrieved from Medium: URL: https://medium.com/@kohlishivam5522/understanding-a-classification-report-for-your-machine-learning-model-88815e2ce397
9. Chawla N. V., Bowyer and Hall L. and Kegelmeyer W. P. Synthetic Minority Over-sampling Technique. Journal of Artificial Intelligence Research, 2002.– P. 321–357.
10. Pedregosa F. V. Scikit-learn: Machine learning in Python. Journal of Machine Learning Research, 2011.– P. 2825–2830.
11. Seaborn Countplot. (n.d.). Retrieved from URL: https://seaborn.pydata.org/generated/seaborn.countplot.html
12. Seaborn distplot. (n.d.). Retrieved from: URL: https://seaborn.pydata.org/generated/seaborn.distplot.html
13. Virani S. S., Alonso A., Benjamin E. J. Heart disease and stroke statistics-2020 update: a report from the American Heart Associationexternal icon. Circulation. 2020.
14. Wijaya C. Y. (n.d.). 5 Smote Techniques for Oversampling your Imbalance Data. Retrieved from towards data science: URL: https://towardsdatascience.com/5-smote-techniques-for-oversampling-your-imbalance-data-b8155bdbe2b5
15. World Health Organization. (2017, May 17). Newsroom / Fact sheets / Cardiovascular diseases (CVDs). Retrieved from World Health Organization: URL: https://www.who.int/news-room/fact-sheets/detail/cardiovascular-diseases-(cvds)
16. Yiu T. Understanding random forest. 2019. June 12. Retrieved from towards data science: URL: https://towardsdatascience.com/understanding-random-forest-58381e0602d2

**https://doi.org/10.29013/ELBLS-21-1.2-34-37**

*Shtrafun I. M.,*
*Alymbaev E. Sh.,*
*Ahmedova H. R.,*
*Shishkina V. G.,*
*Kyrgyz State Medical Academy I. K. Akhunbaeva,*
*National Center for Maternity and Childhood Protection*
*Bishkek, Kyrgyzstan*
*E-mail: sh_inna2013@mail.ru*

# DISORDER OF URODYNAMIC IN CHILDREN WITH INFLAMMATORY DISEASES OF THE UPPER AND LOWER URINARY TRACT

**Abstract.** The material includes an information about a disorder of urodynamic in children with inflammatory diseases of the upper and lower urinary tract. Bladder dysfunction is dominated – 64,5% in the condition contributing to the disturbance of urodynamic and the formation of inflammatory diseases of the upper and lower urinary tract. There is a connection between regression of bladder dysfunction and inflammatory diseases of the upper and lower urinary tract (r = 0, 8). The main symptoms of urinary disorder are pollakiuria- 75% and urgency with urine leakage – 41,2%. The leading role of sphincter-detrusor dyssynergia against the background of a small bladder volume was determined according to the analysis of urodynamic disorders for inflammatory diseases of the upper and lower urinary tract in children.

**Keywords:** disorder of urodynamic, dysfunction of the urine bladder, pyelonephritis, cystitis, children.

*Штрафун И. М.,*
*Алымбаев Э. Ш.,*
*Ахмедова Х. Р.,*
*Шишкина В. Г.,*
*Кыргызская Государственная Медицинская Академия им. И. К. Ахунбаева, Национальный Центр Охраны Материнства и Детства, Бишкек, Кыргызстан*
*E-mail: sh_inna2013@mail.ru*

# НАРУШЕНИЕ УРОДИНАМИКИ У ДЕТЕЙ С ВОСПАЛИТЕЛЬНЫМИ ЗАБОЛЕВАНИЯМИ ВЕРХНИХ И НИЖНИХ МОЧЕВЫХ ПУТЕЙ

**Аннотация.** Представлен материал о нарушении уродинамики у детей с воспалительными заболеваниями верхних и нижних мочевых путей. В структуре состояний, способствующих

нарушению уродинамики и формированию воспалительных заболеваний верхних и нижних мочевых путей преобладают дисфункции мочевого пузыря – 64,5% при этом отмечается взаимосвязь между регрессией дисфункции мочевого пузыря и воспалительными заболеваниями верхних и нижних мочевых путей (r = 0,8) Основные симптомы нарушения мочеиспускания представлены поллакиурией-75% и императивными позывами с подтеканием мочи – 41,2%.

При анализе уродинамических нарушений определена ведущая роль сфинктерно- детрузорной диссинергии на фоне малого объема мочевого пузыря у детей с воспалительными заболеваниями верхних и нижних мочевых путей.

**Ключевые слова:** нарушение уродинамики, дисфункция мочевого пузыря, пиелонефрит, цистит, дети.

**Введение.** Высокие цифры распространенности воспалительных заболеваний верхних и нижних мочевых путей у детей и тенденция к росту, диктуют необходимость пристального внимания к данной проблеме. Актуальность проблемы пиелонефрита обусловлена не только его высокой распространенностью среди детей и большой вариабельностью клинической картины заболевания, но и учащением латентных форм, склонностью к рецидивированию, хроническому течению заболевания и формированию хронической болезни почек [1; 2]. Одной из основных причин острой и рецидивирующей инфекции мочевой системы у детей является нарушение уродинамики [7]. Проблема нарушений уродинамики занимает одно из центральных мест в детской урологии. Это обусловлено большой распространненостью и многообразием причин, вызывающих эвакуатрную несостоятельность мочевых путей, а также наличием прямо пропорциональной зависимости между степенью нарушений уродинамики, активностью пиелонефрита и сроками возникновения функциональной недостаточности почек [3; 4]. На сегодняшний день известно, что функциональные нарушения мочевой системы, способствуют нарушению уродинамики и в дебюте структурных воспалительных заболеваний органов мочевыделения доминируют при этом отмечается взаимосвязь с уровнем поражения нервной системы [5; 6]. Однако анализ нарушений уродинамики без выраженной обструкции обычно не поводится. В то время как своевременное их выявление и успешная коррекция могут привести к существенному снижению рецидивов заболевания, и предупредить развитие и прогрессирование хронической болезни почек у детей.

**Цель исследования:** изучение влияния и характера уродинамических нарушений у детей с воспалительными заболеваниями верхних и нижних мочевыводящих путей.

**Материалы и методы исследования**. Проспективное динамическое наблюдение проводилось с 2018 года по 2020 год в отделении урологии НЦОМиД МЗ Кыргызской Республики. Было обследовано 145 детей с воспалительными заболеваниями органов мочевыделения в возрасте от 4 до 18 лет. Алгоритм обследования включал последовательную оценку жалоб, анамнеза заболевания и жизни, данных осмотра, стандартного урологического исследования, а также по показаниям проводились экскреторная урография и микционная цистография. Оценка уродинамики нижних мочевых путей проводилась в фазы накопления и опорожнения с использованием ритма спонтанных мочеиспусканий и урофлоуметрии на 7 и 10 день антибактериальной терапии с целью исключения влияния активного воспалительного процесса на показатели уродинамики.

**Результаты исследования и их обсуждение.**

В структуре воспалительных заболеваний мочевыводящих путей с нарушениям уродинамики,

преобладали острый пиелонефрит – 48,7% случаев и острый цистит 15% в возрастной группе 4–7 лет, в возрастной группе 8–11 лет острый пиелонефрит диагностировался в 38,6% случаев, а острый цистит в 8%, тогда как в возрастной группе старше 12 лет наблюдались преимущественно хронические формы пиелонефрита в периоде обострения в 13,5% случаев. Достоверной разницы по полу выявлено не было ($p < 0,01$). При анализе микробно – воспалительных изменений в 91,8% случаев высеяна патогенная флора ($p < 0,002$), которая представлена следующим образом: кишечная палочка – 35,8%, стрептококк –15%, энтерококк – 12,9%, стафилококк – 12,3%, клебсиелла – 8,8%, протей –5,5%.

В 64,5% случаев микробно-воспалительные поражения почек и мочевых путей отмечались при дисфункциях мочевого пузыря, а аномалии почек отмечались в 22,4% случаев. В структуре аномалий почек достоверно преобладала ($p <0,0001$) пиелоэктазия – 11,4% ($p <0,0001$), тогда как удвоение чашечно-лоханочной системы и гипоплазия почек составили 9% и 2% соответственно. При оценке ритма спонтанных мочеиспусканий у данной категории детей достоверно доминировали частые мочеиспускания свыше 15 раз в сутки ($p < 0,001$), малый интервал между ними от 30 минут до 1 часа ($p < 0,005$), а средний эффективный объем составил 72,2 ± 7,4 (56,5÷87,9) мл ($p < 0,02$). Императивный характер мочеиспускания с периодическим подтеканием мочи небольшими порциями отмечался в 41,2% случаев. У 75% детей отмечена поллакиурия. Редкое мочеиспускание у обследуемых детей наблюдалось в 9,8% случаев. Достоверной разницы по полу и возрасту у них не отмечалось. Число мочеиспусканий составило 3,8 ± 0,4 (2,9 ÷ 4,7) раз, средний эффективный объем мочеиспускания находился в пределах 299,9 ± 23,5 мл, максимальный – 505,5 ± ±54,7 мл ($p < 0,0001$). При качественной оценке показателей урофлоуметрии повышенная скорость потока мочи отмечалась у 30,5% детей при этом максимальная скорость находилась в пределах 29,5 ± ± 0,6 (28,1 ÷ 30,9) мл и 44,9± 2,0 (40,5 ÷ 49,3) мл ($p < 0,002$), прерывистый тип отмечался в 32,8%, тогда как обструктивный тип достоверно встречался реже в 1,2% случаев ($p < 0,05$). При этом возрастные различия достоверно выявлены не были.

**Выводы:**

1. Воспалительные заболевания нижних и верхних мочевых путей у детей в подавляющем большинстве случаев – 64,5%, обусловлены дисфункциями мочевого пузыря.

2. Возрастная динамика регрессии дисфункции мочевого пузыря находится в прямой сильной корреляционной зависимости ($r = 0,8$) с воспалительными заболеваниями верхних и нижних мочевых путей.

3. Среди нарушений уродинамики нижних мочевых путей преобладает сфинктерно- детрузорная диссинергия на фоне малого объема мочевого пузыря ($p < 0,005$).

## Список литературы:


1. Данилова Т. И. Данилов В. В. Значение коррекции уродинамики в комплексной терапии детей с инфекцией мочевыводящих путей // Урология. 2004.– № 2.– С. 65–70.
2. Коровина Н. А., Захарова И. Н., Герасимова Н. П., Савельева О. В. Функциональное состояние почек при пиелонефрите у детей // Российский педиатрический журнал. 2004.– № 4.– С. 15–19.
3. Митрофанов К. В. Циститы у детей // Мать и дитя в Кузбассе. 2005.– № 1(20).– С. 3–9.
4. Нестеренко О. В., Горемыкин В. И., Мещерякова Е. Е. Нарушения уродинамики у детей с вторичным хроническим пиелонефритом// Научное обозрение. Медицинские науки. 2014.– № 2.– С. 82–83.
5. Узакбаев К. А., Штрафун И. М., Эсембаев Б. И. Нейрогенная дисфункция мочевого пузыря у детей// Вестник КГМА. 2017.– № 3.– С. 81–83.

6. Штрафун И. М., Алымбаев Э. Ш., Ахмедова Х.Р., Шишкина В. Г. Взаимосвязь и взаимообусловленность функциональных нарушений мочевой системы и вомпалительных заболеваний почек у детей // Вестник КГМА. 2013.– № 4 (1).– С. 121–123.
7. Jones K. V. Urinary tract infection of childhood. Practioner. 2002.– Vol. 235.– P. 303–307.

# Section 2. Biomedical science

**https://doi.org/10.29013/ELBLS-21-1.2-38-42**

*Karamzina Lyudmila Antonovna,*
*senior researcher,*
*SI "O.M. Marzieiev Institute for Public Health" NAMSU, Ukraine*
*E-mail: lyudka2008@ukr.net*

## ACOUSTIC REFLEX INVERSION: BIOPHYSICAL REALITY

**Abstract.** The article describes problems of the acoustic reflex inversion interpretation from the biophysics standpoint. The finding of this study showed important significance of the acoustic reflex inversion as result of analysis scientific publications and our own researches. Its diagnostic is significant for biomedical researches.

**Keywords:** acoustic reflex, inversion.

*Карамзина Людмила Антоновна,*
*доктор биологических наук, ГУ «Институт общественного здоровья»*
*им. А.Н. Марзеева Национальной академии*
*медицинских наук Украины, старший научный сотрудник, Украина*
*E-mail: lyudka2008@ukr.net*

## ИНВЕРСИЯ АКУСТИЧЕСКОГО РЕФЛЕКСА: БИОФИЗИЧЕСКАЯ РЕАЛЬНОСТЬ

**Аннотация**: В статье описаны проблемы интерпретации инверсии акустического рефлекса с точки зрения биофизики. На основании анализа литературных данных и собственных исследований делается вывод о значимости фазоинверсии акустического рефлекса. Обоснована его диагностическая значимость для медико-биологических исследований.

**Ключевые слова**: акустический рефлекс, инверсия.

**Введение.** Проблема точности дифференциально-топической диагностики нарушений слуха расширяется по мере обеспечения исследований новыми измерительными устройствами. Диагностика слуховой функции базируется исключительно на данных субъективных и объективных ответных реакций. С момента технической реализации метода импедансометрии O. Metz (1946) [9] для усовершенствования слуховой диагностики и до сегодняшнего дня исследователи так и не могут прийти к единому объяснению диагностической важности фазоинверсии акустического рефлекса (АР) внутриушных мышц. Решение проблемы уходит на периферию исследований, скрываясь под маской ненадёжности результата теста.

**Цель** – обоснование значимости противофазного АР в исследовании слуха.

**Материал и методы.** В группу изучения были включены 80 пациентов обоего пола трудоспособного возраста с различными уровнями тонального слуха в конвенциональном диапазоне частот: 10 чел. с нормальным слухом, 30 чел. с социально-адекватным слухом, 30 чел. с социально-неадекватным слухом и 10 чел. с аудиометрической глухотой по данным стандартных психоакустических исследований. Снижение тонального слуха оценивали по классификации ВОЗ (1997). Здесь нужно отметить, что ранее, в 1989 г. украинскими учёными (В. Г. Базаров, А. И. Розкладка) была разработана, опубликована и принята к применению классификация оценки слуха, с которой практически совпадает классификация ВОЗ.

Техническое сопровождение исследований: аудиометр МА-31 (Präcitronik, Германия); импедансометр Immittance System ZO-2020 (Madsen Electronics, Дания).

**Обсуждение результатов.** У всех отобранных для изучения пациентов были зарегистрированы противофазные АР в ответ на звуковую стимуляцию.

Патологию среднего уха исключили методом тимпанометрии.

При проведении исследования между акустическим зондом импедансометра и барабанной перепонкой создается замкнутое пространство (рис. 1). Отраженный от барабанной перепонки звуковой сигнал предоставляет информацию о сократительной способности не только стременной мышцы, а обеих внутриушных мышц в виде графики АР. Если функция «вход-выход» слухового анализатора не нарушена, то в ответ на прирост громкости звукового стимула пропорционально растет сокращение внутриушных мышц, что выглядит как прирост амплитуды АР и её графическое отображение имеет вид, как на (рис. 2).

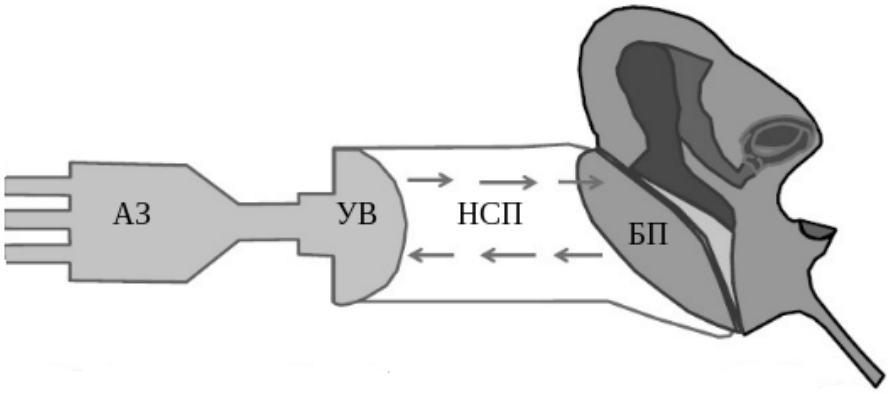


Рисунок 1. Расположение акустического зонда (АЗ) с ушным вкладышем (УВ) внутри наружного слухового прохода (НСП). БП – барабанная перепонка

*адаптировано автором из: http://www.ihsinfo.org/IhsV2/Education/pdf/Acoustic_Reflexes_Presentation_Slides.pdf;*

Во время сокращения внутриушных мышц в замкнутом пространстве наружного слухового прохода происходит изменение объёма этого пространства. При этом барабанная перепонка, как неотъемлемая часть подвижной цепи слуховых косточек, тоже отклоняется от своего равновесного положения, изменяя объём замкнутого пространства наружного слухового прохода и, следовательно, изменяя также и время прохождения звукового сигнала в этом же пространстве.

Такой процесс происходит синфазно с отклонением барабанной перепонки.

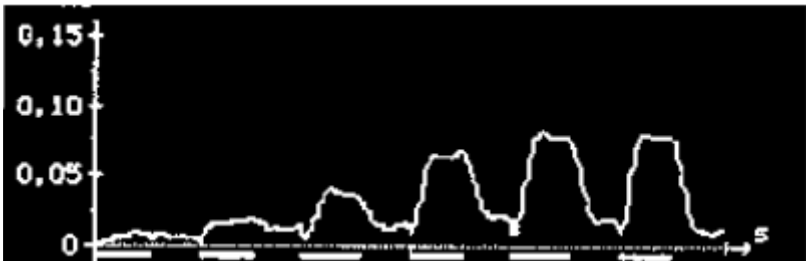


Рисунок 2. Динамика акустического рефлекса
*адаптировано автором из: https://docplayer.ru/58572675-Impedansnaya-audiometriya.html*

Как считает [4], применительно к мышцам среднего уха, повышенная чувствительность к вибрации означает, что любой звук высокого уровня, поступающий в среднее ухо, вызывает немедленное сокращение внутриушных мышц, обеспечивая тем самым мгновенную защиту от перегрузки.

Противофазность АР является следствием такого изменения подвижности цепи слуховых косточек, которое ограничивает не только подвижность барабанной перепонки, но и изменяет её пространственное положение внутри замкнутого НСП. Вследствие этого отражённый от изменённой барабанной перепонки акустический сигнал уже является противофазным, что и регистрирует импедансометр. Очевидно, что такое изменение положения барабанной перепонки и не даёт прироста амплитуды инвертированного АР, что и отображается в противофазной графике АР (рис. 3).

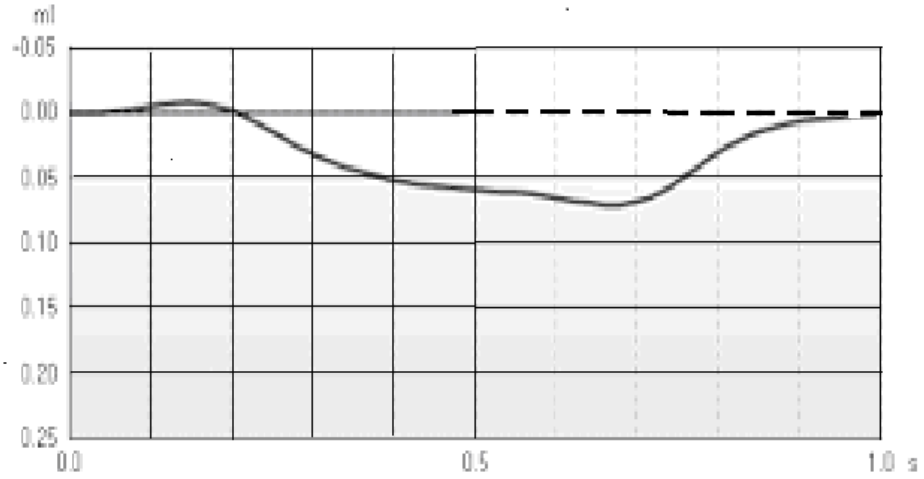


Рисунок 3. Противофазный АР
*взято из: interacoustics.com*

Аргументом в пользу этого утверждения выступает противофазный АР, вызываемый на уровнях громкости звукового сигнала, близким к дискомфортным (порог возникновения регистрируется на 105 дБ УЗД). Дальнейший прирост громкости звука не даёт ожидаемого прироста амплитуды АР, как отображено на (рис. 2). Данная ситуация расценивается автором этой статьи как наличие ретрокохлеарного нарушения в слуховом анализаторе. Обоснованность подобного суждения базируется на том, что регуляция сократительной деятельности внутриушных мышц осуществляется нервными структурами, дающими команду мышцам среднего уха на сокращение. А сокращение внутриушных мышц – это не что иное, как механическое движение, в котором

участвует и барабанная перепонка. Отсюда и заключение, что в ответ на подачу звукового сигнала сокращаются обе мышцы. Поэтому утверждения некоторых исследователей, что противофазный АР – это изолированная реакция исключительно барабанной перепонки не до конца убедительны [5, 13]. Если бы это имело место, то отсутствовал бы разрыв барабанной перепонки вследствие громких кратковременных звуков (например, взрывов). В этом случае сократилась бы только мышца стремени как механизм защиты внутреннего уха, тогда как барабанная перепонка осталась бы целой. Но в реалиях это не так, поскольку имеет место совместное сокращение обеих внутриушных мышц.

Те же авторы [5, 13] расценивают противофазный АР как артефакт и описывают это как отсутствие АР. Но и это не так. Графика противофазного АР говорит о том, что сократительный ответ возникает на действие звука и прекращается в момент прекращения озвучивания, т.е. плато имеет место и свидетельствует в пользу срабатывания внутриушных мышц. Противофазный АР не исчезает после глубокого мышечного расслабления, вызванного анестезией, и присутствует даже у трупов в то время, когда невральная деятельность больше не может иметь место. И поэтому учёные [14] расценивают это как физиологический артефакт.

Отсутствие АР наблюдали [7] у 1374 человек с нормальным слухом. Такое явление по мнению С. Гельфанда с соавт. требует подробного изучения и объяснения. Здесь нужно отметить, что С. А. Гельфанд является автором монографии «Слух: введение в психологическую и физиологическую акустику», которая на сегодня стала бестселлером в среде русскоговорящих аудиологов и специалистов смежных профессий.

Не спешат с категорическими выводами [6], проводившие кинетический анализ АР. Исследователи предполагает существование единого базового явления, которое сможет объяснить сложную морфологию, часто наблюдаемую даже в нормальном ипсилатеральном АР.

Признание таких отрицательных рефлексов увеличивает специфичность и чувствительность рефлекторного теста для акустических опухолей [8].

Однако, наличие противофазного АР принимается всеми исследователями доказательным признаком наличия отосклеротического процесса, хотя графическая модель противофазного АР, как и в остальных случаях остаётся одинаковой.

Автором данной статьи неоднократно были зарегистрированы противофазные АР как при нормальном слухе, так и при нерегистрируемом слухе – аудиометрической глухоте. У пациентов с глухотой других маркеров слуховых ответов вообще нет.

В исследовании группы индийских авторов [10] рассмотрена ситуация участия АР в механизме кодировании речи стволом мозга у лиц с нормальным слухом. Отсутствие АР при нормальном слухе не является достаточным для диагностики такого ретрокохлеарного нарушения как слуховая нейропатия (термин введен Starr et al.,1996 [12]). Но это не отрицает наличия ретрокохлеарной патологии. По определению слуховая нейропатия – это нарушение слуха, которое характеризуется нормальным проведением звукового сигнала до внутреннего уха, а дальнейшая передача звукового сигнала от внутреннего уха к мозгу нарушена. Не согласны с этими авторами группа других индийских специалистов [11], подтверждая аномалии АР у лиц с гиперакузией без учёта влияния уровня слуха. Здесь же подчеркивается важность вовлечения тестирования методом АР в оценке гиперакузиса, при условии, что гиперакузис не связан с потерей слуха или любым другим медицинским состоянием, приведшим к снижению толерантности к звукам.

Противоположные по фазе АР наблюдали и другие исследователи, работавшие с приборами различных производителей [1; 2; 3].

Как следует из данной статьи, вопрос об инверсии фазы далёк от разрешения. Автором предпринята попытка установить истину в возникновении противофазного АР с позиций биофизического подхода.

Перспективным в научно-практическом плане представляется изучение частоты выявления отрицательного АР на популяционном уровне.

**Выводы.**

1. Инверсия АР является диагностическим признаком нарушенного функционирования слухового анализатора.

2. В прогностическом плане, особенно при нормальном слухе, инверсия фазы АР свидетельствует о скрытой потере слуха, которая будет приводить к дефектам слухо-речевой коммуникации.

## Список литературы:


1. Блувштейн Г. М., Амосов В. В. О диагностическом значении и причинах инверсии акустического рефлекса // Журн, ушн., нос. и горл. болезней. 2003. – № 1. – С. 2–10.
2. Карамзина Л. А. Инверсия фазы акустического рефлекса как признак ретрокохлеарных нарушений // Журн. вушних, носових і горлових хвороб. 2005. – № 5-с. – С. 81.
3. Сагалович Б. М., Цуканова В. И. Диагностический смысл ипсилатеральной регистрации акустического рефлекса и артефакты в импедансометрии // Вестн. оториноларинг. 1980. – № 4. – С. 20–24.
4. Bell A. A fast, “zero synapse” acoustic reflex: middle ear muscles physically sense eardrum vibration // Journal of Hearing Science. 2017. – V. 7, № 4. – P. 33–44.
5. Blanco Labrador M., Rodríguez de la Fuente F., Alvarez-Vicent J. J. The inverted ipsilateral reflex: is it an artefact? // Acta Otorrinolaringologica Espanola. 1990. – V. 41. – No. 3. – P. 163–164.
6. Ciardo A., Garavello W., Rossetti A., Manghis P. V., Merola S., Gaini R. M. The Reversed Ipsilateral Acoustic Reflex: Clinical Features and Kinetic Analysis // Acta Oto-Laryngol. 2003. – Vol. 123. – No. 1. – P. 65–70.
7. Gelfand S. A., Schwander T., Silman Sh. Acoustic Reflex Thresholds in Normal and Cochlear-Impaired Ears Effects of No-Response Rates on 90$^{th}$ Percentiles in a Large Sample // Journal of Speech and Hearing Disorders. 1990. – Vol. 55. – No. 1. – P. 198–205.
8. Mangham Ch. A., Lindeman R. C. The negative acoustic reflex in retrocochlear disorders // Laryngoscope. 1980. – Vol. 90. – No. 11. – P. 1753–1761.
9. Признание этих отрицательных рефлексов увеличивает специфичность и чувствительность рефлекторного теста для акустических опухолей.
10. Metz O. The acoustic impedance measured on normal and pathological ears // Acta otolaryngol. 1946. – Suppl. – 63. – P. 1–254.
11. Rajkishor M., Himanshu K. S., Preeti S. Brainstem encoding of speech in normal-hearing individuals with absent acoustic reflex / The Egyptian Journal of Otolaryngology. 2015. – Vol. 31. – P. 156–161.
12. Saxena U., Singh B. P., Kumar S. B.R., Chacko G., Bharath K. N. S. V. Acoustic Reflexes in Individuals Having Hyperacusis of the Auditory Origin // Indian Journal of Otolaryngology and Head & Neck Surgery. 2020. – Vol. 72. – P. 497–502.
13. Starr A., Picton T. W., Sininger Y., Hood L. J., Berlin C. I. Auditory neuropathy // Brain. 1996. – Vol. 119. – P. 741–753.
14. Vallejo L. A., Herrero D., Sánchez C., Sánchez E., Gil-Carced E., Gil-Carcedo L. M. Inverted acoustic reflex: an analysis of its morphological characteristics in different physiological and pathological situations // Acta Otorrinolaringologica (eng. ed.). 2009. – Vol. 60. – No. 4. – P. 238–252.

# Section 3. Life science

https://doi.org/10.29013/ELBLS-21-1.2-43-51

*Zhou Rui,*
*Zhangjiagang Foreign Language School, China*
*E-mail: ZhouRuiAda@gmail.com*

## DETECTING COMMON FACTORS INFLUENCING ADHD IN CHILDREN: DEVELOPMENT AND VALIDATION OF A PREDICTIVE MODEL

**Abstract.** Attention-deficit/hyperactivity disorder (ADHD) is a common chronic condition that is characterized as hyperactivity, difficulty sustaining attention, and impulsive behavior. Without radical caret, symptoms of ADHD patients can only be eased with treatments like behavior therapy, including training for parents, and medications [1].

The objective of this research is to build a predictive model to determine the possibility for a child to develop ADHD caused a variety of factors including gender, race, age, and parents' education. Two models, a logistic regression and an artificial neural network, were tested using the data from National Health Interview Survey (NHIS) 2017. And we compared the two models using various evaluation metrics like the receiver operating characteristic (ROC) curve and the area under the curve (AUC) score. We found that the AUC score for the artificial neural network is 0.69, while that for the logistic regression model is 0.66. Therefore, we concluded that, overall, the artificial neural network has better performance.

According to the logistic regression, older children, non-Hispanic children, and males are more likely to be a victim of ADHD. Asian kids and kids with more educated parents were less likely to have early interventions services. The neural network indicates that the most important predictors of developing ADHD are age, followed by Asian children, mother's education level, White children, sex, Black children, Hispanic origin, and father's education level. We believed those results are useful for doctors and parents to evaluate the possibility of having children with ADHD, and to provide suggestions schoolteachers and peers to change the disruptive behaviors of ADHD children.

**Keywords:** ADHD, children, a predictive model, treatment, suggestions

### 1. Introduction

Attention-deficit/hyperactivity disorder (ADHD) is one of the most common chronic conditions that tortures millions of children. Over the years, it has serious impacts on the lives of children who suffer from ADHD. According to the latest study, more than 16 million (9.4 percent) children in the U.S. have an ADD diagnosis [2]. The disease is first diagnosed in childhood, but ADHD can continue as children mature, resulting in their hyperactiv-

ity as well as their disability in maintaining attention and controlling impulsion. People with ADHD tend to be daydreaming, insomniac, and overly talkative. They usually have great difficulty in resisting temptation and getting along well with others. These conditions in children dramatically affect their school performance, including inattentive in class, excessive talking at an appropriate time, and frequently interrupt others' conversations.

According to a Swedish cohort study of 544 children, a considerable association was observed between symptoms of inattentiveness (as measured by the Conners 10-item scale) in children aged 7 and 10 years and academic underachievement at age 16 years [3]. Thus, it is likely that people with ADHD have comparably lower educations levels which leads to their hardship in finding well-paid jobs. In this case, the affecting factors of ADHD in children are in imperious need for people to know to conduct and ensure better prevention of the detrimental consequences triggered by ADHD.

The hypothesis of this study is that "the possibility for a child to develop ADHD is related to one or more common factors such as gender, race, age, and parents' educational level." The objective of this study is to develop a predictive model to detect the likelihood for a child to suffer from ADHD in a family. With the help of the model, parents can evaluate the possibility of having a child with ADHD or that of their children to develop ADHD over time, thus taking appropriate measures such as changing daily habits or parenting methods to prevent the disease.

**2. Method**

***2.1 Data***

The National Health Interview Survey (NHIS) is the principal source of information on the health of the civilian noninstitutionalized population of the United States and is one of the major data collection programs of the National Center for Health Statistics (NCHS) which is part of the Centers for Disease Control and Prevention (CDC). The National Health Interview Survey (NHIS) Data 2017 was used in this study.

**2.2 Model**

*2.2.1 Logistic regression model development*

Logistic regression models were used to calculate the predicted risk. Logistic regression is a part of a category of statistical models called generalized linear models, and it allows one to predict a discrete outcome from a set of variables that may be continuous, discrete, dichotomous, or a combination of these. Typically, the dependent variable is dichotomous, and the independent variables are either categorical or continuous. The percentage of students who developed Attention Deficit/Hyperactivity Disorder was the dependent variable in this study.

The logistic regression model can be expressed with the formula:

$$\ln\left(\frac{y}{1-y}\right) = w_0 + w_1 x_1 + \ldots + w_m x_m$$

In the logistic regression, each feature $x_i$ has its specific weight $w_i$, where $w_0$ is the intercept while $w_1$ through $w_m$ are the coefficients of the independent variables.

Our task is to find a set of parameters $w_0, \ldots, w_m$ such that the loss function between the output $y$ and the actual values $u$

$$l(y,u) = l|y-u|l_2^2$$

is minimized.

*2.2.2 Artificial neural network*

An artificial neural network is a computational model vaguely inspired by the biological neural networks that constitute animal brains. An artificial neuron that receives a signal then processes it and can signal neurons connected to it. The "signal" at a connection is a real number, and the output of each neuron is computed by some non-linear function of the sum of its inputs.

A typical artificial neural network consists of one input layer, several hidden layers, and one output layer. The input layer is the first layer, the output layer is the last layer, and any layers between them are hidden layers. The data are passed into the input

layer, processed by the hidden layers, and finally transformed into predicted labels in the output layer. In this study, the model has one hidden layer.

A package called "neuralnet" in R was used to conduct neural network analysis. The package neuralnet focuses on multi-layer perceptrons (MLP, Bishop, 1995), which are well applicable when modeling functional relationships.

### *2.3 Variables*

The outcome variable is the percentage of students who developed Attention Deficit/Hyperactivity Disorder (LAHCC13).

Table 1.– Variables used in this study

| | |
|---|---|
| LAHCC13 | Attention Deficit/Hyperactivity Disorder (ADD/ADHD) causes limitation |
| SEX | 1: male<br>2: female |
| ORIGIN_I | Hispanic Ethnicity:<br>1: yes; 2: no |
| RACRECI3 | 1: White<br>2: Black<br>3: Asian |
| AGE_P | Age <18 years old<br>0–17 |
| MOM_ED | 01 Less than/equal to 8th grade<br>02 9–12th grade, no school diploma<br>03 School graduate/GED recipient<br>04 Some college, no degree<br>05 AA degree, technical or vocational<br>06 AA degree, academic program<br>07 Bachelor's degree<br>08 Master's, professional, or doctoral degree |
| DAD_ED | 01 Less than/equal to 8th grade<br>02 9–12th grade, no school diploma<br>03 School graduate/GED recipient<br>04 Some college, no degree<br>05 AA degree, technical or vocational<br>06 AA degree, academic program<br>07 Bachelor's degree<br>08 Master's, professional, or doctoral degree |

### *2.4 Data pre-processing*

The data set is pre-processed in this step to improve both the training speed and accuracy. As most machine learning algorithms are not able to deal with missing values, all the data points with missing entries are excluded from training. Then we center and scale each feature variable independently. Feature standardization transforms different features into comparable scales and ensures all features weigh equally in the training process. The standard scaler function standardizes features by scaling the feature means to zero and standard deviations to unit variance. Finally, we partitioned the dataset into two sets, the training dataset (50%) for model development and the test dataset (50%) for model test.

The nominal variable is one kind of categorical variables whose levels are simply labels and thus does not contain any meaning of order. For example, in the variable "RACRECI3", "White" is encoded as 1, and "Black" is encoded as 2, and "Asian" is encoded as 3. Even though we want these three levels to be equally weighted, it is usually problematic, as the logistic regression will mistakenly assume that Black is greater than White. A way to solve this is to use the one-hot encoding technique. The idea behind this approach is to create a separate variable for each race group. Here, a new binary feature was created whose value was used to indicate the particular race group of a student.

## 3. Results

### *3.1 Chorogram*

Basically, a chorogram is a graphical representation of the cells of a matrix of correlations. The idea is to display the pattern of correlations in terms of their signs and magnitudes by using visual thinning and correlation-based variable ordering. Moreover, the cells of the matrix can be shaded or colored to show the correlation value. The positive correlations are shown in blue, while the negative correlations are shown in red; the darker the hue, the greater the magnitude of the correlation.

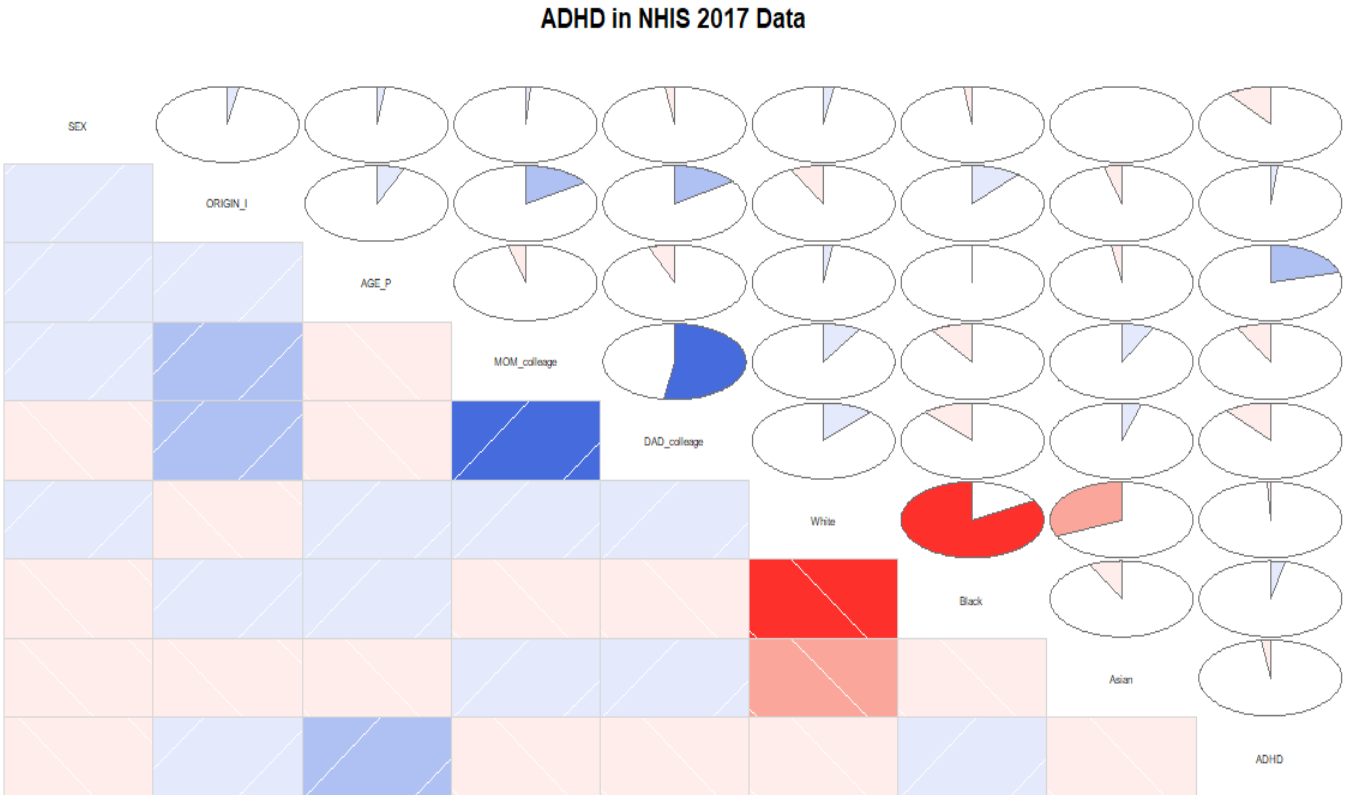


Figure 1. Matrix of correlations among variables

According to the chorogram above, ADHD had the strongest positive correlation with age, followed by non-Black people and non-Hispanic origin. Meanwhile, it has the strongest negative relationship with dad's education level, followed by sex, mom's educational level, Asian people and White people.

### *3.2. Logistic regression model*

From the table above, sex, origin, and father's educational level are significant predictors of the dependent variable. Females are less likely to develop Attention Deficit/Hyperactivity Disorder (ADD/ADHD) than males. Non-Hispanic children were more likely to have Attention Deficit/Hyperactivity Disorder

(ADD/ADHD) than Hispanic kids. Kids are more likely to be a victim of ADHD when they aged. Asian kids and kids with more educated parents were less likely to have early interventions services.

Table 2. – Logistic Regression for Having Attention Deficit/Hyperactivity Disorder (ADD/ADHD)

| | Estimate | Std. Error | z value | Pr(>\|z\|) | |
|---|---|---|---|---|---|
| (Intercept) | –2.402 | 0.553 | –4.347 | 0.000 | *** |
| SEX | –0.606 | 0.135 | –4.498 | 0.000 | *** |
| ORIGIN_I | 0.121 | 0.153 | 0.788 | 0.431 | |
| AGE_P | 0.116 | 0.014 | 8.203 | 0.000 | *** |
| MOM_colleage | –0.168 | 0.164 | –1.024 | 0.306 | |
| DAD_colleage | –0.624 | 0.191 | –3.266 | 0.001 | ** |
| White | 0.624 | 0.452 | 1.381 | 0.167 | |
| Black | 0.699 | 0.468 | 1.491 | 0.136 | |
| Asian | 0.469 | 0.600 | 0.782 | 0.434 | |

### *3.3. Artificial Neural Network*

The structure of the neural network used in this study is shown in (Figure 2).

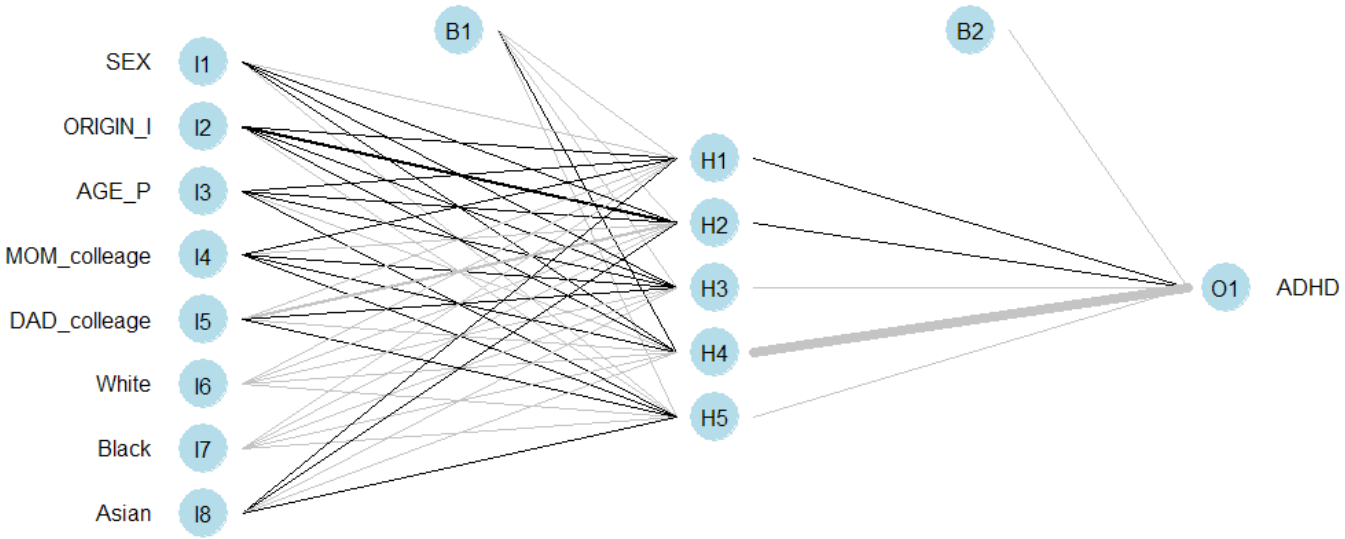


Figure 2. Artificial Neural Network in training sample

In the figure above, line thickness represents weight magnitude and line color weights sign (black = positive, gray = negative). The network is essentially a black box, so we cannot say that much about the fitting, the weights, and the model. However, it suffices to say that the training algorithm has converged. Therefore, the model is ready to be used.

*3.3.1 Variable Importance in Artificial Neural Network*

Variable importance represents the statistical significance of each variable in the data with respect to its effect on the generated model. It ranks each predictor based on the contribution predictors make to the model. This technique helps data scientists weed out certain predictors that are con-

tributing to nothing and that instead add time to processing [4]. Garson's algorithm was used to calculate relative importance of input variables in this neural network. The importance for each variable is shown in (Figure 3).

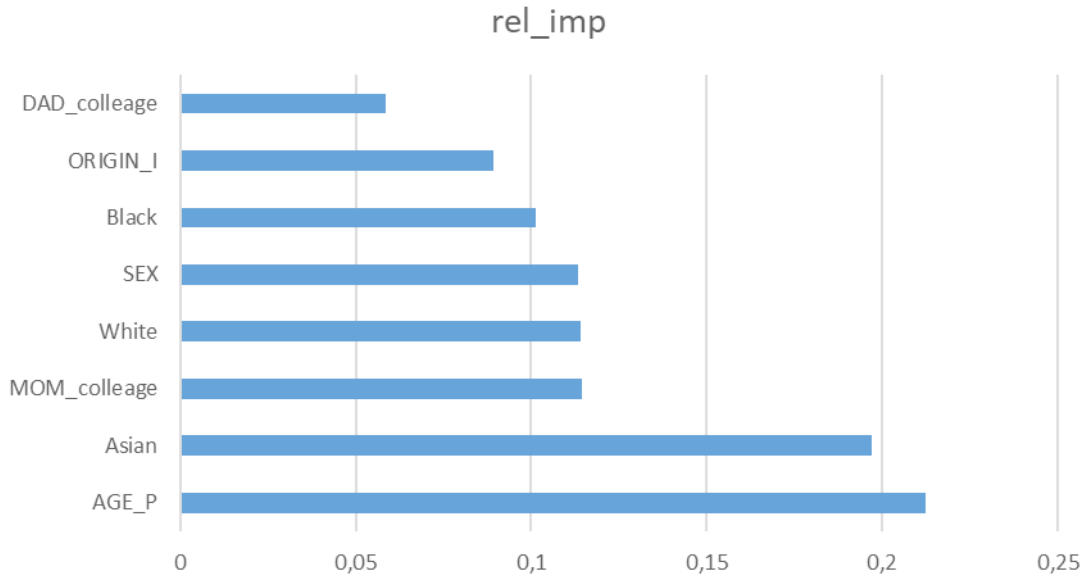


Figure 3. Variable Importance in Artificial Neural Network

The most important predictor was age, followed by Asian children, mother's education level, White children, sex, Black children, Hispanic origin, and father's education level.

***3.4 ROC***

A receiver operating characteristic curve (ROC curve), is a graph showing the performance of a classification model at all classification thresholds [5]. The x-axis of ROC plot represents false positive rate, while the y-axis represents true positive rate. When the decision threshold changes, a better classifier will have a lower false positive rate and a higher true positive rate. In other words, when the false positive rate of two models are the same, the better one will have a higher true positive rate, which makes the curve come closer to the upper left corner of the ROC space. We can use the ROC curve to compare the performance of logistic regression model and the neutral network. Sometimes, it might be hard to identify which model performs better by directly looking at ROC curves, as one curve may not completely encompass the other. Area Under Curve (AUC) overcomes this drawback by finding the area under the ROC curve, making it easier to find the optimal model. Usually, a better model has a higher AUROC score.

*3.4.1 ROC in the training sample*

For the training sample, the AUROC was 0.70 for the logistic regression and 0.72 for the artificial neural network. Artificial neural network performed better than logistic regression did.

*3.4.2 ROC in the testing sample*

In the testing sample, the AUROC was 0.66 for the Logistic regression and 0.69 for the artificial neural network. Artificial neural network had better performance in the testing sample.

**4. Discussion**

***4.1 Logistic regression analysis and interpretation of the results***

Of the 1752 school students participating in the study, 21.2% had Attention Deficit/Hyperactivity Disorder (ADD/ADHD), and 79.8% did not have. Among those patients, about 15.8% were female and 24.2% male. At the significance level of 0.01, the predictive model of Attention Deficit/Hyperactivity Disorder is:

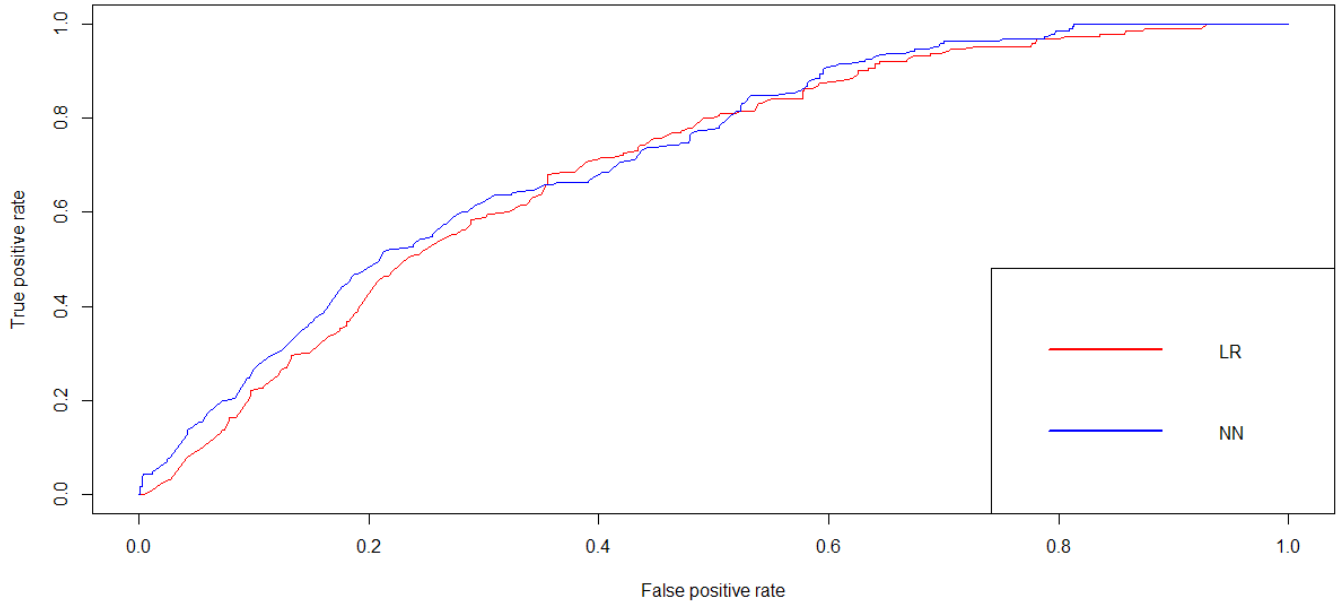


Figure 4. ROC in the training sample for Logistic Regression (Red) vs Neural Network (Blue)

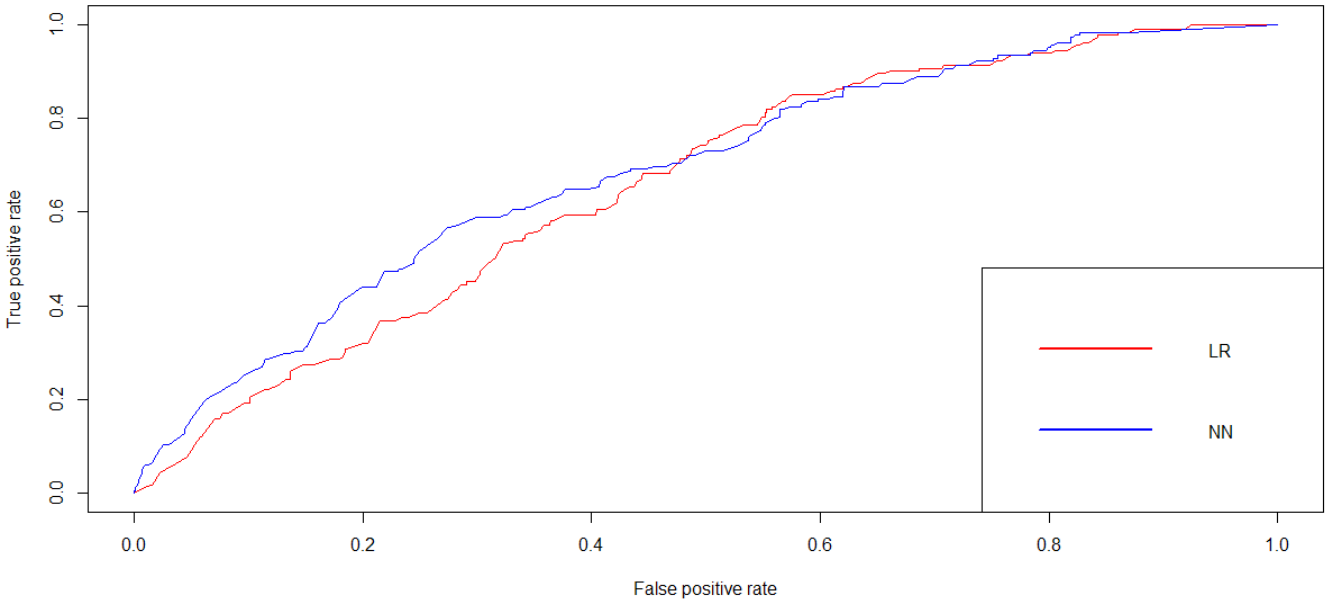


Figure 5. ROC in the testing sample for Logistic Regression (Red) vs Neural Network (Blue)

Predicted logit of adolescent depression:

−2.402−0.606*SEX+0.121*ORIGIN_I+0.116*AGE_P-0.168*MOM_college-0.624*DAD_colleage+0.624*White+0.699*Black+0.469*Asian

The coefficients of the parameters were interpreted as follows. At the significance level of 0.01:

- On average, controlling other variables, a female student is 45 percent less likely to report to develop Attention Deficit/Hyperactivity Disorder (ADD/ADHD) than a male student.
- On average, controlling other variables, a non-Hispanic student is 13 percent more likely to report to develop Attention Deficit/Hyperactivity Disorder (ADD/ADHD) than a Hispanic student.
- On average, controlling other variables, a one-year older student is 12 percent more

likely to develop Attention Deficit/Hyperactivity Disorder (ADD/ADHD) than a younger student.

- On average, controlling other variables, a student who has a higher educational mother is 15 percent less likely to develop Attention Deficit/Hyperactivity Disorder (ADD/ADHD) than a student whose mother is poorly educated.
- On average, controlling other variables, a student who has a higher educational father is 46 percent less likely to develop Attention Deficit/Hyperactivity Disorder (ADD/ADHD) than a student whose father is poorly educated.
- On average, controlling other variables, a White student is 87 percent more likely to develop Attention Deficit/Hyperactivity Disorder (ADD/ADHD) than a student from other race groups.
- On average, controlling other variables, a Black student is 101 percent more likely to develop Attention Deficit/Hyperactivity Disorder (ADD/ADHD) than a student from other race groups.
- On average, controlling other variables, an Asian student is 60 percent more likely to develop Attention Deficit/Hyperactivity Disorder (ADD/ADHD) than a student from other race groups.

It is indicated in the model that being male, being non-Hispanic, being older, having a more educated mother, having a more educated father, being White or Black or Asian are significant predictors in predicting Attention Deficit/Hyperactivity Disorder (ADD/ADHD). Having a more educated mother or father will decrease the probability of suffering from Attention Deficit/Hyperactivity Disorder (ADD/ADHD); while being a male, being non-Hispanic, getting older may increase the probability of developing Attention Deficit/Hyperactivity Disorder (ADD/ADHD). Moreover, compared to being White or Black, Asians are less likely to develop Attention Deficit/Hyperactivity Disorder (ADD/ADHD).

According to the study, parents can reflect on themselves, and then take appropriate measures to reduce the possibility of having children with Attention Deficit/Hyperactivity Disorder (ADD/ADHD). For example, for parents' with a relative low education level, they can improve their prenatal and postnatal care by pursuing a higher education, which provides them with well-paid jobs and thus enough money to take better care of their children. However, since most factors involved in the study are innate and generally unchangeable, treatment and mental comfort are more essential in the face of ADHD patients.

Treatments can be divided into drug intervention and human intervention. For children younger than 6, the American Academy of Pediatrics (AAP) recommends that human intervention like parents' help should be the first line of treatment before medication is tried. However, for older children, both behavior therapy and medications can be applied to help treat ADHD [6]. To achieve success, it is the parents' responsibility to receive training in behavior management first to treat their children's disruptive behaviors. This requires both time and effort, but the benefits to their children will be considerable. Despite parents' commitment, schoolteachers and peers play important roles. School-based management training led by teachers can have an enormous impact on students' constructive manners. For example, a reward system can be applied to encourage positive behavior such as concentrating in class, actively but appropriately participating in a discussion, making progress in academic performance. For peers, they can help classmates with ADHD by caring for them more, playing some concentrating games with them instead of isolating them. In this way, they can help these ADHD patients integrate into the collective, thus providing mental comfort.

### *4.2 Limitations and future study*

Although this study gives predictions on developing ADHD for kids, and a great deal of treatments and suggestions can be evoked from the results of the study, it has limitations. In this study, factors leading to ADHD are innate and determined after birth, which can only be treated by the environmental and medical intervention. If we want to lower the incidence of ADHD more effectively, factors that trigger ADHD even before birth play an important role. In other words, a life's formation and growth in a mother's embryo are susceptible to external influences. A pregnant woman's behavior may have a colossal impact on her child's possibility of developing ADHD. Therefore, to better prevent the development of ADHD in children, factors such as the mother's smoking or drinking history during pregnancy may be included as prime suspects for future study.

## 5. Conclusion

In this study, logistic regression was used to develop a predictive model to evaluate the probability of Attention Deficit/Hyperactivity Disorder (ADD/ADHD). The National Health Interview Survey (NHIS) Data 2017 was used, and factors such as gender, race, age, and parents' educational level were included in the study. The results indicated that this model can be used for doctors and parents to evaluate the possibility of having children with ADHD. With this model, doctors can provide suggestions for parents, schoolteachers, as well as peers to change the disruptive behavior of ADHD children, help them concentrate in class, and offer them better mental care. An application of this model can also be distributed to parents who are worried about their children's potential mental problems and to teachers who deal with ADHD children every day. With this diagnosis model, we believe that the percentage of children with ADHD will decline and fewer children will suffer from ADHD. In the future, more factors such as the mother's smoking or drinking history during pregnancy may be in need of further study.

## Refernces:

1. "Treatment of ADHD." Centers for Disease Control and Prevention. Centers for Disease Control and Prevention, September 21, 2020. URL: https://www.cdc.gov/ncbddd/adhd/treatment.html
2. ADHD Editorial Board Medically reviewed by Sharon Saline, ADHD Editorial Board, and Sharon Saline. "ADHD Statistics: New ADD Facts and Research." ADDitude, August 6, 2020. URL: https://www.additudemag.com/statistics-of-adhd
3. Holmberg, Kirsten, and Sven Bölte. "Do Symptoms of ADHD at Ages 7 and 10 Predict Academic Outcome at Age 16 in the General Population?" Journal of attention disorders. U. S. National Library of Medicine, November 2014. URL: https://www.ncbi.nlm.nih.gov/pubmed/22837550
4. Chauhan, Avkash. "What Is Variable Importance and How Is It Calculated? – DZone AI." dzone.com. DZone, June 15, 2017. URL: https://dzone.com/articles/variable-importance-and-how-it-is-calculated
5. "Classification: ROC Curve and AUC | Machine Learning Crash Course." Google. Google. Accessed February 3, 2021. URL: https://developers.google.com/machine-learning/crash-course/classification/roc-and-auc
6. "Treatment of ADHD." Centers for Disease Control and Prevention. Centers for Disease Control and Prevention, September 21, 2020. URL: https://www.cdc.gov/ncbddd/adhd/treatment.html

# Section 4. General biology

**https://doi.org/10.29013/ELBLS-21-1.2-52-70**

*Hubert Chen,*
*Ivymind Academy, New Jersey, USA*
*E-mail: lenanikinj@gmail.com*

## SYSTEMATIC ANALYSIS OF GENETIC VARIATION OF DUCHENNE MUSCULAR DYSTROPHY AND IMPLICATION FOR CANCER

**Abstract.** Duchenne muscular dystrophy (DMD) is a rare, severe, progressive genetic disorder causing disability and premature death. Mutations in the DMD gene encoding the dystrophin protein lead to the dystrophinopathies DMD. Phenotypic variations in DMD may also occur in patients with the same primary mutation due to secondary genetic modifiers. Recent advances in molecular therapies for DMD have need of precise genetic diagnosis, since a large number of therapeutic approaches are mutation specific [1]. Interestingly, it has also been reported that muscular dystrophy patients may be at increased risk of malignancy [2; 3]. Although mutations in the DMD genes have been widely studied, to our knowledge, a systematic genetic analysis of all variants, especially single nucleotide polymorphisms (SNPs), of the gene in human have not been reported. In this study, we performed a systematic analysis of the DMD genetic variants via the Single Nucleotide Polymorphism Database (dbSNP), and annotated the functions of the variants with wANNOVAR [4]. The protein-protein interaction (PPI) network for genetic modifiers identified in DMD patients was explored. DMD genetic alternations in different tumors have also been investigated via cBioPortal [5].

We examined a total of 3,627 exonic SNPs in the DMD gene. SNPs distributed across all exons. The largest category was nonsynonymous account for nearly 64% of all mutations. Exon 19 appeared to have most density of pathogenic SNP distribution. Nonsense mutation (i.e. stopgain) or frameshift mutation likely lead to more pathogenic. Among the genetic modifiers identified in DMD patients, THBS1 has higher network topological parameters, followed by SPP1, ACTN3 and LTBP4. Network analysis highlighted non-random interconnectivity between the genetic modifiers identified in DMD patients, and potentially shed light on new genetic modifiers by their functional coupling to these known genes. Gene therapy is a promising experimental approach to treat genetic disease such as DMD [6]. In addition, our results also suggest DMD gene may serve as a diagnostic and therapeutic target for certain types of cancer.

**Keywords:** Duchenne muscular dystrophy (DMD), data mining, genetic, protein-protein interaction (PPI), single nucleotide polymorphisms (SNPs), tumor.

## 1. Introduction

Duchenne muscular dystrophy (DMD), a rare X-linked disorder, is caused by a genetic mutation that prevents the body from producing dystrophin [7], a protein that enables muscles to work properly. It is one of the most common types of muscular dystrophy.

DMD symptom onset is in early childhood, usually between ages 3 and 5 years. Over time, children with Duchenne will have difficulty walking and breathing, then lead to disability, dependence, and premature death. The disease primarily affects boys, but in rare cases it also can affect girls. The prevalence of DMD is approximately 1 in 3500 to 5000 male births worldwide [8]. Muscle weakness is the principal symptom of DMD and worsen over time, first affecting the proximal muscles and later affecting the distal limb muscles. Patients with DMD progressively lose the ability to perform activities independently and often require a wheelchair by their early teens. As the disease progresses, life-threatening heart and respiratory conditions can occur [9]. In general, patients succumb to the disease in their 20s or 30 s [9]; however, disease severity and life expectancy can vary.

DMD is caused by mutations in the DMD gene, which encodes the protein product called dystrophin. DMD gene is one of the largest of the identified human genes, spanning 2.4 Mb of a genomic sequence and corresponding to about 0.1% of the total human genome [10]. The gene consists of 79 exons encoding a 14,000 bp messenger RNA transcript that is translated into dystrophin [11]. The most common mutation responsible for DMD is a deletion spanning one or multiple exons. Such deletions account for 60–70% of all DMD cases. Point mutations are responsible for around 26% of DMD cases [12]. Exonic duplications account for 10 to 15% of all DMD case. Mutations in the DMD gene disrupt the protein's reading frame causing premature stop codons, leaving little or no functional dystrophin protein produced in cells. In addition, phenotypic variations in DMD may also occur in patients with the same primary mutation. A wide range of clinical manifestations suggest that genetic modifiers can influence the severity of DMD disease [13].

Dystrophin protein consists of 3,685 amino acids with molecular weight of 427 kDa and plays a crucial role in muscle function. Cytoplasmic face of the sarcolemma is where dystrophin is located[14]. Based on sequence homology, dystrophin is divided into four distinct structural domains. (i) amino terminal actin binding domain that contains two calponin homology domain which directly interacts with cellular actin cytoskeleton[15]; (ii) a long central rod shaped domain is composed of 24 structurally similar spectrin-type repeats[16]; (iii) cysteine rich domain binds to the intrinsic membrane protein β-dystroglycan; (iv) the carboxy-terminal domain binds to dystrobrevin and syntrophins[17]. Dystrophin is a cytoskeletal protein that binds actin and associates with the dystrophin–glycoprotein complex (DGC) to link the cytoskeleton to the extracellular matrix (ECM)[18, 19]. The DGC consists of integral and peripheral proteins: dystroglycans, sarcoglycans, and syntrophins [18, 19]. Defects in dystrophin and/or other components of the DGC are responsible for several phenotypes of muscular dystrophy including DMD.

The DMD gene produces different transcripts encoding at least seven protein isoforms of various sizes and tissue distributions, each translated from a unique message initiated from one of the seven distinct promoters in the gene. Three full-length, large molecular weight isoforms (427 kDa), expressed primarily in skeletal muscle cells and cardiomyocytes, cortical neurons and the hippocampus of the brain and cerebellar Purkinje cells [20]. The shorter Dp260 and Dp116 isoforms are expressed primarily in the retina and the peripheral nerve, respectively [21]. Dp140 is expressed in the central nervous system (CNS) and kidney. There have been studies linking the lack of Dp140 expression in some DMD patients to cognitive impairment [22]. Finally, the Dp71 isoform is ubiquitously expressed, with higher

levels in the CNS [23]. The literatures usually only describe seven protein coding isoforms. However, the Ensembl.org automatic annotation software predicts the presence of more protein coding splice variants of the dystrophin gene [24].

Although mutations in DMD genes have been widely studied, to our knowledge, a systematic genetic analysis of all variants, especially single nucleotide polymorphisms (SNPs), of the gene in human have not been reported. In this study, we carried out a systematic analysis of the DMD genetic variants via the dbSNP database, and annotated functions of these variants with wANNOVAR[4]. Protein-protein interactions for genetic modifiers identified in DMD patients were explored. In addition, potential relationships of genetic alternations in the DMD gene with cancer were also investigated.

## 2. Materials and Methods

### *2.1 Research workflow*

The DMD genetic research mainly focus on using public-domain human genome databases to perform a systematic analysis of genetic variants especially SNPs in human populations, explore protein-protein interactions for genetic modifiers identified in DMD patients and examine relationships of genetic alternations in DMD gene and types of cancer. No statements of approval or informed consent were required for our study as we obtained data from an open access database. A research workflow was presented in (Figure 1).

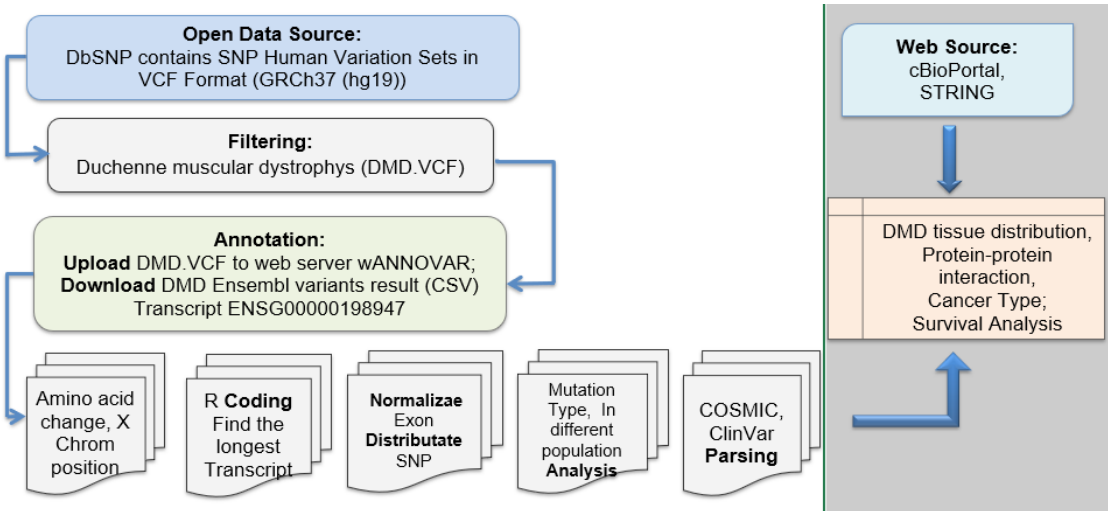


Figure 1. Research Workflow

In brief, all the genetic variants of DMD genes were extracted from the open access Single Nucleotide Polymorphism Database (dbSNP) database with variant call format (VCF). Variants using the online wANNOVAR server to generate output results files. These output files were annotated with function, distribution and disease etc [4]. Data mining and visualization were further performed based on the annotation.

### *2.2 Source dbSNP database and SNPs extraction*

The source data for the DMD gene comes from the dbSNP, which was established by National Center for Biotechnology Information (NCBI) in collaboration with the National Human Genome Research Institute (NHGRI) in 1998 for GenBank of publicly available nucleic acid and protein sequences [32]. In order to extract specific human DMD gene data, build-in Unix compress tool "MacCompress" under a Mac environment was selected to unzip the large size vcf.gz file. To extract DMD variants, we used the command 'grep DMD00-All.vcf > DMD.vcf', then added the header lines of 00-All.vcf into the file.

### *2.3 Functional annotation with wANNOVAR*

Online server wANNOVAR was used to annotate functional consequences of genetic variation [26]. Online annotating single nucleotide variants,

insertions and deletions functions effects on genes, ClinVar database information(Clinvar_DIS, Clinvar_ID), calculating predicted importance scores (SIFT_pred,Polyphen2) of each variant, retrieving allele frequencies in public databases (the 1000 Genomes Project and Genome Aggregation Database (gnomAD) of 15,708 genomes)[27], and implementing a 'variants reduction' protocol to identify a subset of potentially deleterious variants/genes[26].

***2.4 Retrieve ensembl transcript***

The dystrophin gene ENSG00000198947 has different transcripts which described at Ensembl.org [28]. According to wANNOVAR instruction, the most popular approach was to use the longest transcript which provided the most genetic annotation information if multiple transcripts were available [24]. The full-length transcript variant of the dystrophin gene was ensembl transcript (ENST) ID ENST00000357033.9, with13992 length in base pairs (bp) [28]. The R program (R-4.0.2) identified the longest transcript start and end, then split long characters string for AAChange.ensGene. It also picked the exon number and variant type, protein coding information (R scripts in appendix 6.1).

***2.5 Protein-protein interaction map***

Protein-protein interaction map for genetic modifiers identified in DMD patients was constructed using search tool for the retrieval of interacting genes/proteins (STRING v11) [29]. Active interaction sources were restricted to "Textmining," "Experiments," and "Databases." Only interactions with confidence score over 0.9 were mapped to the network. The network obtained from STRING was subsequently analyzed using Cytoscape 3.8.1 plugin Network Analyzer [30]. The nodes in the PPI network represented the genes/proteins, and the edges between the nodes represented the interactions between them. Nodes with high degree and betweenness centrality (BC) value were considered as key parameters to analyze the network. The node with a high degree was deemed with an essential biological function.

***2.6 Integrative analysis genetic alternations in the DMD gene with cancer***

Genetic alternations in the DMD gene with cancer was examined by using Cancer Genomics Portal (cBioPortal) [5]. This web portal provides query interface combined with customized data enabled us to interactively explore genetic alterations across DMD samples, genes mutation site and frequency. Kaplan-Meier curves stratified by genotype were plotted and comparisons were tested using the Log-rank test.

**3. Results**

***3.1 Variant prioritization***

| Func.ensGene | Count |
|---|---|
| downstream | 151 |
| exonic | 3626 |
| exonic;splicing | 1 |
| intergenic | 203 |
| intronic | 376096 |
| ncRNA_exonic | 340 |
| ncRNA_intronic | 251 |
| ncRNA_splicing | 1 |
| splicing | 99 |
| upstream | 167 |
| UTR3 | 1069 |
| UTR5 | 156 |
| Total | 382160 |

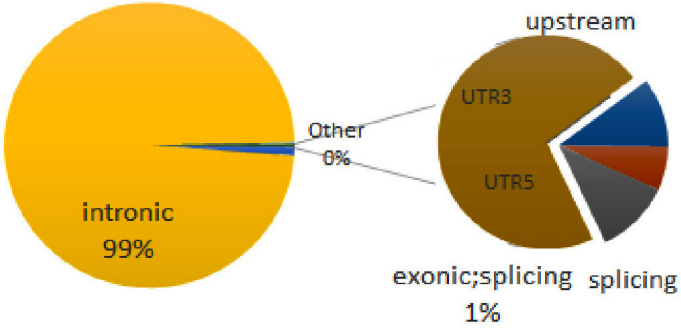


Figure 2. Catalog of genomic regions in the DMD gene

Online wANNOVAR submission for DMD.vcf processed a total of 382160 variants. Variants located mainly in intronic, exonic, and UTR3 variant regions (Figure 2). In this study, genetic variants in exons rather than introns were focused on, because variants in exonic (coding) region often can alter the protein function.

### *3.2 DMD gene annotation output*

DMD exome summary contains a total of 3627 rows and 140 columns, which includes information such as function class of exonic variant. We presented some selected key information (Table 1) in the annotated file that is crucial for our research.

Table 1.– Example of selected key columns in the annotated file

| Columns Name | Description | Annotation |
|---|---|---|
| Start | Start nucleotide number on X chromosome. | 31140001 |
| End | End nucleotide number on X chromosome. | 31140003 |
| Ref | Original nucleotide(s) present before mutation. | C |
| Alt | Alternative nucleotide(s) present after mutation. | G |
| Gene.ensGene | Gene Variant number. | ENSG00000198947 |
| Func.ensGene | Regions (e.g., exonic, intronic, non-coding RNA)) that one variant hit | |
| ExonicFunc.ensGene | Exonic variant function, e.g., synonymous, nonsynonymous, frameshift insertion. | nonsynonymous SNV |
| AAChange.ensGene | Amino Acid Change | ENST00000357033.9: exon45: c.G6502C: p.E2168Q ENST00000378677: exon45: c.G6490C: p.E2164Q |
| COSMIC_DIS | Distribution in Catalogue of Somatic Mutations in Cancer | 1(prostate) |
| ClinVar_SIG | ClinVar uses standard terms for clinical significance recommended by an authoritative source when available. These standards include five terms for diseases [33] | Pathogenic |
| ClinVar_DIS | Clinical significance parameter | Duchenne muscular dystrophy |
| SIFT_score SIFT_pred | SIFT score (deleterious or tolerated) [31] D: Deleterious (sift<=0.05); T: Tolerated (sift>0.05) | *0.239* *D* |
| Polyphen2 HDIV_score | Impact on amino acid sequence and protein function. | 0.291 |
| 1000_exome_ALL | 1000 Genomes Project dataset with allele frequencies in six populations including ALL, AFR (African), AMR (Admixed American), EAS (East Asian), EUR (European), SAS (South Asian). These are whole-genome variants[31]. | 0.005 |

### *3.3 Exonic SNPs frequency in the DMD gene*

We choose wANNOVAR's default definitions of exonic functional categories in order of precedence: deletions, insertions or substitutions for frameshift; stop gain; start loss; deletions, insertions, or substitutions for nonframeshift; nonsynonymous

and synonymous (Table 2). A total of 3627 exonic SNPs in the DMD gene has been examined. The largest category was nonsynonymous account for nearly 64% of all mutations. Synonymous accounted for nearly 43% and followed by stop gain account for nearly 6.7% of all mutations.

Table 2.– Variants Type and Frequency in the DMD Gene

| Variants Definition | Variants Type | Count | Frequency |
|---|---|---|---|
| Insertion, deletion or substitution of one or more nucleotides that cause frameshift changes in protein coding sequence. | frameshift insertion | 47 | 1.30% |
| | frameshift deletion | 116 | 3.20% |
| | frameshift substitution | 3 | 0.08% |
| Variant that leads to the immediate creation of stop codon at the variant site; | stopgain | 242 | 6.67% |
| Variant that leads to the immediate elimination of stop codon at the variant site | startloss | 1 | 0.03% |
| Insertion, deletion or substitution of 3 or multiples of 3 nucleotides that do not cause frameshift changes in protein coding sequence. | nonframeshift insertion | 4 | 0.11% |
| | nonframeshift deletion | 27 | 0.74% |
| | nonframeshift substitution | 1 | 0.03% |
| A single nucleotide change that cause an amino acid change | nonsynonymous | 2322 | 64.02% |
| A single nucleotide change that does not cause an amino acid change | synonymous | 864 | 23.82% |
| | Total variants | 3627 | |

High frequency nucleotide substitutions have been observed in the DMD gene. The largest category was Guanine (G) to Adenine (A) with 17%, followed by Cytosine (C) to Thymine (T) with 15% and Thymine (T) to Cytosine (C) with 15%, respectively (Figure 3).

| Count and Percentage of High frequency AAChange | | |
|---|---|---|
| G-->A | 614 | 17% |
| C-->T | 561 | 15% |
| T-->C | 533 | 15% |
| A-->G | 303 | 8% |
| C-->A | 259 | 7% |
| G-->C | 213 | 6% |
| T-->A | 203 | 6% |
| C-->G | 182 | 5% |
| T-->G | 178 | 5% |
| G-->T | 177 | 5% |
| A-->T | 100 | 3% |
| A-->C | 93 | 3% |
| Other | 211 | 6% |
| *Toatl* | *3627* | |

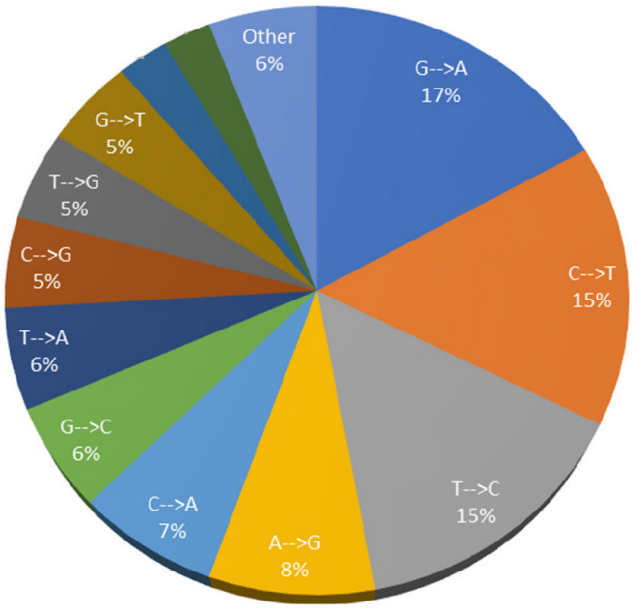


Figure 3. Summary of amino acid change in the DMD gene

### *3.4 DMD gene variants in Human 1000 Genomes Project*

DMD ensemble in this project contains the 1000 Genomes project data in annotation. 1000 Genomes project was designed to provide a comprehensive description of human genetic variation through sequencing multiple individuals. Populations were classified into 5 major continental groups: Africa (AFR), America (AMR), Europe (EUR), East Asia (EAS), and South Asia (SAS)[34].The DMD gene variants frequency from several different continents were showed in Table 3 and Figure 4. Approximately 7% nonsynonymous mutations were observed from 1000 Genomes project, with relatively higher alteration frequency in African (~3%). Similar frequency distributions were observed among America, Europe, East Asia, and South Asia. No frameshift and nonframeshift mutations and startloss were reported in 1000 Genomes project.

Table 3.– DMD gene variants frequency in Human 1000 Genomes Project

| Variants Type | All DMD Exome | 1000G ALL | 1000G AFR | 1000G AMR | 1000G EAS | 1000G EUR | 1000G SAS |
|---|---|---|---|---|---|---|---|
| nonsynonymous | 2320 | 165(7.1%) | 67(2.9%) | 34(1.6%) | 47(2%) | 35(1.5%) | 41(1.8%) |
| stopgain | 242 | 2(0.8%) | 0 | 1(0.4%) | 0 | 0 | 0 |
| synonymous | 735 | 83(11.3%) | 33(4.5%) | 19(2.6%) | 19(2.6%) | 16(2.2%) | 21(2.9%) |
| frameshift deletion | 95 | 0 | 0 | 0 | 0 | 0 | 0 |
| frameshift insertion | 37 | 0 | 0 | 0 | 0 | 0 | 0 |
| frameshift substitution | 2 | 0 | 0 | 0 | 0 | 0 | 0 |
| nonframeshift deletion | 22 | 0 | 0 | 0 | 0 | 0 | 0 |
| nonframeshift insertion | 2 | 0 | 0 | 0 | 0 | 0 | 0 |
| nonframeshift substitution | 1 | 0 | 0 | 0 | 0 | 0 | 0 |
| startloss | 1 | 0 | 0 | 0 | 0 | 0 | 0 |
| Total | 3297 | 250 (7.6%) | 100 (3%) | 154 (4.7%) | 66 (2%) | 41 (1.2%) | 63 (1.9%) |

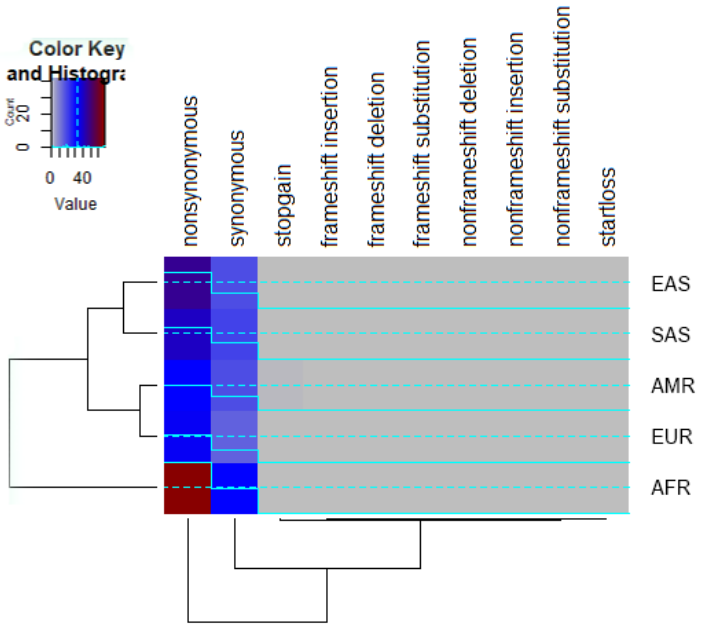


Figure 4. DMD gene variants frequency from different continents. Different colors represent for different levels of frequency values by R Heatmap Script in the appendix 6.2.

### *3.6 SNPs distribution by exons*

In the DMD gene, SNPs were distributed across all the exons. Exon 79 is the longest with 2703 bp in length. Exon 78 is the shortest with 32 bp. To a better understanding of SNPs distribution density, we normalized the length of the exon, and as such high-frequency SNPs were observed in exon 19, 13, 71, respectively (Figure 5). Interestingly, although Exon 79 is the longest exon, there is a low distribution of genetic variants in this gene region. A further investigation revealed that the majority region of the exons belongs in the 3'untranslated region (3'-UTR). With consideration for the low SNP frequency in the 5'-UTR, demonstrates that the genetic variation of DMD gene mainly occurs in the protein-coding region. This implies a potential genetic interaction between variation and protein function.

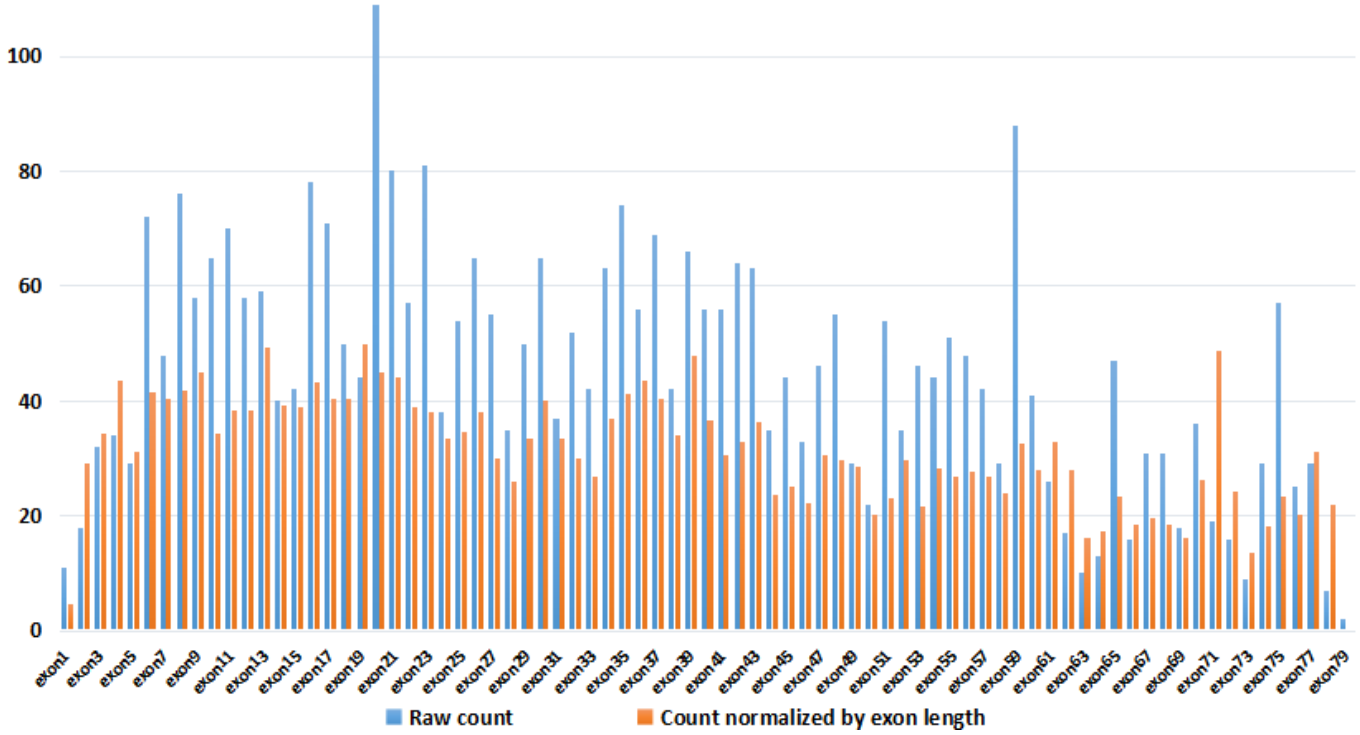


*The x-axis only shows exon odd-number due to space*

Figure 5. The frequency and distribution density of genetic variants in the exons of DMD gene

### *3.7 SNPs distribution by ACMG classification*

Variants according to ACMG Standards and Guidelines for clinical laboratories were classified as: 'Benign', 'Likely benign', 'Pathogenic', and 'Likely pathogenic [35].

Distribution of SNPs by ACMG Classifications in the DMD Gene presented in (Figure 6). Stop-gain caused 57% pathogenic, followed by frameshift (22%). In general, most of synonymous mutation have no functional consequence. Interestingly, we observed a few cases with synonymous mutation (2%) also associated with pathogenic DMD in the current analysis.

Distribution of SNPs by exonic region and ACMG classification in the DMD gene presented in (Figure 7). In general, pathogenic variants were distributed across almost all exons. In many exons (i.e. exon 19), most variants were pathogenic. However, in some other exons (i.e. exon 37), benign variants occurred more frequently. Exon 19 has most density of pathogenic SNP distribution and followed by exon 20.

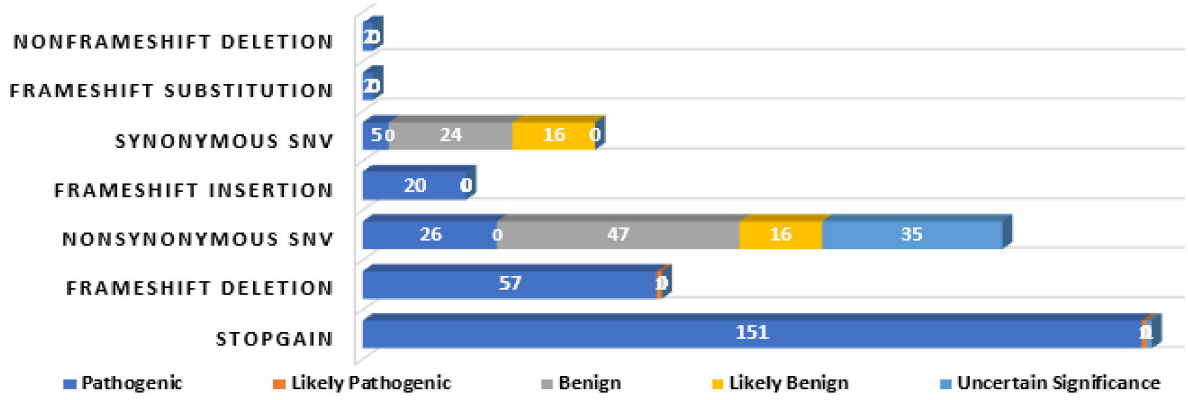


| | Stopgain | Frameshift deletion | Nonsynonymous SNV | Frameshift Insertion | Synonymous SNV | Frameshift Substitution | Nonframeshift Deletion |
|---|---|---|---|---|---|---|---|
| Pathogenic | 151 | 57 | 26 | 20 | 5 | 2 | 2 |
| Likely Pathogenic | 1 | 1 | 0 | 0 | 0 | 0 | 0 |
| Benign | 0 | 0 | 47 | 0 | 24 | 0 | 0 |
| Likely Benign | 0 | 0 | 16 | 0 | 16 | 0 | 0 |
| Uncertain Significance | 1 | 0 | 35 | 0 | 0 | 0 | 0 |

Figure 6. Distribution of SNPs by ACMG-AMP classifications in the DMD gene

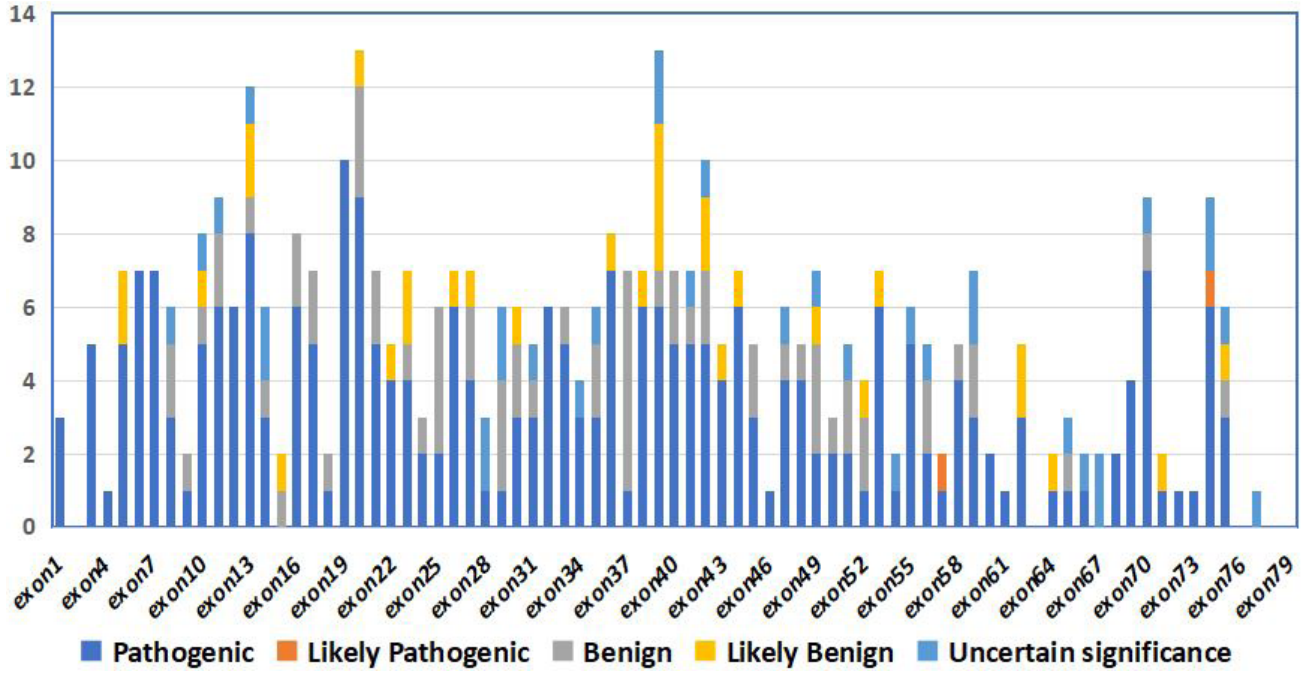


*The x-axis only shows every third exon number due to space*

Figure 7. Distribution of SNPs by exonic region and ACMG classification in the DMD gene

***3.8 Network analysis highlights non-random interconnectivity between the genetic modifiers identified in DMD patient***

Genetic modifiers have been associated with variability in human DMD sub-phenotypes[13]: SPP1, LTBP4, and THBS1 are mapped to the TGF-β pathway, and implicated in several interconnected molecular pathways regulating inflammatory response to muscle damage, regeneration, and fibrosis. ACTN3 deficiency triggered an increase in oxidative muscle metabolism through activation of calcineurin, and then ameliorated the progression of

dystrophic pathology. We considered SPP1, LTBP4, ACTN3 and THBS1 as the "seed" genes/proteins to construct the PPI network associated with DMD (Figure 8) [36]. Fifteen additional interactors were allowed in the network to identify the most significant interactions and achieve a meaningful size for network analysis. PPI analyses showed that ACTN3 had direct interaction with DMD. SPP1 may interact with DMD through ITGB1, which has the highest node degree and BC values in the network. ITGB1 is one of the most common forms in muscle. Disruptions of integrins are responsible for a further class of muscular dystrophies [37]. Among the "seed" genetic modifiers, THBS1 has higher network topological parameters, followed by SPP1, ACTN3 and LTBP4. The network enrichment p-value was < 3.09e-08, meaning that this connected network has significantly more interactions than expected at random, and that the genetic modifiers have more interactions among themselves than what would be expected for a random set of genes/proteins of similar size. Such enrichment also indicates that these genetic modifiers are, at least partially, biologically connected. In addition, the PPI network may be possible to shed light on new genetic modifiers by their functional coupling to these known "seed" genes.

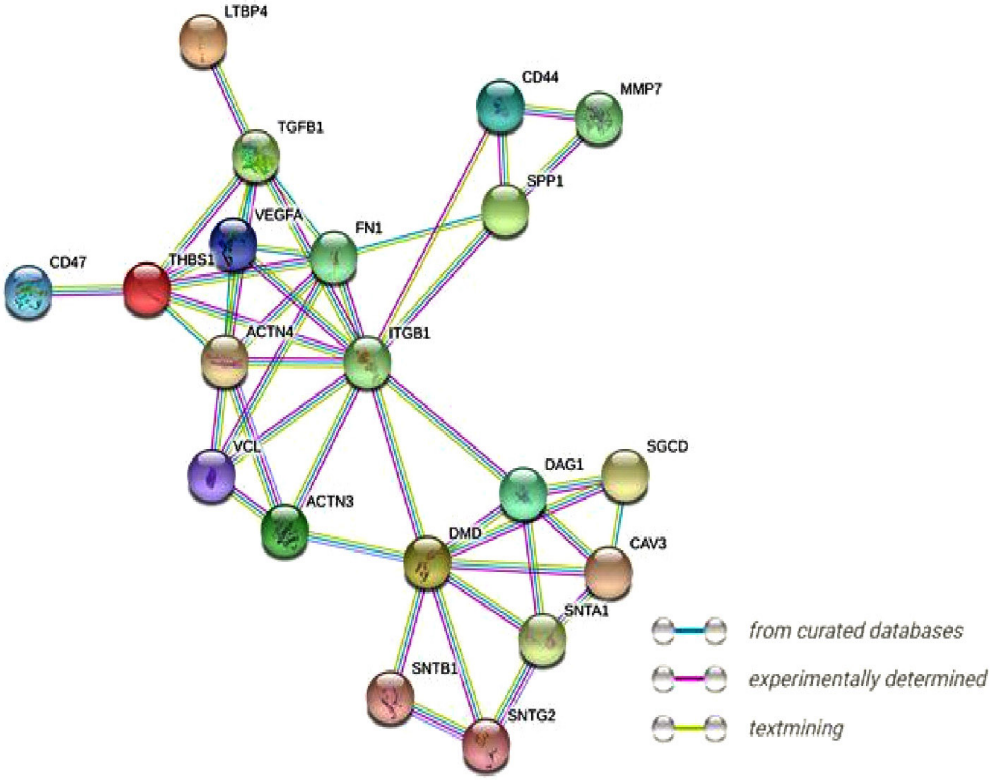


Figure 8. Interaction network resulting from the genetic modifiers identified in DMD patients

***3.9 Exon DMD genetic alternations in different tumors***

After examining SNPs distribution by ACMG Classification from DMD functional annotation output file, it appeared genetic alternations in the DMD gene associated with different types of cancers. It has also been reported that DMD gene is involved in tumor development and progression [38–41]. Therefore, we further analyzed data from 25 published cancer studies from The Cancer Genome Atlas (TCGA) and 4 pediatric cancer studies that included a minimum of 100 samples in the cBioPortal database. Since people with DMD could develop rare and aggressive type of muscle cancer (i.e. rhabdomyosarcoma), we also included one study that analyzed 43 rabdomyosarcomas cases. Total 11927

patients (age from ~ 3 years to 90 years; ~ 48% male and ~ 46% female; ~ 60% white, ~7% black or africa america and ~ 5% asian) and 11977 samples from 30 studies have been included in the analysis. Approximately 10% of the cases have an alteration in the DND gene, consisting mainly of missense mutation and truncating mutation. The studies analyzed were listed in the appendix 6.4.

Table 4. – Example of DMD gene mutations with cancers

| Cancer Type | Functional Impact | Mutation Type | Variant Type | HGVSc | Exon |
|---|---|---|---|---|---|
| Bladder Urothelial Carcinoma | MutationAssessor: NA; SIFT: impact: deleterious, score: 0; Polyphen-2: impact: probably_damaging, score: 0.994 | Missense_Mutation | SNP | ENST00000357033.4: c.1940T>C | 16/79 |
| Bladder Urothelial Carcinoma | MutationAssessor: NA; SIFT: impact: tolerated, score: 0.76; Polyphen-2: impact: probably_damaging, score: 0.985 | Missense_Mutation | SNP | ENST00000357033.4: c.2215G>A | 18/79 |
| Bladder Urothelial Carcinoma | MutationAssessor: NA; SIFT: NA; Polyphen-2: NA | Nonsense_Mutation | SNP | ENST00000357033.4: c.4222C>T | 30/79 |
| Bladder Urothelial Carcinoma | MutationAssessor: NA; SIFT: impact: tolerated, score: 0.25; Polyphen-2: impact: benign, score: 0.219 | Missense_Mutation | SNP | ENST00000357033.4: c.4117C>A | 30/79 |
| Rectal Adenocarcinoma | MutationAssessor: NA; SIFT: impact: tolerated, score: 0.19; Polyphen-2: impact: possibly_damaging, score: 0.475 | Missense_Mutation | SNP | ENST00000357033.4: c.5824G>A | 41/79 |
| Bladder Urothelial Carcinoma | MutationAssessor: NA; SIFT: NA; Polyphen-2: NA | Missense_Mutation | SNP | ENST00000357033.4: c.7213G>T | 50/79 |
| Bladder Urothelial Carcinoma | MutationAssessor: NA; SIFT: impact: deleterious, score: 0.03; Polyphen-2: impact: probably_damaging, score: 0.926 | Missense_Mutation | SNP | ENST00000357033.4: c.7891C>T | 54/79 |
| Adrenocortical Carcinoma | MutationAssessor: NA; SIFT: impact: tolerated, score: 0.4; Polyphen-2: impact: benign, score: 0.164 | Missense_Mutation | SNP | ENST00000357033.4: c.8464C>A | 57/79 |
| Adrenocortical Carcinoma | MutationAssessor: NA; SIFT: NA; Polyphen-2: NA | Frame_Shift_Ins | INS | ENST00000357033.4: c.8528dup | 57/79 |
| Bladder Urothelial Carcinoma | MutationAssessor: NA; SIFT: impact: tolerated, score: 0.35; Polyphen-2: impact: benign, score: 0.005 | Missense_Mutation | SNP | ENST00000357033.4: c.8641C>G | 58/79 |
| Adrenocortical Carcinoma | MutationAssessor: NA; SIFT: impact: deleterious, score: 0; Polyphen-2: impact: probably_damaging, score: 1 | Missense_Mutation | SNP | ENST00000357033.4: c.9766G>A | 67/79 |

The majority of DMD genetic alterations corresponded to mutations and deep deletions, and a low frequency of gene amplifications. The occurrence of DMD alterations varied across the studies/tumor types (Figure 9). The highest ratio of genetic alternations was approximately 31% (Esophagus, TCGA PanCan), and followed by 25% (Uterine TCGA PanCan 2018). There were approximately 967 missense

mutations and 246 truncating mutation in the tumor samples, with highest frequency (8 of nonsense mutation) being R1459*/Q in the kinase domain. There appeared to be no hot spots of alteration in the gene region (Figure 10). Interestingly, DMD alterations were not found in rabdomyosarcomas samples.

***3.10 Patients with DMD alterations have poorer overall survival***

To study the overall survival (OS) of patients with and without DMD genetic alterations, Kaplan-Meier curves stratified by genotype were plotted and the comparisons were tested using the Log-rank test [5]. OS analysis has been initially conducted using cBioPortal with pooled all patient data from 30 different cancer studies as mentioned in previous section (appendix 6.4). We observed that patients with genetic alterations in DMD had significantly shorter OS (63.8 months) compared to patients with wild-type DMD (82.9 months) (Figure 11).

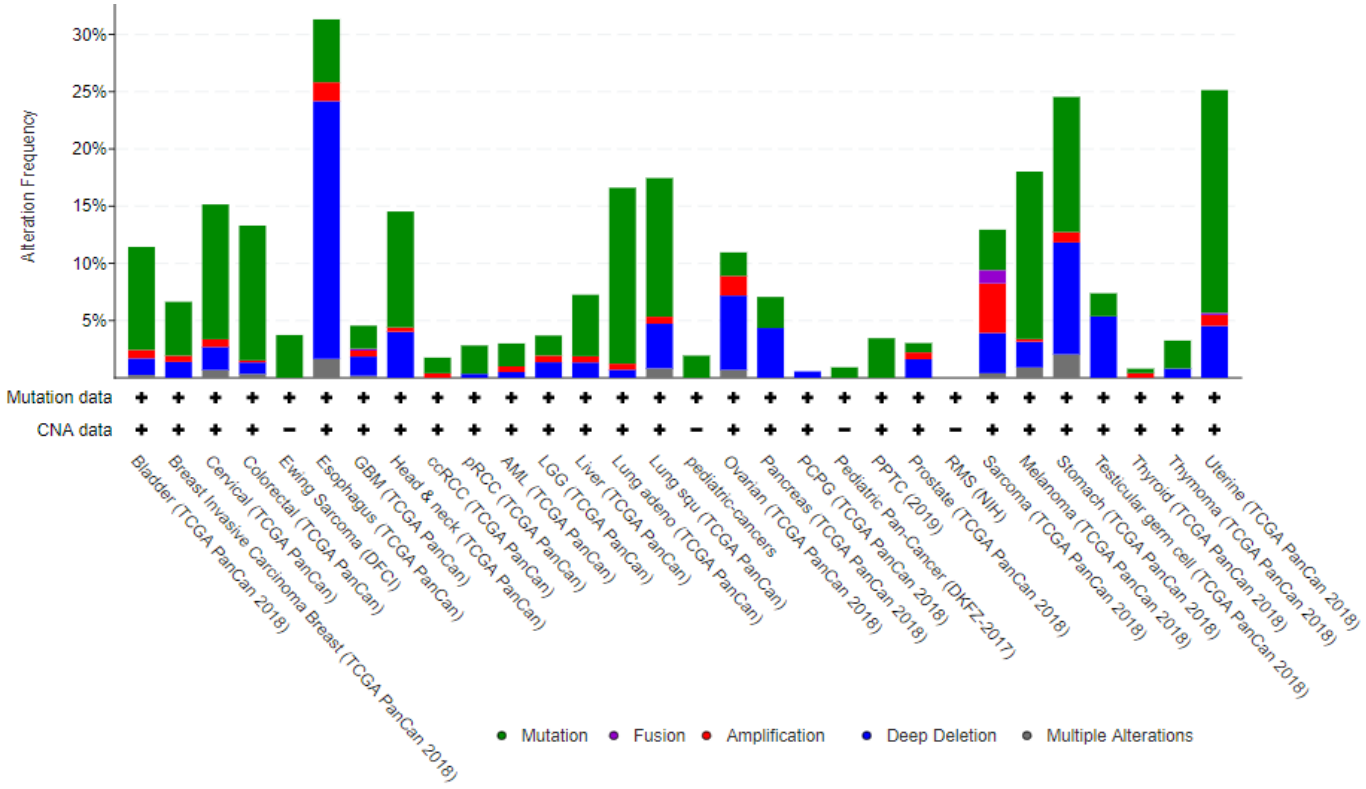


*The x-axis shows the types of cancer (color coded), availability of mutation and copy number variation data, and the study abbreviation*

Figure 9. Frequency of genetic alternations in the DMD gene in different types of tumors

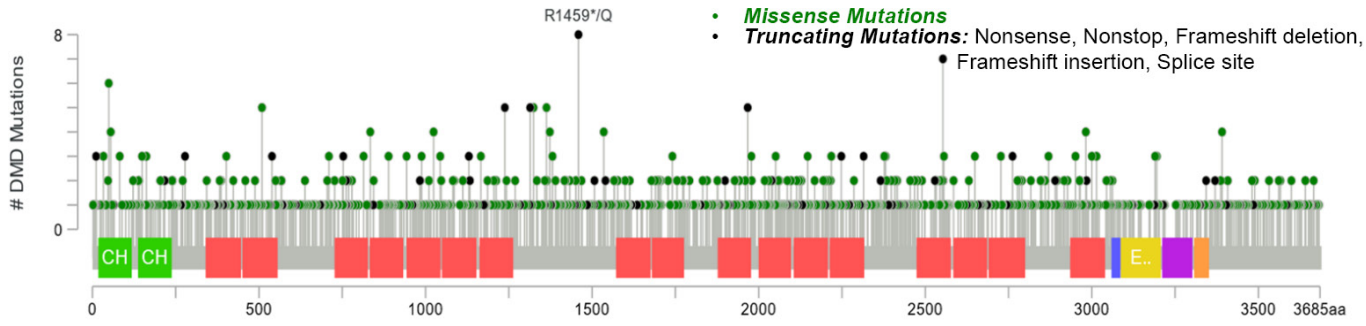


Figure 10. Mutation diagram of DMD gene in the tumor samples

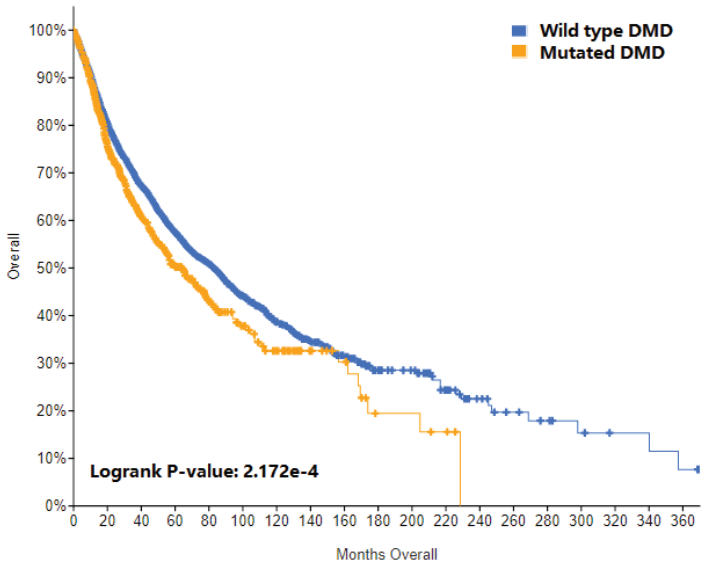


Figure 11. Overall survival analyses using c BioPortal data

Additional OS analysis has been performed by various tumor types with greater than 5% DMD genetic alteration frequency[5]. Invasive breast carcinoma and esophageal carcinoma that revealed significant differences between by wild-type DMD or mutated DMD groups (Figure 12). Others such as ovarian carcinomas showed similar trend, but not statistically significant (Figures not presented). OS analysis of breast cancer patients with low or high expression of DMD gene has been further conducted by using Kaplan-Meier Plotter (www.kmplot.com/analysis) [42]. Likewise, low DMD expression is associated with poorer survival in breast cancer patients. These results demonstrate that the relationship between DMD genetic status and prognosis may be tumor-type specific. Moreover, its biological function in tumorigenesis as well as prognosis is complicated and co-regulated with other factors.

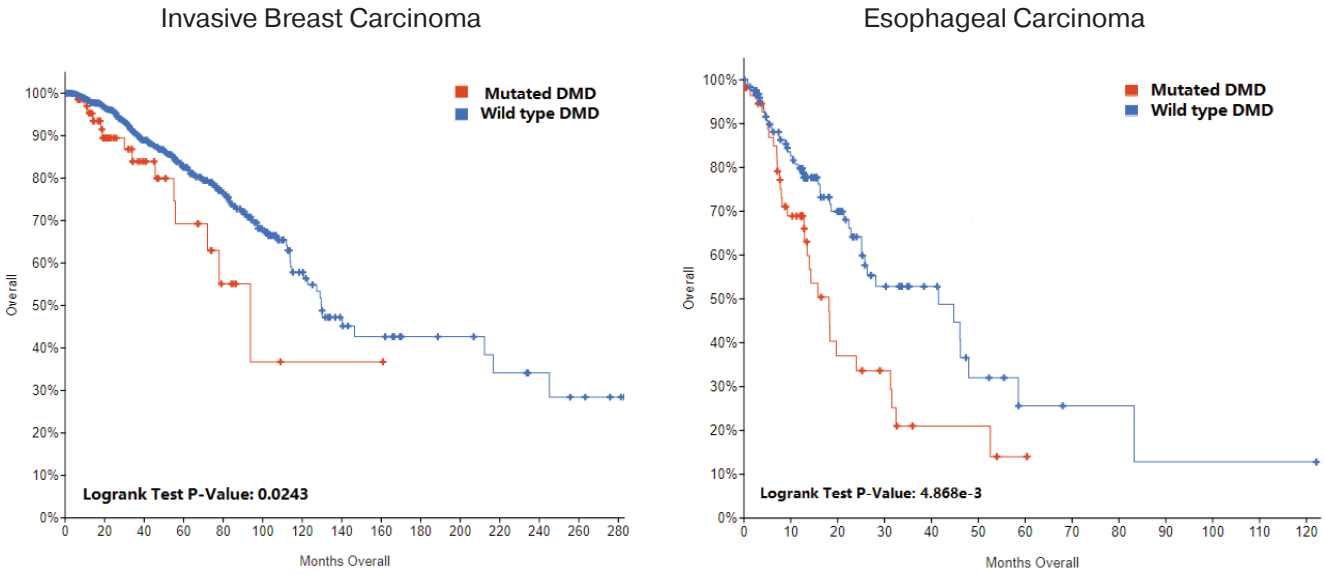


Figure 12. Overall survival for invasive breast carcinoma and esophageal carcinoma using cBioPortal data

**4. Discussions**

DMD is a rare, severe, progressive genetic disorder causing disability and premature death. DMD caused by mutations in the dystrophin-encoding DMD gene, which is one of the largest of the identified human genes. There are currently no curative therapies for DMD. Gene therapy is a promising experimental method that uses genes (the fundamental units of heredity) to treat disorders that result from genetic mutations. Currently, several kinds of gene-based therapies including exon skipping are being developed to treat DMD.

Although mutations in DMD genes have been widely studied, to our knowledge, a systematic genetic analysis of all variants, especially SNPs, of the gene in human have not been reported. In general, Variants in exonic (coding) region can alter the protein function. Therefore, we focused on a total of 3627 exonic SNPs. In the DMD gene, SNPs distributed across all exons. The largest category was nonsynonymous account for nearly 64% of all mutations. Exon 19 appeared to be most pathogenic region. As expected, nonsense mutation (i.e. stopgain) or frameshift mutation likely lead to more pathogenic DMD. Of note, the limitation of current database may not perfectly represent the DMD patient population, since the database collects all genetic variations from various individuals, but not merely DMD patients. Therefore, the result in the study reveals richer variations in human populations than in DMD patients. Interestingly, some pathogenetic variants were also observed in healthy individuals. For example, a few nonsynonymous and stop gain cases were observed in the 1000 Genomes project, although the allele frequency was very low. Healthy individuals may also carry DMD related genetic alternations. However, for each gene, there are homologous alleles from the mother and father, so the abnormality of one of the alleles will not lead to disease. This may explain why normal individuals carry DMD mutations without clinic symptoms.

Phenotypic variations in DMD may also occur in patients with the same primary mutation. A wide range of clinical manifestations suggest that genetic modifiers such as SPP1, LTBP4, ACTN3, and THBS1 can modify the clinical severity of DMD disease [13]. As expected, our PPI analysis highlighted non-random interconnectivity between the genetic modifiers identified in DMD patients, and potentially shed light on new genetic modifiers by their functional coupling to these known genes.

The genomic, functional and clinicopathological evidence demonstrate dystrophin tumor suppressor roles in human cancers. People with DMD may increase risks to develop aggressive and rare muscle cancer such as rhabdomyosarcoma[38, 43]. In the current study, we have used the cBioPortal for cancer genomics as a tool for visualizing, exploring and analyzing the biological and clinical characteristics of DMD genetic alterations with cancer. Total 11927 patients and 11977 samples from 30 studies with various types of tumors have been included in the analysis. Approximately 10% of the cases had an alteration in the DMD gene, consisting mainly of missense mutation and truncating mutation. We observed DMD genetic alterations varied across the studies/tumor types. Patients with DMD genetic alterations appeared to have shorter overall survival, particularly with esophageal carcinoma and invasive breast carcinoma. Similarly, Stephens et al. also reported poorer survival for patients with upper gastrointestinal cancer and low expression of DMD[39]. However, there were no significant correlations between DMD genetic alterations and overall survival in some other types of human cancers. These results demonstrate that the relationship between DMD genetic status and prognosis may be tumor-type specific. Moreover, its biological function in tumorigenesis as well as prognosis is complicated and co-regulated with other factors.

Leonela N. Luce et al conducted paired tumor/normal tissues showed that majority of tumor specimens had lower DMD expression compared to the normal adjacent tissue [44], in concordance to the

other reports suggesting the tumor suppressor role of DMD[38]. Contrastingly, overexpression of the DMD gene has also been reported in leukemias, renal carcinomas, ependymomas, and astrocytomas [44]. The function and molecular mechanism involved in altered DMD gene expression in different cancer types remains to be further investigated.

**5. Conclusions**

In conclusion, to our knowledge, this is first data mining study with a systematic genetic analysis of all variants, especially SNPs, of the DMD gene in human. SNPs distributed across all Exons. The largest category was nonsynonymous account for nearly 64% of all mutations. Exon 19 appeared to have most density of pathogenic SNP distribution. Nonsense mutation (i.e. stopgain) or frameshift mutation likely lead to more pathogenic. Network analysis highlighted non-random interconnectivity between the genetic modifiers identified in DMD patients, and potentially shed light on new genetic modifiers by their functional coupling to these known genes. In addition, our results also suggest DMD gene may serve as a diagnostic and therapeutic target for certain types of cancer.

**6. Appendix**

***6.1 R Script of "Extract the longest length transcript with Exon Number, amino acid change from DMD gene exome file"***

```
# String work
library(stringr)
library(dplyr)
# Read Path where your CSV file is located
DMD<- read.csv(file = 'Read Path where CSV file
located\\DMD_query.output.exome_summary.
csv')
head(DMD)
library(stringr)
location<-str_locate(DMD$AAChange.
ensGene,"ENST00000357033")
location
startpos<-location[,1] startpos
endpos<-location[,2] endpos
str_sub(DMD$AAChange.ensGene, startpos,
 endpos+25)
# Export ENST00000357033 segment CSV
DMD_ENST_Output<-str_
sub(DMD$AAChange.ensGene, startpos, end-
pos+25)
write.csv(DMD_ENST_putput, file = "DMD_
ENST_Output.csv")
```

***6.2 R Script for Heatmap of DMD variants frequency from different population in 1000 Genomes project***

```
# Read DMD variants frequency VS1000 gene popu-
lation file from ENSG0000019894
DMDgeneExp <- read.csv'Read Path where CSV
file located\\heatmap\\1000genomeproject.csv")
install.packages('caTools')
library(gplots)
head(DMDgeneExp)
rownames(DMDgeneExp) <- make.unique(as.
character(DMDgeneExp $Variants.Type))
DMDgeneExp_matrix <- as.matrix(DMDgeneExp
[2:6])
head(DMDgeneExp_matrix)
dist_no_na <- function(mat) {
edist <- dist(mat)
edist[which(is.na(edist))] <- max(edist,
na.rm=TRUE) * 1.1
return(edist)
}
colors = c(seq(–3,-2, length=100),
seq(–2,0.5, length=100),
seq(0.5,6, length=100))
my_palette <- colorRampPalette(c("grey","blue","d
arkred"))(n = 100)
# Heatmap plotted
heatmap.2(DMDgeneExp_matrix, distfun=dist_
no_na, col=my_palette,
key=TRUE, symkey=FALSE,
cexRow=0.01, cexCol=1.2,
offsetRow = 0,
densadj = 0.15,
margins=c(4,16),
lwid = c(5,20))
```

### *6.3 Amino acid descriptions*

| One letter code | Three letter code | Amino acid | Possible codons |
|---|---|---|---|
| A | Ala | Alanine | GCA, GCC, GCG, GCT |
| B | Asx | Asparagine or Aspartic acid | AAC, AAT, GAC, GAT |
| C | Cys | Cysteine | TGC, TGT |
| D | Asp | Aspartic acid | GAC, GAT |
| E | Glu | Glutamic acid | GAA, GAG |
| F | Phe | Phenylalanine | TTC, TTT |
| G | Gly | Glycine | GGA, GGC, GGG, GGT |
| H | His | Histidine | CAC, CAT |
| I | Ile | Isoleucine | ATA, ATC, ATT |
| K | Lys | Lysine | AAA, AAG |
| L | Leu | Leucine | CTA, CTC, CTG, CTT, TTA, TTG |
| M | Met | Methionine | ATG |
| N | Asn | Asparagine | AAC, AAT |
| P | Pro | Proline | CCA, CCC, CCG, CCT |
| Q | Gln | Glutamine | CAA, CAG |
| R | Arg | Arginine | AGA, AGG, CGA, CGC, CGG, CGT |
| S | Ser | Serine | AGC, AGT, TCA, TCC, TCG, TCT |
| T | Thr | Threonine | ACA, ACC, ACG, ACT |
| V | Val | Valine | GTA, GTC, GTG, GTT |
| W | Trp | Tryptophan | TGG |
| X | X | any codon | NNN |
| Y | Tyr | Tyrosine | TAC, TAT |
| Z | Glx | Glutamine or Glutamic acid | CAA, CAG, GAA, GAG |
| * | * | stop codon | TAA, TAG, TGA |

### *6.4 Cancer studies analyzed from cBioPortal*

| Type of cancer – study abbreviation | Number |
|---|---|
| *1* | *2* |
| Bladder Urothelial Carcinoma (TCGA, PanCancer Atlas) | 411 |
| Colorectal Adenocarcinoma (TCGA, PanCancer Atlas) | 594 |
| Breast Invasive Carcinoma (TCGA, PanCancer Atlas) | 1084 |
| Brain Lower Grade Glioma (TCGA, PanCancer Atlas) | 514 |
| Glioblastoma Multiforme (TCGA, PanCancer Atlas) | 592 |
| Cervical Squamous Cell Carcinoma (TCGA, PanCancer Atlas) | 297 |
| Esophageal Adenocarcinoma (TCGA, PanCancer Atlas) | 182 |
| Stomach Adenocarcinoma (TCGA, PanCancer Atlas) | 440 |
| Head and Neck Squamous Cell Carcinoma (TCGA, PanCancer Atlas) | 523 |
| Kidney Renal Clear Cell Carcinoma (TCGA, PanCancer Atlas) | 512 |
| Kidney Renal Papillary Cell Carcinoma (TCGA, PanCancer Atlas) | 283 |

| *1* | *2* |
|---|---|
| Liver Hepatocellular Carcinoma (TCGA, PanCancer Atlas) | 372 |
| Lung Adenocarcinoma (TCGA, PanCancer Atlas) | 566 |
| Lung Squamous Cell Carcinoma (TCGA, PanCancer Atlas) | 487 |
| Acute Myeloid Leukemia (TCGA, PanCancer Atlas) | 200 |
| Ovarian Serous Cystadenocarcinoma (TCGA, PanCancer Atlas) | 585 |
| Pancreatic Adenocarcinoma (TCGA, PanCancer Atlas) | 184 |
| Prostate Adenocarcinoma (TCGA, PanCancer Atlas) | 494 |
| Skin Cutaneous Melanoma (TCGA, PanCancer Atlas) | 448 |
| Pheochromocytoma and Paraganglioma (TCGA, PanCancer Atlas) | 178 |
| Sarcoma (TCGA, PanCancer Atlas) | 255 |
| Testicular Germ Cell Tumors (TCGA, PanCancer Atlas) | 149 |
| Thymoma (TCGA, PanCancer Atlas) | 123 |
| Thyroid Carcinoma (TCGA, PanCancer Atlas) | 500 |
| Uterine Corpus Endometrial Carcinoma (TCGA, PanCancer Atlas) | 529 |
| Pediatric Pan-Cancer (DKFZ, Nature 2017) | 961 |
| Pediatric Ewing Sarcoma (DFCI, Cancer Discov 2014) | 107 |
| Pediatric Preclinical Testing Consortium (CHOP, Cell Rep 2019) | 261 |
| Pediatric Pan-cancer (Columbia U, Genome Med 2016) | 103 |
| Rhabdomyosarcoma (NIH, Cancer Discov 2014) | 43 |

## References


1. Mohammed F., et al., Mutation spectrum analysis of Duchenne/Becker muscular dystrophy in 68 families in Kuwait: The era of personalized medicine. PLoS One, 2018.– 13(5).– e0197205 p.
2. Gadalla S. M., et al. Cancer risk among patients with myotonic muscular dystrophy. Jama, 2011.– 306(22).– P. 2480–6.
3. Win A. K., et al. Increased cancer risks in myotonic dystrophy. Mayo Clin Proc, 2012.– 87(2).– P. 130–5.
4. Lab W. G. wANNOVAR. 2010–2020. Available from: URL: http://wannovar.wglab.org/
5. cBio Portal for Cancer Genomics. 2020. Available from: URL: https://www.cbioportal.org/
6. Nelson S. F., et al. Emerging genetic therapies to treat Duchenne muscular dystrophy. Current opinion in neurology, 2009.– 22(5).– 532 p.
7. Salmaninejad A., et al. Duchenne muscular dystrophy: an updated review of common available therapies. Int J Neurosci, 2018.– 128(9).– P. 854–864.
8. Wang R. T. and Nelson S. F. What can Duchenne Connect teach us about treating Duchenne muscular dystrophy? Curr Opin Neurol, 2015.– 28(5).– P. 535–41.
9. BioIncept L. Potential to effectively protect muscle function, combatting Duchenne muscular dystrophy. 2020. Available from: URL: https://bioincept.com/product-development/duchenne-muscular-dystrophy/
10. Van Belzen D. J., et al. Mechanism of Deletion Removing All Dystrophin Exons in a Canine Model for DMD Implicates Concerted Evolution of X Chromosome Pseudogenes. Mol Ther Methods Clin Dev, 2017.– 4.– P. 62–71.

11. Lee B. L., et al. Genetic analysis of dystrophin gene for affected male and female carriers with Duchenne/Becker muscular dystrophy in Korea. J Korean Med Sci, 2012.– 27(3).– P. 274–80.
12. Gao Q. Q. and E. M. Mc Nally. The Dystrophin Complex: Structure, Function, and Implications for Therapy. Compr Physiol, 2015.– 5(3).– P. 1223–39.
13. Bello L., Pegoraro E. The "Usual Suspects": Genes for Inflammation, Fibrosis, Regeneration, and Muscle Strength Modify Duchenne Muscular Dystrophy. J Clin Med. 2019 May 10; – 8(5).– 649 p.
14. Porter G. A., et al. Dystrophin colocalizes with beta-spectrin in distinct subsarcolemmal domains in mammalian skeletal muscle. J Cell Biol, 1992.– 117(5).– P. 997–1005.
15. Norwood F. L., et al. The structure of the N-terminal actin-binding domain of human dystrophin and how mutations in this domain may cause Duchenne or Becker muscular dystrophy. Structure, 2000.– 8(5).– P. 481–91.
16. Muthu M., Richardson K. A. and Sutherland-Smith A. J. The crystal structures of dystrophin and utrophin spectrin repeats: implications for domain boundaries. PLoS One, 2012.– 7(7).– e40066 p.
17. Broderick M. J. and Winder S. J. Spectrin, alpha-actinin, and dystrophin. Adv Protein Chem, 2005.– 70.– P. 203–46.
18. Henry M. D. and Campbell K. P. Dystroglycan: an extracellular matrix receptor linked to the cytoskeleton. Curr Opin Cell Biol, 1996.– 8(5).– P. 625–31.
19. Blake D. J., Tinsley J. M. and Davies K. E. Utrophin: a structural and functional comparison to dystrophin. Brain Pathol, 1996.– 6(1).– P. 37–47.
20. Heikoop J. C., Hogervorst F. B.L., Meershoek E. J. et al. Expression of the Human Dp 71 (Apo-Dystrophin-1) Gene from a 760-kb DMD-YAC Transferred to Mouse Cells. Eur J Hum Genet 3, 1995.– P. 168–179.
21. D'Souza V.N. et al. A novel dystrophin isoform is required for normal retinal electrophysiology. Human molecular genetics – Vol. 4,5. 1995.– P. 837–42.
22. Taylor P. J., et al. Dystrophin gene mutation location and the risk of cognitive impairment in Duchenne muscular dystrophy. PLoS One, 2010.– 5(1).– e8803 p.
23. Lederfein D. et al. A 71-kilodalton protein is a major product of the Duchenne muscular dystrophy gene in brain and other nonmuscle tissues. Proceedings of the National Academy of Sciences of the United States of America – Vol. 89.– 12. 1992.– P. 5346–50.
24. Yates A., et al. Ensembl 2016. Nucleic Acids Res, 2016.– 44(D1).– P. D710–6.
25. dbSNP. 2020. Available from: URL: https://www.ncbi.nlm.nih.gov/snp
26. Chang X. and Wang K. wANNOVAR: annotating genetic variants for personal genomes via the web. J Med Genet, 2012.– 49(7).– P. 433–6.
27. Genomics Lab. 2010–2020. Available from: URL: http://wannovar.wglab.org
28. Institute, E.M.B.L.s.E.B. DMD ENSG00000198947 Transcripts. August 2020. Available from: URL: http://Aug2020.archive.ensembl.org/Homo_sapiens/Gene/Summary?g=ENSG00000198947;r=X:31097677–33339441
29. Szklarczyk Damian et al. STRING v11: protein-protein association networks with increased coverage, supporting functional discovery in genome-wide experimental datasets. Nucleic acids research – Vol. 47.– D1 (2019).– D607-D613.

30. Cytoscape: a software environment for integrated models of biomolecular interaction networks. Shannon P., Markiel A., Ozier O., Baliga N. S., Wang J. T., Ramage D., Amin N., Schwikowski B., Ideker T. Genome Res. 2003.– Nov,– 13(11).– P. 2498–504.
31. ANNOVAR Documentation. Utilize update-to-date information to functionally annotate genetic variants detected from diverse genomes, wANNOVAR supports only human genome annotation 2010–2018. Available from: URL: https://doc-openbio.readthedocs.io/projects/annovar/en/latest
32. Gao J., et al. Integrative analysis of complex cancer genomics and clinical profiles using the cBioPortal. Sci Signal, 2013.– 6(269).– l1 p.
33. Information N. C. f.B. Clinical significance on ClinVar submitted records. 2020–03. Available from: URL: https://www.ncbi.nlm.nih.gov/clinvar/docs/clinsig
34. Belsare S., et al. Evaluating the quality of the 1000 genomes project data. BMC Genomics, 2019.– 20(1).– 620 p.
35. New ACMG Guidelines. September 30, 2015. Available from: URL: https://www.genedx.com/whats-new/new-acmg-guidelines
36. Garton Fleur C. et al. The Effect of ACTN3 Gene Doping on Skeletal Muscle Performance. American journal of human genetics – Vol. 102.– 5. 2018.– P. 845–857.
37. Smith Lucas R. et al. Systems analysis of biological networks in skeletal muscle function. Wiley interdisciplinary reviews. Systems biology and medicine – Vol. 5,1. 2013.– P. 55–71.
38. Wang Y., et al. Dystrophin is a tumor suppressor in human cancers with myogenic programs. Nat Genet, 2014.– 46(6).– P. 601–6.
39. Sgambato A., et al. Dystroglycan expression is frequently reduced in human breast and colon cancers and is associated with tumor progression. Am J Pathol, 2003.– 162(3).– P. 849–60.
40. Hosur V., et al. Dystrophin and dysferlin double mutant mice: a novel model for rhabdomyosarcoma. Cancer Genet, 2012.– 205(5).– P. 232–41.
41. Körner H., et al. Digital karyotyping reveals frequent inactivation of the dystrophin/DMD gene in malignant melanoma. Cell Cycle, 2007.– 6(2).– P. 189–98.
42. Kaplan-Meier Plotter. 2009–2020. Available from: URL: http://www.kmplot.com/analysis
43. Boscolo Sesillo F., Fox D. and Sacco A. Muscle Stem Cells Give Rise to Rhabdomyosarcomas in a Severe Mouse Model of Duchenne Muscular Dystrophy. Cell reports, 2019.– 26(3).– P. 689–701.e6.
44. Luce L. N., et al. Non-myogenic tumors display altered expression of dystrophin (DMD) and a high frequency of genetic alterations. Oncotarget, 2017.– 8(1).– P. 145–155.
45. Rania Horaitis N. b. J. T. D. D. Codons and amino acids. October, 2009. Available from: URL: https://www.hgvs.org/mutnomen/codon.html

# Section 5. Physiology

**https://doi.org/10.29013/ELBLS-21-1.2-71-76**

*Basistaya Yekaterina Igorevna,*
*postgraduate student of physiology department*
*Dnipro State Medical University, Dnipro, Ukraine*
*Dnipropetrovsk, Ukraine*
*E-mail: katerinkaabas@gmail.com*

*Rodinskiy Aleksandr Georgievich,*
*M.D., Professor, Head of Physiology Department*
*Dnipro State Medical University, Dnipro, Ukraine*

*Guz Ludmila Vasilyevna,*
*Candidate of biological sciences, teacher of physiology department*
*Dnipro State Medical University, Dnipro, Ukraine*

## MORPHOLOGICAL CHARACTERISATION OF THE PANCREAS IN GERONTOGENESIS UNDER EXPERIMENTAL HYPERGLYCAEMIA

**Abstract.** The article assessed the development of diabetes mellitus at a reduced dose of alloxan by morphological examination of the pancreas. Middle-aged and elder rats were used in the experiment. The development of hyperglycaemia and its further effects on the pancreas were confirmed during the experiment.

**Keywords:** experimental hyperglycaemia, pancreas, diabetes mellitus, morphology, β-cells, islets of Langerhans.

**Introduction**

Diabetes mellitus (DM) is a metabolic disease resulting from impaired insulin secretion by the pancreas, insulin response or a combination of these factors. In terms of prevalence, DM can be considered a pandemic of the 21st century [2]. Major health problems develop as a result of the resulting hyperglycaemia [3]. There are no curative treatments for these conditions, and a deeper understanding of the mechanisms of disease development is required [4].

Experimental research models are widely used to study the pathogenesis of the disease. The alloxan-induced diabetic animal model is widely considered to be the classical model. Alloxan causes destruction of the β-cells of the pancreatic islets of the pancreas [5]. But despite the similarity of subdiabetogenic to lethal doses of the drug, the wide range of recommended doses for modeling, the absence of morphological evidence of DM development in conditions of administration of certain doses, the wide range of hyperglycaemic values, the emergence of specific insular apparatus functioning during gerontogenesis, our work is relevant. We chose a dose of 120 mg/kg animal weight.

**Materials and methods**

The experiment was carried out on 60 white Wistar rats kept in standard vivarium conditions. Animals were represented by two age groups – middle aged rats (6–7 months) weighing 140–160 g and elder rats (18–22 months) weighing 260–340 g(according to classification of I. P. Zapadnyuk, 1983). Each age group was divided into intact (control) and experimental (with experimental hyperglycemia) groups. Hyperglycemia was modeled by intraperitoneal injection of alloxan monohydrate solution (120 mg/kg, Sigma, Germany).

The development of hyperglycaemia was monitored by blood glucose, which was determined (glucose oxidase method) using a Bionime portable glucometer. On the third day, animals were selected that had persistent hyperglycaemia with peripheral blood glucose higher than 28 mmol/l.

The animals were euthanized by inhalation anesthesia with ethyl ether for tissue sampling [6; 7]. After decapitation, the pancreas was extracted, and microslides of the pancreas were made according to standard histological techniques, followed by hematoxylin and eosin staining. Fragments of pancreas were preserved in 10% neutral formalin. The material was dehydrated in a Leica TP1020 automatic station and embedded in paraffin. Paraffin sections (5 μm) were placed on slides coated with poly-L-lysine film (Sigma). Morphometric analysis was carried out using a system of computer analysis of microscopic images, consisting of a Nikon Eclipse E400 microscope, a Nikon DXM1200 digital camera, a personal computer and Video-Test-Morphology4.0 software (Avtandilov grid).

The results were statistically processed using Student's t-test and determination of criterion of normality of values distribution of the studied series [1]. We adhered to General Ethical Principles of Animal Experiments (Kyiv, 2001) and the European Convention for the Protection of Vertebrate Animals Used for Experimental and Other Scientific Purposes (Strasburg, 1986).

**Results and discussion**

To assess the peculiarities of the structure and functional activity of endocrine and exocrine parts of the pancreas in experimental animals we used standard criteria, including measurement of islets of Langerhans, number of islets per unit conventional area (per 0.1 $mm^2$), diameter of α- and β-cells, number of endocrine cells in pancreatic islets, area of parenchyma and organ stroma [8].

In the course of the study we found that in the middle-aged animals of the intact group there was a gradual decrease in the relative volume density of the stroma and, conversely, an increase in the relative volume density of the parenchyma (Fig. 1).

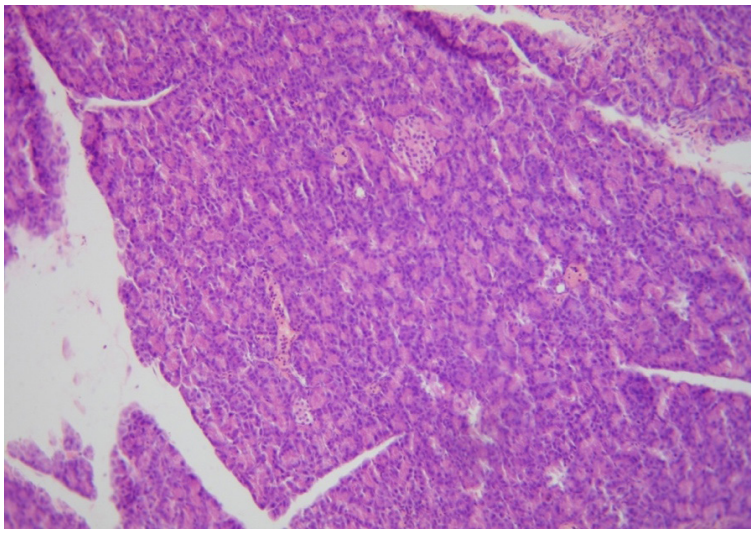

Figure 1. The pancreas of the middle-aged intact rat

3 groups of stromal changes were observed in animals with experimental hyperglycaemia: the occurrence of inflammatory infiltrate, fibrosis and vascular reaction. In most cases there was productive inflammation, which was either isolated in some lobules or diffusely distributed in the stroma of the organ. Foci of exudative inflammation were rare and detected around the excretory ducts. Fibrosis in most cases was combined with productive inflammation and venous vascular congestion. In some areas the parenchyma was separated by broad interlayers of connective tissue. Connective tissue development was more prominent in the immediate vicinity of the ducts (Figure 2). The excretory ducts were dilated and contained homogeneous oxyphilic contents.

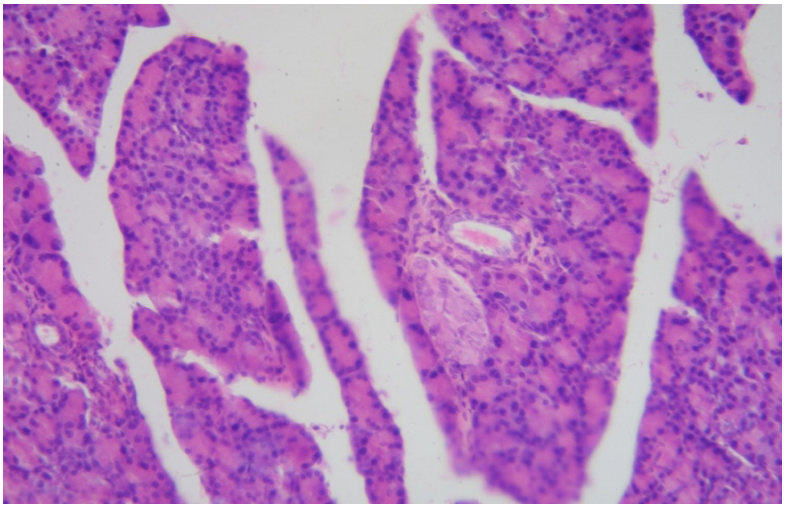

Figure 2. Pancreas of the middle-aged rat with experimental hyperglycaemia

Pancreatic exocrine tissue consists of 4 types of cells: acinar cells; centroacinarductal cells; mucin-secreting ductal cells; and connective interstitial cells [9].

The acini in the middle-aged intact animals consisted of a pyramidal, single-layered epithelium lining the basal membrane with curves directed towards the centre. Basal part of cell cytoplasm contained basophilic granules and stained more intensively in comparison with apical part of cell cytoplasm (by hematoxylin-eosin staining). Pancreatic secretory activity correlated with the size of acinocytes and their nuclei. Along the course of the ducts, cells with round nuclei, well visualized chromatin and 1 or 2 nuclei appeared. Mitotic markers were rarely observed (up to 1%). The small-calibre ducts were lined by flattened cube-shaped epithelium, the outlet terminal ducts by tall cylindrical epithelium and surrounded by dense fibrous connective tissue. Islets of Langerhans were few and irregularly rounded and accounted for 3% of the total structure of the pancreas. Diameter of islets ranged from 50 to 200 μm, most of them were 55–65 μm and 145–170 μm in diameter. Histologically, they were predominantly syncytium-like bands of heterogeneous prismatic cells. The boundaries of the islets were clear, and β-cells were predominantly located in the centre of the islets. Despite the rarity of mitoses, apoptosis markers (0.3%-0.5%) were found in islets of Langerhans.

In the exocrine part, histological examination in hyperglycemic middle-aged rats showed both focal and diffuse infiltration of the acini with lymphocytes. There was wrinkling of the affected acini, in isolated cases there was their enlargement with flattening of the epithelium. There were also areas of acinar dislocation into fatty tissue. Ducts with dilatation underwent the greatest changes. On sagittal slices the ducts had a tortuous course and were filled with condensed homogeneous masses. There was a decrease in accumulation of zymogen granules in acini of peripheral marginal sections and a high degree of their accumulation in

perinsular areas of lobules. In most animals there were foci of marked fatty dystrophy up to "fattening" of cells in exocrinocytes. This was accompanied by compensatory hypertrophy and hyperplasia of adjacent cells.

The islet part in this group decreased to 2%-2.5%, islet boundaries were blurred with moderately pronounced infiltration by lymphocytes at the periphery (initiation of insulinitis). Diameter of islets ranged from 50 to 150 μm with the predominance of islets with a diameter of 80–90 μm of irregular shape. We have noted heterogeneity of islets cell structure: in some cells there was active degranulation and hydrophic cytoplasmic dystrophy and prominent pycnosis of nuclei, in other part against the background of a low mitotic index (less than 1%) increased apoptosis up to 2.5%-3%.

In elder intact rats, the organ retained a lobular structure and was represented by tubular-alveolar structures. The outside of the pancreas was covered by a connective-tissue capsule dominated by fibrosis and venous vasculopathy (in contrast to young animals). From the capsule inside the organ there were thickened connective tissue interlayers that divided the pancreas into lobules, but the parenchymatous component decreased due to fibrosis and redistribution of adipose tissue. In the experimental group, organ fibrosis developed on the background of productive inflammation. There was noted a replacement of the parenchymatous comonte of the organ by the adipose tissue, in which there was an inflammatory infiltrate of lymphocytes, plasma cells, histiocytes and neutrophils. The pancreatic capsule was significantly thickened. On the capsule side, connective tissue bands with fatty tissue compounds were growing into the pancreas and squeezing the organ parenchyma (Fig. 3).

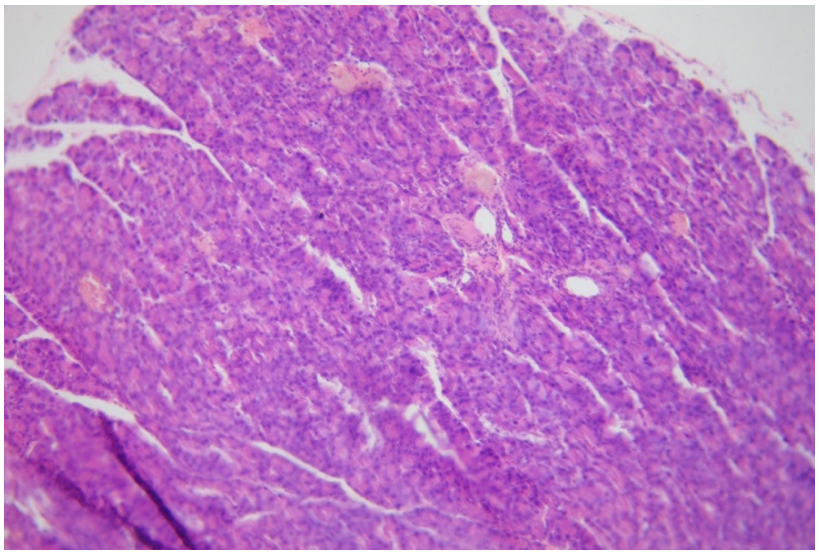

Figure 3. Elder intact rat pancreas

In animals without DM, the acinar structure and pyramidal shape of exocrinocytes was preserved, but in some acini the microvilli in the apical part of the cells were desquamated and lost. In some acini the heterogeneity of staining of basal and apical parts of cytoplasm was lost (basophilic and acidophilic component was leveled). Single exocrinocytes showed fine vacuolization of cytoplasm and pycnotic changes of nuclei. Small exit ducts were lined by cubic epithelium, terminal sections by cylindrical, but in some ducts there was flattening of epithelium and relative dilatation of duct with fibrosis of surrounding stroma and venous fullness. Mitotic patterns were absent. In old rats with DM, the gland retained a lobular structure, but the lobules varied in size, predominantly decreasing due to connective and adipose tissue overgrowth. In most cases the gland had acinar structure with single row pyramidal cells, however dystrophic changes prevailed in cells – diffuse hydrophic cytoplasmic dystrophy, pycnosis of nuclei and chromatin fragmentation in cells

with loss of apical microvessels, apical and then total desquamation of exocrinocytes into acinus lumen. In some animals, foci of fine fatty dystrophy were detected. On the background of dystrophic-degenerative changes of cells, there were also areas of compensatory adenomatosis of exocrinocytes. Among the dilated exit ducts with flattened epithelium there were ducts with epithelium hyperplasia. Fibrosis with residual lymphocytes and plasma cells developed around the vessels and the exit ducts. Fibrosis also developed and the ducts were tortuous, dilated and filled with homogeneous oxyphilic substance (Fig. 4).

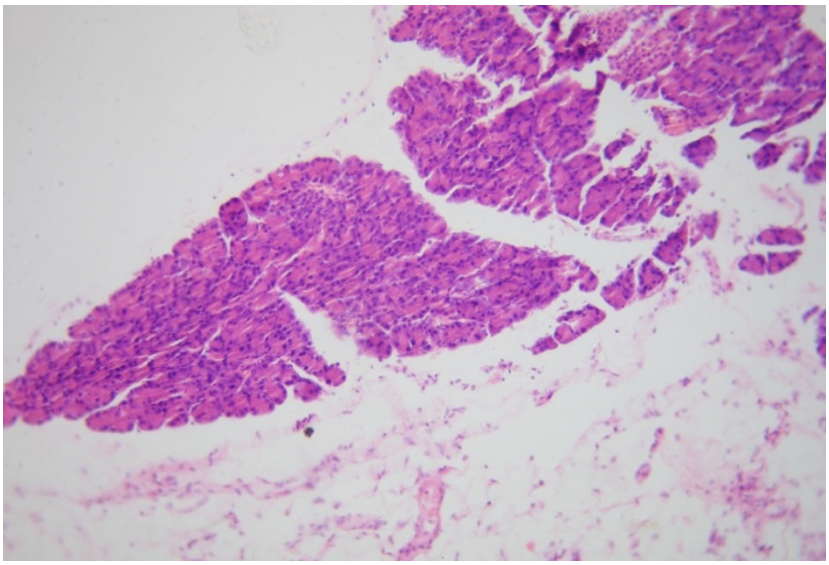

Figure 4. Pancreas of the elder rat with DM

Islets of Langerhans in the elder animals of the intact group were few in number, their shape was more rounded compared to younger animals and amounted to 1%-1.5%. The diameter of islets also ranged from 50 to 200 μm, but islets of different diameters were evenly distributed and no significant patterns of islet size were detected. The boundaries of islets were clear, and β-cells were located both in the centre of the islet and were diffusely scattered. Apoptosis markers were not observed, and individual cells with signs of cytoplasmic hydropic dystrophy and nuclear pycnosis were found in islet cells. In hyperglycaemic rats, the islet part was reduced to 1%-1.5% without signs of inflammatory infiltration. Islets of Langerhans had an irregular shape and blurred borders. The diameter of the islets decreased and ranged from 50 to 100 μm. Mitotic and apoptotic markers were absent. Degranulation, vacuolization of cytoplasm and nucleus, chromatin condensation and cell shrinkage developed in most islets.

**Conclusion.** The data obtained during morphological study of pancreas in rats of different age groups correlate with similar parameters of glycaemic levels and confirm the development of DM. The effect of the same dose of alloxan on rats of different ages was found to be slightly different. The damage to the exo- and endocrine parts of the BP of older rats was less pronounced, which may be related to age-related features of glucose metabolism, namely an increase in basal blood glucose and insulin levels.

## References:

1. Lakin G. V. Biometriya.– M.: Vyisshaya shkola; 1990.– 352 p.
2. Semenko V. Serdyuk V. Savytskyi I. Development of experimental alloxan model of diabetes mellitus. International Journal of Endocrinology (Ukraine), [S. l.],– Vol. 13.– No. 4. 2017.– P. 276–280. DOI: 10.22141/2224–0721.13.4.2017.106657.

3. Sharofova M. U., Sagdieva Sh. S., and Yusufi S. D. "Diabetes mellitus: current state of the art (part 1)" Vestnik Avitsennyi,– Vol. 21.– No. 3. 2019.– P. 502–512.
4. Garbuzov V. V., Morozov V. A., Maslov A. V., Hafizov R. F. Diabetes mellitus: risk factors of development and complications. modern tendencies. Alleya nauki,– 2(1). 2020.– P. 171–177.
5. Gritsyuk M. I. Comparative characteristics of experimental models of diabetes mellitus / M. I. Gritsyuk, T. M. Boychuk, O. I. Petrishen // SvIt meditsini ta bIolog IYi. 2014.– No. 2(44).– P. 199–203.– Rezhim dostupu: URL: http://nbuv.gov.ua/UJRN/S_med_2014_2_57.
6. International guidelines for biomedical research using animals// Hronika VOZ. 1985.– T. 39.– No. 3.– P. 3–9.
7. European convention for the protection of vertebrate animals used for experimental and other scientific purposes.– Council of Europe, Strasbourg, 1986.– 53 p.
8. Yanko R. V., Chaka E. G., Levashov M. I. Age differences in the morphofunctional state of the pancreas in rats after the administration of magnesium chloride. Rossiyskiy fiziologicheskiy zhurnal im. I. M. Sechenova. 105, 4.– fev. 2019.– P. 501–509. DOI: https://doi.org/10.1134/S0869813919040
9. Balabina N. M. B20 Chronic pancreatitis: diagnosis, treatment and prevention in outpatient: a study guide / N. M. Balabina; GBOU VPO IGMU Minzdrava Rossii, Kafedra poliklinicheskoy terapii i obschey vrachebnoy praktiki.– Irkutsk: IGMU, 2016.– 91 p.

# Contents